UNIVERSITY OF TARTU
Faculty of Science and Technology
Institute of Technology

Avishan Aghayari

T-cell receptor repertoire analysis in CVID patients post Comirnaty vaccination

Master's Thesis (30 ECTS)

Curriculum Bioengineering

Supervisor(s):

Professor, MD, PhD Kai Kisand

PhD student, MSc, Alexandra Elsakova

Tartu 2024

T-cell receptor repertoire analysis in CVID patients post Comirnaty vaccination

Abstract:

Common variable immunodeficiency (CVID) is one the most diagnosed primary immunodeficiencies (PID) with a complex etiology, characterized by low levels of serum immunoglobulins mainly due to B-cell deficiencies with potential T-cell dysregulations and abnormalities. This immune system dysfunction puts CVID patients at a higher risk for developing severe infections, including COVID-19. Despite its critical importance, their immune response to SARS-CoV-2 infection and vaccination remains unclear. Studying the T-cell-receptor (TCR) repertoire of these patients sheds light on the dynamics of their cellular immune response, knowing that T-cells recognize antigens through their TCR. In this study, we utilized high throughput sequencing to investigate and profile the TCR repertoire of PID patients, particularly those with CVID following the second dose of the Pfizer-BioNTech Comirnaty-BNT162b2 vaccine. We report on the diversity and clonality of TCR repertoires between diseased and healthy individuals post-vaccination. Investigating gene segment usage, we found a bias in the frequency of TCR V beta gene segment usage between patients and controls. Lastly, we examined the clonal expansion of T-cells following Spike-antigen (S Ag) stimulation to provide insights into the T-cell response post-vaccination.

Keywords:

T-cell receptor repertoire, CVID, PID, COVID-19, Vaccination

CERCS: B500 Immunology, serology, transplantation

T-raku retseptorite repertuaari analüüs üldise variaabli immuunpuudulikkusega patsientidel Comirnaty vaktsiini järgselt

Lühikokkuvõte:

Üldine variaabel immuunpuudulikkus (*CVID*) on üks kõige sagedamini diagnoositavaid primaarseid immuunpuudulikkuseid (PID), millel on keeruline etioloogia, mida iseloomustab seerumi immunoglobuliinide madal tase peamiselt B-rakkude puudulikkuse tõttu koos võimalike T-rakkude funktsiooni kõrvalekalletega. Immuunsüsteemi häire tõttu on CVID-ga patsientidel suurem risk raskete infektsioonide, sealhulgas komplitseeritud COVID-19 tekkeks. Vaatamata selle kriitilisele tähtsusele on nende patsientidevastus SARS-CoV-2 infektsioonile ja vaktsineerimisele endiselt ebaselge. Nende patsientide T-raku retseptori (TCR) repertuaari uurimine heidab valgust nende rakulise immuunvastuse dünaamikale, arvestades et T-rakud tunnevad antigeene oma TCR-i kaudu ära. Selles uuringus kasutasime järgmise põlvkonna sekveneerimist, et uurida PID-patsientide TCR-i repertuaari eripärasid Pfizer-BioNTech Comirnaty-BNT162b2 vaktsiini teise annuse järel. Kirjeldame TCR repertuaaride mitmekesisust ja klonaalsust haigetel ja tervetel. Leidsime TCR V beeta geenisegmendi kasutamise sageduse kallutatuse patsientide ja kontrollrühmade vahel. Lõpuks uurisime T-rakkude kloonide laienemist pärast Spike-antigeeni stimulatsiooni, et anda ülevaade T-rakkude vastusest pärast vaktsineerimist.

Võtmesõnad:

T-raku retseptorite repertuaar, CVID, immuunpuudulikkus, COVID-19, vaktsineerimine

CERCS: B500 Immunoloogia, seroloogia, transplantoloogia

TABLE OF CONTENTS

TERMS, ABBREVIATIONS AND NOTATIONS

ACE2	Angiotensin-converting enzyme 2
APC	Antigen presenting cell
CDR	Complementarity determining region
COVID-19	Coronavirus Disease of 2019
cTfh	Circulating Tfh cells
CVID	Common variable immunodeficiency
E	Envelope
EF	Extrafollicular phase
GC	Germinal center
Ig	Immunoglobulins
IFN	Interferon
IL-1	Interleukin-1
IL-6	Interleukin-6
LNP	Lipid nanoparticles
M	Membrane
MHC	Major histocompatibility complex
N	Nucleocapsid
NGS	Next generation sequencing
PBMC	Peripheral blood mononuclear cell
PBS	Phosphate buffered saline
PID	Primary immunodefeciency
RACE	Rapid Amplification of cDNA Ends
RB	Running buffer
RBD	Receptor binding domain
S	Spike

SARS-CoV-2	Severe Acute Respiratory Distress Syndrome Coronavirus 2
TCR	T-cell Receptor
Tfh	T follicular helper cells
Th17	T helper 17 cell
TNF	Tumor necrosis factor
TLR	Toll-like receptor
UMI	Unique molecular identifier
XLA	X-linked agammaglobulinemia

INTRODUCTION

Primary immunodeficiencies (PID) are a heterogeneous group of monogenic or polygenic diseases that can affect both the adaptive and innate arms of the immune system. Common Variable Immunodeficiency (CVID) is one of the most diagnosed PIDs, resulting in significant antibody deficiency. CVID is mainly thought of as a B-cell immunodeficiency; however, the disease is also associated with possible T-cell dysregulations and abnormalities. This results in impaired antibody responses to infections or vaccinations. Thus, these patients are at a higher risk for severe infections compared to the public. This vulnerability extends to Coronavirus disease 2019 (COVID-19) and the recent pandemic, as their immune system impairment could increase morbidity. However, their immune response to severe acute respiratory distress syndrome Coronavirus 2 (SARS-CoV-2) remains unclear to this day based on varying reports and conclusions. The vaccine response in these patients is also highly variable depending on the specific immune defect and the vaccine type. This highlights the need for more studies focusing on the immune responses of these patients post-infection and vaccination. Studying the T-cell receptor (TCR) repertoire of CVID patients post-vaccination allows for a better understanding of their cellular immune response dynamics, such as the antigen specificity and clonal dynamics of the T-cell response. T-cells recognize peptide antigens in combination with HLA molecules through their highly specific TCR. This is followed by the clonal expansion of the specific T-cells and their establishment as memory T-cells, enhancing the immune response upon subsequent encounters with the same antigen. T-cell response post-vaccination is induced by the vaccine antigen, and the TCR repertoire dynamics can be studied with high-throughput TCR repertoire sequencing (Fink, 2019; Miyasaka et al., 2019; Pogorelyy et al., 2018).

In this work, we focused on studying the TCR repertoire of PID patients post second dose of Pfizer-BioNTech Comirnaty-BNT162b2, especially those with CVID, to help fill the knowledge gaps regarding the TCR repertoire of these individuals. We investigated the clonality of the TCR repertoire between the healthy and diseased, the overlap of CDR3 region in these cohorts, and diversity. We also reported changes in the TCR V beta gene segment usage between different groups in the cohort. Lastly, clonal expansion post-spike-protein stimulation was also investigated.

LITERATURE REVIEW

1.1 Coronavirus disease 2019 (COVID-19)

In December 2019, a previously unknown coronavirus belonging to the *β-coronavirus* genus, severe acute respiratory syndrome coronavirus 2 (SARS-CoV-2), was identified in Wuhan, China, causing the disease known as Coronavirus disease 2019 (COVID-19). The pandemic caused by this virus highlighted the need for effective vaccines and therapeutics (Walls et al., 2020). This enveloped, single-stranded positive-sense RNA virus belongs to the *Coronaviridae* family of viruses consisting of 4 genera: *α-coronavirus*, *β-coronavirus*, *γ-coronavirus*, and *δ-coronavirus*, primarily infecting birds and mammals. *α-coronaviruses* and *β-coronaviruses* are the two genera known to infect humans, with SARS-CoV-2 emerging as a particularly virulent and transmissible member of the *β*-genus, highlighting the critical importance of understanding coronavirus diversity and cross-species transmission potential (Hartenian et al., 2020). The coronavirus's virion is characterized by four structural proteins: spike (S), envelope (E), membrane (M), and nucleocapsid (N), among which the spike glycoprotein is central to hosT-cell entry (Tortorici & Veesler, 2019). S is composed of two functional subunits: S1, which is responsible for binding the hosT-cell receptor containing the receptor-binding domain (RBD), and the S2 subunit, which facilitates the fusion of the viral and cellular membranes, enabling the virus to enter the host cytoplasm; as a result, S determines the host range of the virus and is also the main target of the neutralizing antibodies post-infection and the central target for vaccine development (Tortorici & Veesler, 2019; Walls et al., 2020).

1.1.1 COVID-19 and risk factors

SARS-CoV-2 threatens human health and public safety by being highly transmissible and pathogenic, causing mild to severe respiratory infections (Cascella et al., 2023). It is mainly spread through infected individuals via respiratory droplets while talking, sneezing, coughing, or any face-to-face contact, as suggested by epidemiologic data. Notably, infection transmission can happen by carriers who are asymptomatic, pre-symptomatic, or symptomatic (Wiersinga et al., 2020). Clinically speaking, although completely asymptomatic

SARS-CoV-2 infection is not rare, around 30-50% of patients present with progressive respiratory involvement, such as interstitial pneumonia (da Rosa Mesquita et al., 2021; Tong et al., 2020).

People of all ages are susceptible to SARS-CoV-2. However, age and certain medical conditions affect the infection's intensity and the virus's clinical manifestation. Individuals aged 60 and higher and patients with underlying medical comorbidities such as obesity, heart disease, chronic kidney disease, diabetes, cancer, or those who have undergone solid organ or hematopoietic stem cell transplants and immunocompromised patients face a higher risk of experiencing severe COVID-19 (Cascella et al., 2023).

The respiratory system is the main target for SARS-CoV-2 due to the high expression of the angiotensin-converting enzyme 2 (ACE2) receptor protein and the transmembrane protease serine protease 2, which are the virus entry mediators into the hosT-cell, in nasal epithelial cells, lungs, and bronchial branches(Cascella et al., 2023b; Hu et al., 2020). Thus, the primary symptoms are experienced mainly in the respiratory system. The common symptoms include fever, headache, shortness of breath, cough, muscle aches, and exhaustion (Esakandari et al., n.d.).

1.1.2 Immune response to COVID-19

The immune system's innate and adaptive components are involved in the dynamic and well-coordinated immune response to COVID-19. The exposure of human cells to the virus and its particles is the first step of this response. This initial encounter occurs in the upper respiratory tract, causing the innate immune response to act first through pattern recognition receptors (Brandtzaeg, 2015; Primorac et al., 2022). with SARS-CoV-2 immune evasion strategies, a downmodulated antiviral type-I-interferon (IFN) response follows. Plasmacytoid dendritic cells (pDCs), which are present in the blood and the mucosa, are highly specialized cells that primates evolved for the generation of type-I IFNs, which also act as the main link between the innate immune response and the activation of the adaptive immune response via upregulating major histocompatibility complex class I (MHC-I) molecules for better virus antigen presentation for CD8+ T-cells and potentiating the function of T and B-cells (Hartmann et al., 2006; Tezuka et al., 2011). Virus-infected cells can be targeted by NK cells that sense the stressed cells, activate their killing machinery, and help get rid of the

virus together with the infected cells. B-cells, CD4+ T-cells, and CD8+ T-cells are the major components of the adaptive immune system. B-cells produce antibodies, CD4+ T-cells possess helper and effector functionalities, and CD8+ T-cells kill the infected cells (Sette & Crotty, 2021). Thus, one of the roles of the innate immune response is to prime and trigger the adaptive immune system. The adaptive immune response requires several days, typically 6-10 days after initial exposure to the virus, to generate enough specialized cells capable of controlling a viral infection. This delay is due to the time needed for extensive proliferation and differentiation of naive immune cells into active effector cells. Once a sufficient number of effector T-cells (helper and cytotoxic) and effector B-cells responsible for antibody production (plasma cells) have proliferated and differentiated, they work together to eliminate infected cells and circulating virions (Sette & Crotty, 2021).

1.1.3 Antibody response (humoral immunity)

Antibodies play a crucial role in adaptive immunity, specifically against viral infections. This antibody response can be divided into two phases based on predominant isotypes and the profile of somatic hypermutations of the antibodies: the extrafollicular (EF) phase and the germinal center (GC) phase. In the EF phase of the response, B-cells differentiate into plasma cells in foci outside the follicle shortly after infection (Elsner & Shlomchik, 2020). These plasma cells produce antibodies with fewer somatic hypermutations that still possess high enough affinity, enabling the neutralization of the virus (Lam et al., 2020). However, this rise of neutralizing antibodies by the EF response is insufficient for controlling the infection. Prevention of re-infection depends on the GC response, which gives rise to enduring neutralizing antibodies with enhanced affinity and binding strength, as well as a durable humoral memory through memory B-cells and long-lived plasma cells (Qi et al., 2022; Woodruff et al., 2020). Neutralizing antibody responses are likely markers of protective immunity, and they exclusively target the viral S protein, specifically the RBD within the S1 sub-domain (Robbiani et al., 2020; Wheatley et al., 2021). Neutralizing immunoglobulins IgA, IgM, and IgG have been reportedly found in cases of COVID-19, with IgM being the primary one being produced (Suthar et al., 2020). The antibody response is expected to be generated 5-15 days post-onset of the symptoms and peak after 3-4 weeks before starting to go down. Additionally, the magnitude of the neutralizing antibody response has been shown to correspond with the severity of the disease in a way that patients with the most severity

typically show the most intense antibody response. On the other hand, patients experiencing mild disease or who are asymptomatic may have lower levels of detectable neutralizing activity in their blood; this is explained by the significant expansion of antibody-secreting cells in severe cases due to prolonged contact with viral antigens (Woodruff *et al*., 2020).

1.1.4 T-cell response (cellular immunity)

Understanding the T-cell response in disease pathogenesis and longer-term protective immunity is crucial when guiding therapeutic approaches and efficient vaccine design (Peng et al., 2020).

Multiple studies of acute and convalescent COVID-19 patients have shown the importance of T-cell responses for the control and resolution of a primary SARS-CoV-2 infection, suggesting that there is a correlation between robust T-cell responses and milder forms of the disease(Rydyznski Moderbacher et al., 2020; Sekine et al., 2020). However, T-cell responses are commonly detected following approximately all COVID-19 infections, and CD4+ T-cell responses are more significant than those of CD8+ T-cells. Moreover, the neutralizing antibody response also depends on the CD4+ T-cell response (Grifoni et al., 2020; Sekine et al., 2020). Thus, CD4+ T-cell responses play a vital role in the efficacy of most vaccines (Rydyznski Moderbacher et al., 2020). Most CD4+ T-cells in COVID-19 patients specifically target the S, M, N, and open reading frames (ORFs) of SARS-CoV-2, which are abundantly expressed (Grifoni et al., 2020).

Virus-specific CD4+ T-cells typically differentiate into effector cells with more direct anti-pathogen activities, such as Th1 cells and T follicular helper cells (Tfh), where Th1 cells exhibit antiviral activity by IFNγ production and Tfh cells play a vital role in assisting B-cells and developing neutralizing antibody responses, as well as memory B-cells and long-term adaptive immunity (Crotty, 2019). Circulating Tfh cells (cTfh) specific to SARS-CoV-2 and memory cTfh cells are also formed during acute infection (Rydyznski Moderbacher et al., 2020).

Furthermore, IFNγ+ CD4+ T-cells have been shown to confer protection against lethal SARS-CoV infection, and IFNγ is known to be the most dominant cytokine produced by T-cells in COVID-19 patients(Weiskopf et al., 2020; Zhao et al., 2016).

Additionally, CD4+ T-cells also assist CD8+ T-cells, and IL-21, which is a canonical cytokine of Tfh cells, is known to be important for CD4+ T-cells to help CD8+ T-cells (Buchholz & Busch, 2019; Zander et al., 2019).

It has also been reported that a CD4-CTL (CD4+ T-cells with cytotoxic activity) transcriptional signature has been seen in COVID-19 patients; however, the cytotoxicity degranulation marker CD107a has been minimally detected on SARS-CoV-2-specific CD4+ T-cells (Peng et al., 2020; Sekine et al., 2020; Weiskopf et al., 2015).

Another function of the SARS-CoV-2 specific CD4+ T-cells through gene expression of CCL3/4/5 (MIP-1α) and XCL1 chemokine could be recruiting other effector cells to viral antigen sites (Meckiff et al., 2020).

Furthermore, the expression of CCR6, which is a chemokine receptor known to be associated with migration to mucosal tissue, by a sub-population of SARS-CoV-2 specific CD4+ T-cells may suggest that these cells may possess characteristics of Th17 cell lineage (T helper 17); however, expression of IL-17α which is typically produced by Th17 cells is either undetectable or low (Braun et al., 2020; Juno et al., 2020; Rydyznski Moderbacher et al., 2020; Weiskopf et al., 2020). On the other hand, there is a robust expression of IL-22, which is commonly produced by mucosal CD4+ T-cells in the SARS-CoV-2 Tspecific CD4+ T-cells, and IL-22 expression is commonly associated with tissue repair, especially of lung or epithelial cells. This suggests that SARS-CoV-2-specific CD4+ T-cells may play a role in lung tissue repair during COVID-19 infection (Dudakov et al., 2015; Rydyznski Moderbacher et al., 2020).

CD8+ T-cells are known for the critical role they play in viral infections by their ability to kill infected cells. In the case of COVID-19, it has been reported that SARS-CoV-2 specific CD8+ T-cells were more present in milder cases of infection, and scarcity of naïve CD8+ T-cells is associated with a risk of severe COVID-19 (Peng et al., 2020). However, SARS-CoV-2 specific CD8+ T-cells are less frequently observed compared to CD4+ specific cells however, they are still directed against different SARS-CoV-2 antigens such as S, N, M, and ORF3a, which is a nonstructural accessory protein of SARS-CoV-2 which is hypothesized to promote virus uptake, replication, and release through exocytosis (Grifoni et al., 2020; Sekine et al., 2020; Zhang et al., 2022). SARS-CoV-2 specific CD8+ T-cell's cytotoxic activity is correlated with the expression of IFNγ, granzyme B, perforin, and the cytotoxicity degranulation marker CD107a (Rydyznski Moderbacher et al., 2020; Schulien et al., 2021).

1.2 COVID-19 vaccines

Despite the protective measures taken to control the transmission of SARS-CoV-2, such as wearing masks and contact limitations, vaccination against the disease was established as a solution by developing acquired immunity. The vaccine-mediated immune activation mimics the natural immune activation of SARS-CoV-2, resulting in the proliferation of the same effector and memory cell subsets without the real infection or severe inflammatory side effects (Mistry et al., 2022). Most COVID-19 vaccines are focused on and target the S protein with which the virus can enter the host cell via the ACE2 receptor; by targeting the S protein, vaccines tend to block this receptor-mediated entry of the virus (Martínez-Flores et al., 2021).

There are currently eight Covid-19 vaccines that have been approved for use in Europe, which can be categorized into 4 different types: mRNA-based vaccines, viral vector-based vaccines, inactivated vaccines, and protein-based vaccines (*Covid-19 Vaktsiinid | Ravimiamet*, n.d.) **(Table 1)**.

Table 1. Authorized SARS-CoV-2 vaccines for use in Europe and Estonia. The Table describes different types of SARS-CoV-2 vaccines, their manufacturers, adjuvant, and active ingredients. (Ravimiamet, 2024).

	Vaccine and manufacturer	Vaccines active ingredient	Adjuvant
mRNA based	**Comirnaty** BionTech Manufacturing GmbH	SARS-CoV-2 spike protein-encoding mRNA packaged in a lipid nanoparticle	Does not contain
	Spikevax Moderna Biotech Spain S.L		Does not contain
Adeno-virus-based	**Vaxzervia** AstraZenecaAB	DNA encoding the spike protein of SARS-CoV-2 packaged in a chimpanzee adenoviral vector	Does not contain
	Jcovden Jannsen-Cilag International N. V	DNA encoding the spike protein of SARS-CoV-2 packaged in a human adenoviral vector	Does not contain
Inactivated	**Covid-19 Vaccine Valneva** Valneva	Inactivated (killed) SARS-Cov-2 virus particle	Aluminum hydroxide and nucleic acid CpG1018
Protein-based	**Nuvaxovid** Novavax CZ a.s.	SARS-CoV-2 spike protein	Matrix M (soap tree bark extract)
	VidPrevtyn Beta Sanofi Pasteur	SARS-CoV-2 spike protein	AS03 - squalene-based adjuvant
	Bimervax Hipra Human Health S.L.	Alpha and beta variant of SARS-CoV-2 spike protein fragment	SOBA - squalene-based adjuvant

1.2.1 mRNA vaccines

mRNA-based vaccines represent the most recent advancement in vaccine technology. These vaccines contain a single-stranded RNA molecule carrying a part of the coding sequence of a viral peptide or protein. Once synthesized within the cytoplasm, this antigen elicits an immune response, leading to the generation of effector cells and antibody production (Pormohammad et al., 2021). An advantage offered by these vaccines is that there is no need for delivery into the nucleus as opposed to DNA-based vaccines, as protein translation from the mRNA takes place in the cytoplasm. Moreover, these vaccines do not need an adjuvant as mRNA on its own acts as an adjuvant capable of triggering a strong innate immune response (Cagigi & Loré, 2021; Corey et al., 2020).

mRNA-based SARS-CoV-2 vaccines Pfizer-BioNTech Comirnaty-BNT162b2 & Moderna - mRNA-1273) contain mRNA sequences that encode the full-length spike protein, which is packaged into lipid nanoparticles (LNP) (Pormohammad et al., 2021).

The LNP acts as an adjuvant, enhancing the immune response, shielding the mRNA from degradation, and facilitating mRNA entry into the cell (Corey et al., 2020). Encapsulation is essential due to the unstable nature and negative charge of mRNA, ensuring successful entry(E. Fang et al., 2022). Cell entry, in the case of these vaccines, happens solely through endocytosis, creating an endosome that does not damage the cell membrane. This is followed by the immediate direction of the endosomes to lysosomes for degradation, which poses a challenge to maintaining the integrity of the mRNA essential for its translation into proteins. Thus, it is crucial to avoid endosomal fusion to lysosomes; this is facilitated by the ionizable cationic lipids in LNPs, which help with endosomal escape. The acidic environment inside the endosome leads the ionizable lipids to gain a positive charge, making them have an affinity for the negatively charged headgroups of phospholipids in the endosomal membrane. This results in disruption of the stable phospholipid bilayer structure, and this disruption enables the encapsulated mRNA within the lipid nanoparticle to evade the endosome and reach the cytoplasm, where it can be translated by ribosomes (E. Fang et al., 2022).

Following the translation of the mRNA, the translated protein is degraded by the proteasome into antigenic peptides. These peptides are consequently presented to CD8+ cytotoxic T-cells through MHC-I, resulting in the activation of the cell-mediated immune response (Cagigi & Loré, 2021). Moreover, upon the secretion of the translated proteins into the extracellular environment and, thereby, the circulatory system, these proteins can be taken up by APCs. Through these events, antigen presentation to CD4+ T-cells takes place via MHC-II molecules, which results in the activation of CD4+ T-cells, which is followed by various cytokine secretions and B-cell activation, resulting in antibody production (Cagigi & Loré, 2021).

1.3 COVID-19 and vaccine response in primary immunodeficiencies

COVID-19 can affect and threaten the general population. However, those with existing comorbidities are at a greater risk for adverse outcomes. Patients with inborn errors of im-

munity, or in other words, primary immunodeficiencies (PID), belong to this category, making them susceptible to a severe acute and long-lasting SARS-CoV-2 infection (Ameratunga et al., 2021; Hurme et al., 2023). Thus, understanding the immune response of patients with PIDs post-vaccination is of critical importance.

1.3.1 Spectrum of PIDs

PIDs are a large heterogeneous group of diseases with genetic anomalies that arise from adaptive and innate immunity impairments. Patients suffering from PID can have varied clinical presentations depending on the underlying genetic defect causing the immune system dysfunction. However, some of the common manifestations could be named as high susceptibility to infections causing recurrent and severe infections, autoimmunity, autoinflammation, immune dysregulation, extreme allergies, etc. (Amaya-Uribe et al., 2019; Cunningham-Rundles & Ponda, 2005; Raje & Dinakar, 2015).

The classification of primary immunodeficiency disorders (PIDs) depends on which component of the immune system is malfunctioning, whether it's the adaptive immunity (i.e., T-cell, B-cell, or combined immunodeficiencies) or the innate immunity (e.g., phagocyte and complement disorders) and the prevalence of PIDs is approximately estimated to be around 4-10 per 10^5 live births. Moreover, PIDs can manifest themselves at any age, depending on the type; sometimes, they can be diagnosed in newborns, and sometimes, the disease presents itself later in life (Fischer et al., 2017; McCusker et al., 2018; Tangye et al., 2020).

Among the diverse spectrum of PIDs, severe combined immunodeficiency, which is characterized by a lack of functional T-cells, Wiskott-Aldrich syndrome, DiGeorge syndrome, ataxia-telangiectasia, and x-linked lymphoproliferative disease are examples of T-cell and combined immunodeficiencies (Bousfiha et al., 2015).

The common variable immunodeficiency (CVID), relevant to this thesis, is a type of B-cell immunodeficiency. B-cell immunodeficiencies (antibody deficiency) are considered to be the most frequent type of PIDs, accounting for approximately 50% of all PID-confirmed cases (Bonilla et al., 2014).

1.3.2 CVID

Back in 1971, the term “variable immunodeficiency” was used to refer to all PIDs not fitting the diagnosis as x-linked agammaglobulinemia (XLA), selective immunoglobulin A deficiency, x-linked hyper-IgM syndrome, ataxia telangiectasia, Wiskott-Aldrich syndrome, severe combined immunodeficiency, or some other clinically distinct syndromes. to this day, CVID remains challenging to classify as the term encompasses a broad and varied array of conditions and there is little knowledge on definite patterns and underlying causes(Bousfiha et al., 2015; Fudenberg et al., 1971).

However, CVID is considered the most prevalent clinically significant antibody deficiency (humoral primary immunodeficiency) with a possible underlying T-cell dysregulation, and symptoms may present at any age with a usual onset at a later age. Susceptibility to recurrent bacterial infections and viral respiratory tract infections are the major clinical manifestations of this disease(Bonilla & Geha, 2009). Moreover, CVID is also associated with a greater risk of autoimmune and inflammatory complications (Fischer et al., 2017).

From an immunologic perspective, all CVID patients have low serum IgG accompanied by low IgA or IgM and distinctly impaired antibody response to infection or vaccines, resulting in poor or absent responses to immunization, a low percentage of class-switched IgD−CD27+ memory B lymphocytes is also prevalent and associated with low antibody production capacity (Arroyo-Sánchez et al., 2022; Bonilla & Geha, 2009; McCusker et al., 2018). Additionally, another characteristic of this disease could be an inverted CD4/CD8 T-cell ratio pointing to a relative CD4+ T-cell lymphopenia along with T-cell activation and exhaustion markers that could indicate an underlying T-cell dysregulation (Løken & Fevang, 2023).

1.3.3 COVID-19 in CVID

Patients with inborn errors of immunity, especially patients with CVID, are at a higher risk for severe SARS-CoV-2 infection relative to the general population. However, different studies have reported varied conclusions on this matter, making the immune response of these patients into a hot debate (Bonilla & Geha, 2009).

The two primary antiviral cellular immune responses after a viral infection post transcription are the induction of IFNs and the production of cytokines, primarily interleukin-1 (IL-1),

interleukin-6 (IL-6), and tumor necrosis factor-alpha (TNF-α) resulting in the recruitment of specific white blood cells (Blanco-Melo et al., 2020). Studies claim that primary immunocompromised patients have a dysfunctional IL-6 pathway due to the lack of IL-6 receptor expression, which subsequently makes them unresponsive to IL-6 (Nahum et al., 2020; Spencer et al., 2019).

In the case of SARS-CoV-2, research suggests that this virus induces a severe inflammatory response characterized by lowered IFN response and a significant cytokine release (particularly IL-1 and IL-6), ultimately leading to a cytokine storm (Blanco-Melo et al., 2020; McGonagle et al., 2020). B lymphocyte impairment in CVID patients may result in a poor cytokine response; however, this impairment, along with low Ig levels, may not necessarily result in high mortality caused by COVID-19 but rather an increase in morbidity (Abraham et al., 2021). It has also been shown that despite the B-cell impairment and antibody deficiency, CVID patients may still develop SARS-CoV-2 IgM and IgG antibodies 7 weeks post the initial symptoms (Guchelaar et al., 2021). According to Quinti *et al*, CVID patients experienced a more severe illness caused by SARS-CoV-2 compared to those with agammaglobulinemia, implying a potential role of B-lymphocytes in the inflammatory process triggered by SARS-CoV-2 (Quinti et al., 2020).

Furthermore, studies indicate that in CVID patients, there is a notable decrease in the functionality of specific toll-like receptors (TLR), namely TLR-7 (responsive to RNA viruses) and TLR-9, which play crucial roles in both antiviral responses and the production of proinflammatory cytokines (Petes et al., 2017).

Regarding cellular immunity and COVID-19 in CVID patients, findings suggest that T-cells may provide significant protection, making up for the impaired B-cell response. In a study done by Kinoshita *et al.* in which they studied 5 unvaccinated COVID-19 Patients with primary antibody deficiency, three of the patients with CVID experienced mild disease. They demonstrated CD4+ T-cell responses similar to the healthy convalescent patients, evidenced by cytokine production levels in peripheral blood mononuclear cells (PBMC) cultures stimulated by S, M, and nucleocapsid proteins (Kinoshita et al., 2021). Another study suggests that 7 out of 11 uninfected CVID patients with no lymphopenia had spike protein-specific reactive CD4+ T-cells but none against nucleocapsid. However, healthy controls had a higher frequency of reactive T-cell populations (Steiner et al., 2020). In a separate study, 3 unvaccinated CVID patients with severe COVID-19 showed robust T-cell responses, with

all patients displaying reactive CD4+ T-cells against spike and nucleocapsid proteins. Notably, the frequencies of reactive T-cells were significantly higher in CVID patients compared to convalescent healthy controls. Similarly, the reactive CD4+ T-cells produced higher amounts of IFN-γ, TNF, and IL-2 in CVID patients. However, the controls experienced only mild disease. These findings suggest that CVID patients mount strong T-cell responses to COVID-19, even in the absence of a serologic response (Steiner et al., 2022).

1.3.4 Vaccine responses in CVID

Multiple studies have been done on the humoral and cellular response of CVID patients post-vaccination against SARS-CoV-2. However, the response to immunization depends on several factors, such as the antigen type, the vaccine mechanism, and the specific immune defect causing CVID (Arroyo-Sánchez et al., 2022).

It is generally expected for CVID patients not to have robust antibody responses post-vaccination due to B and T-cell impairments and possible hypogammaglobulinemia. However, it has been shown that most CVID patients with mild to moderate IgG deficiency did exhibit specific anti-S antibody concentrations that were slightly lower but comparable to healthy individuals after the second dose of mRNA vaccination (Bitzenhofer et al., 2022). Conversely, other findings indicate a lack of humoral immune response in two-thirds of CVID patients (Salinas et al., 2021). These variations in immune response may be attributed to the severity of humoral immunodeficiency, immunosuppressant treatments, and low IgG baseline titers (Bitzenhofer et al., 2022; Kinoshita et al., 2021). Furthermore, there are also studies suggesting that patients with immune deficiencies can develop robust T-cell responses compared to healthy individuals, making up for the lack of humoral response post-vaccination (Kinoshita et al., 2021; Zonozi et al., 2023).

One way to assess the cellular response is by measuring the cytokine production levels, specifically IFN-γ and IL-2. Multiple studies claim that cellular responses measured by cytokine levels in some CVID patients were defective compared to healthy controls 4-5 weeks after the start of the vaccination (Pfizer-BioNTech Comirnaty-BNT162b2). However, the same CVID patients did have a present but blunted anti-S antibody response. Interestingly, CVID patients showed a weaker cellular response than XLA patients present in the study group, meaning that there was no detected increase in IFN-γ after spike protein inductions of their

cells, this lack of cellular response could be in association with previous oncologic history and defects in the T-cells and cellular arm of immunity (Arroyo-Sánchez et al., 2022; Hagin et al., 2021; Salinas et al., 2021). However, both the humoral and cellular responses could be variable among different CVID populations with different underlying causes and etiologies. Another study has shown that individuals with CVID have increased effector and memory spike protein-specific T-cell responses, specifically CD8+ T-cells, after vaccination with two doses of mRNA-based spike protein vaccines (Moderna mRNA-1273 or Pfizer-BioNTech Comirnaty-BNT162b2) (Zonozi et al., 2023).

The collective conclusion of all studies is showcasing the benefits of vaccination in reducing the disease severity for this vulnerable group. However, solid conclusions require more in-depth studies on immunity post-vaccination.

1.4 T-cell receptor (TCR)

Mature T-cells recognize specific antigens presented on MHC molecules on APCs through specific receptors known as T-cell receptors (TCR). Thus, large numbers of TCRs elicit the cellular arm of adaptive immunity, providing protection against a vast diversity of pathogens (X. Liu & Wu, 2018).

Depending on the TCR expressed on the surface of T-cells, they can be divided into either α/β T-cells or γ/δ T-cells. α/β T-cells make up almost 95% of the T-cell population, and the receptor is a heterodimer consisting of one alpha chain and one beta chain. In the case of γ/δ T-cells, TCR consists of one gamma and one delta chain (H. Liu et al., 2021; X. Liu & Wu, 2018).

TCRα and TCRβ are formed through somatic recombination known as VDJ recombination **(Figure 1)**, which is a combinatorial somatic rearrangement of multiple variable (V), diversity (D) (for the β-chain only), joining (J) and constant (C) gene segments (Davis & Bjorkman, 1988). According to the International Immunogenetics Information System, to this day, there are 45 known V gene segments and 50 J segments for the α chain and 48V, 2 D, and 13 functional J segments for the β chain in humans (Manso et al., 2022).

Vdj recombination, coupled with the insertion or deletion of nucleotides between spliced gene segments, produces a diverse TCR repertoire with an estimated 2×10^{19} distinct TCRαβ

pairs, ensuring that each T-cell is specific to a different antigen. However, selection pressures and the number of present T-cells likely lower this diversity in an individual (Bradley & Thomas, 2019; Davis & Bjorkman, 1988; Nikolich-Žugich et al., 2004). These somatic rearrangements in TCRs occur during T-cell development in the thymus (X. Liu & Wu, 2018).

Within TCR, there are three significant regions known as complementarity-determining regions (CDR1, CDR2, and CDR3). These regions are essential for identifying antigens presented by MHC molecules. CDR1 and CDR2, found in both α and β chains and encoded only by the V genes, typically interact with the MHC molecule. On the other hand, CDR3, encoded by the junctional region including the V, (D) (only in the beta chain), and J genes, primarily recognizes the antigenic peptide itself, and it is also known to be the most diverse region in TCR chains. Therefore, the CDR3 region is considered the main determinant of the antigen-specificity of T-cells (Turner et al., 2006).

The T-cell receptor (TCR) sequence is unique to each T-cell, serving as a specific molecular identifier. This characteristic assists in distinguishing individual T-cells and their grouped clones, referred to as clonotypes. This is possible because all T-cells that are activated and undergoing proliferation carry the same TCR (Turner et al., 2006). Thus, analyzing the TCR repertoire allows for a better understanding of the antigen-driven clonal expansion and dynamics of T-cells as an indicator of antigen specificity and response (Bradley & Thomas, 2019).

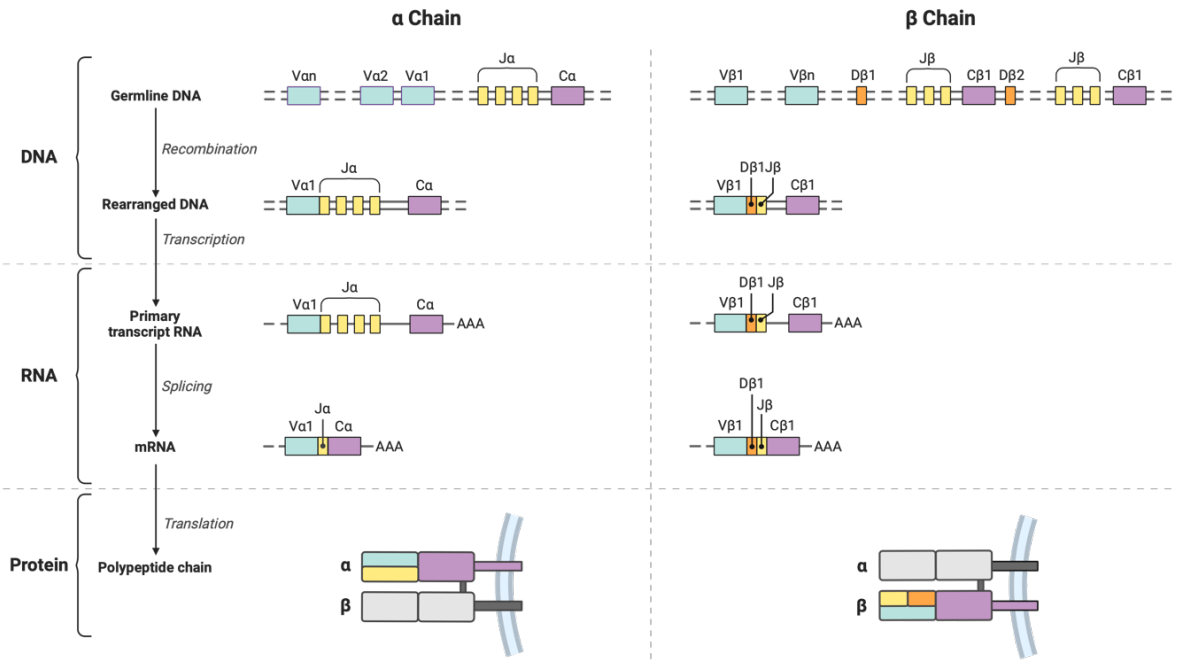

Figure 1. VDJ recombination in the α and the β chain of the TCR. A schematic representation of the V(D)J rearrangement for the alpha and beta chains of α/β T-cells.

THE AIMS OF THE THESIS

The study's general aim was to analyze the properties of the T-cell receptor repertoire of patients with dominant B-cell defects to increase the understanding of the potential involvement of T-cell abnormalities in their disease pathogenesis.

Specific aims:

- Compare the general characteristics of the TCR repertoire of CVID patients to those of healthy individuals and other PID patients, such as clonality, diversity, CDR3 length, V beta gene usage, and clonal expansion.
- Find and characterize the expanded T-cell clonotypes after in vitro restimulation with SARS-CoV2 spike antigen.

EXPERIMENTAL PART

MATERIALS AND METHODS

1.4.1 Study group

Samples for this thesis were taken from 33 individuals with Primary immunodeficiencies (PIDs) **(Table 2)**. Additionally, the study featured samples from 5 individuals serving as healthy controls. All individuals were vaccinated against COVID-19 with the Pfizer-BioN-Tech Comirnaty-BNT162b2 vaccine. Samples were collected from individuals aged 19 to 71, including females and males.

Table 2. The number of samples and the age range included in the study based on the diagnosis and the number of individuals with low antibody levels post Comirnaty vaccination.

Status	Number of Samples	Age Range	Count of impaired antibody response to vaccination
CVID	13	21 - 48	9
XLA	2	19 - 21	2
Antibody deficieny	18	26 - 71	1
Healthy	5	30 - 55	0

1.4.2 PBMC isolation

Blood samples from PID patients and healthy controls were collected in 8 ml CPT tubes (Cell Preparation Tubes) (BD Vacutainer). For PBMC isolation, the blood tubes were first centrifuged (Eppendorf 5810R, rotor A-4-62) at room temperature at 1800 rcf (Relative Centrifugal Force) for 25 minutes with a minimum brake to maintain the required gradient. Post centrifugation, the PBMC-containing layer of the formed gradient was carefully moved to a 15 ml tube (Biosigma ClearLine). Following this step, cells were washed with 15 ml of PBS (Phosphate buffered saline) (Corning) and centrifuged at room temperature for 10 min at 200 rcf. This step was followed by removing the supernatant and a second wash with 10 ml of PBS and 10 minutes of centrifugation at 300 rcf. During the centrifugation, cells were counted using Luna Fluorescence Cell Counter (Logos Biosystems) by taking 18 µl of cell suspension and 2 µl of acridine orange-propidium iodide dye (Logos Biosystems, catalog number F23001). Lastly, the supernatant was removed, and ABC freezing media (Immunospot) was added according to the manufacturer's protocol. The cells were stored at -150 °C. PBMC isolation was done by other lab members.

1.4.3 Proliferation assay

Prior to antigen stimulation of samples from patients, proliferation assay using CTV (cell trace violet staining) was carried out on PBMC samples from healthy controls that had been vaccinated against COVID-19. The assay was carried out with the purpose of comparing T-cell proliferation after stimulation with SARS-CoV-2 S Antigen containing S1 and S2 subunits (BioLegend) versus a S peptide pool containing immunodominant regions from the wild-type virus (PepTivator SARS-CoV-2 Prot_S (WT), Miltenyi Biotec). Moreover, the proliferation in the presence and absence of heat-inactivated 5% human serum was compared (Sigma-Aldrich).

PBMCs were thawed using a warm (37°C) RPMI 1640 medium (Corning), and cell numbers were counted using Luna Fluorescence Cell Counter (Logos Biosystems) by taking 18 µL of cell suspension and 2 µl of acridine orange-propidium iodide dye (Logos Biosystems, catalog number F23001). For staining the cells, thawed PBMCs were resuspended in 37°C PBS (corning) depending on the cell numbers, 1 ml of PBS was used per 1 million cells.

Furthermore, 0.2 µl /mL of CTV Brilliant Violet 421 dye (Invitrogen) was added to the samples, and samples were left to incubate for 20 minutes at room temperature. Post Incubation, 5 volumes of warm (37°C) RPMI 1640 medium supplemented with 10% autologous plasma was added to the samples. This step was followed by another 5 minutes of incubation at room temperature. Samples were then centrifuged (Eppendorf 5810R, rotor A-4-62) at 300 rcf for 10 minutes, and cells were counted another time as CTV is toxic to the cells. CTV-stained cells were then taken up in approximately 1.5 million cells in 250 µl warm (37°C) X-VIVO 15 media (Lonza) supplemented with 10 µM sodium pyruvate (Gibco), 1x MEM-nonessential amino acids (Gibco), 0.01mM 2-mercaptoethanol (Sigma), 2mM L-Glutamine, and plated into a cell culture 48-well plate (Greiner bio-one). 5 µl of each stimulant was then added to the wells at a final concentration of 1 µg/mL. The experiment also had a set of negative controls with no stimulant added to the culture. Cells were then left to proliferate in the 37°C incubator.

1.4.3.1 Flow cytometry

Flow cytometry was performed on the 5th and 7th days post-stimulation to assess differences in proliferation based on both the stimulant and the number of days for the immune response to form. To start, the cells were resuspended and transferred to 1.5 ml tubes. The wells were then washed with 1 ml of 2 mM EDTA-PBS solution, which was then transferred to the tubes containing the cells. Cells were then centrifuged (Centrifuge 5415R, Eppendorf) at 4°C for 5 minutes at 400 rcf. 25 µl of 5x dilution of FcR Blocking reagent (Miltenyi Biotec, catalog number 130-059-901) in running Buffer (RB) (25 mM EDTA, 0.5 % BSA, 1X PBS) was added to the samples after removing the supernatant. The cells were then incubated for 10 minutes while being kept on ice. Next, 25 µl of antibody mix containing anti-CD3 APC, anti-CD4 Alexa Fluor 700, and CD8 Brilliant Violet 605 (all from Biolegend) was added to the samples. This was followed by 30 minutes of incubation at 4°C. Compensation beads were used to prepare single stains for each dye during the incubation. Post incubation, cells were washed with RB and centrifuged at 400 rcf for 5 minutes and finally taken up in 200 µl RB. 7-AAD (BioLegend) was added to the samples prior to acquiring samples for the discrimination of dead cells at a final concentration of 0.75 µg/ml. Flow cytometry was performed using LSRFortessa (BD Biosciences) and results were obtained by Cell Sorter Software version 3.1.2.6151.

1.4.4 PBMC antigen stimulation

35 PBMC samples of PID patients from time point VD2-1 (1 month after the second vaccine dose) along with 5 samples from healthy controls were first thawed using warm (37°C) RPMI 1640 medium (Corning). Consecutively, cell numbers were counted using Luna Fluorescence Cell Counter (Logos Biosystems) by taking 18µL of cell suspension and 2 µl of acridine orange-propidium iodide dye (Logos Biosystems, catalog number F23001). For antigen stimulation, thawed PBMCs were centrifuged (Eppendorf 5810R, rotor A-4-62, 18 rad) for 10 minutes at 200 rcf. Next, approximately 1.5 million cells were taken up in 250 µl warm (37°C) X-VIVO 15 media (Lonza) supplemented with 10 µM sodium pyruvate (Gibco), 1x MEM-nonessential amino acids (Gibco), 0.01mM 2-mercaptoethanol (Sigma), 2mM L-Glutamine and plated into a cell culture 48-well plate (Greiner bio-one). Following the plating, 5 µl of SARS-CoV-2 S protein S1 + S2 (BioLegend) was added to the samples at a final concentration of 1 µg/mL, and 5 µl of RPMI 1640 to unstimulated controls, and cells were left in the incubator (37°C) for 7 consecutive days. On the second day of stimulation, 50 µl of the medium was removed and stored at -20°C for IFN-γ quantification, and 300 µl of the X-VIVO 15 medium was respectively added to all the wells. On the 7th Day, cells were resuspended and transferred to 1,5 ml tubes, and the wells were washed with 2 mM EDTA-PBS solution and added to the corresponding tubes. After centrifugation for 5 minutes at 400 rcf (Centrifuge 5415R, Eppendorf), the supernatant was removed, and cells were resuspended in 1 ml of Trizol (Invitrogen- Thermo Fisher Scientific) to be kept at -80°C for RNA Isolation.

1.4.5 Total RNA isolation

The frozen stimulated and unstimulated cells kept in Trizol were removed from -80°C and thawed at room temperature. 200 µl of Chloroform (FisherScientific) was added to the thawed samples. This step was followed by vigorous vertexing of the sample to create a harmonized pink solution. After 2-3 minutes of incubation at room temperature, the samples were centrifuged (Centrifuge 5415R, Eppendorf) at 12000 rcf for 15 minutes at 4°C. Post centrifugation, the aqueous phase of the separated solution was carefully removed using a pipette and transferred into a new 1.5 ml Eppendorf tube. This was followed by an addition of 650 µl of freshly made 70% ethanol, resuspension using a pipette, and finally, transfer to

the RNeasy Mini kit column (Qiagen). Further, RNA isolation was conducted following the manufacturer's protocol (Qiagen - RNeasy mini kit), with DNase I treatment performed between the two washing steps as specified in the protocol. The RNA was eluted in 30 µL of RNase-free water (Qiagen), and concentrations were measured using a NanoDrop spectrophotometer (Thermo Fisher Scientific), yielding results ranging from 4.6 to 86.3 ng/µL. Subsequently, the RNA was stored at -80 °C.

1.4.6 RNA-based 5'-RACE protocol

To prepare an NGS (next-generation sequencing) library of TCR repertoire, the unbiased 5'RACE (Rapid amplification of cDNA ends) protocol was used, which amplifies TCR genes using one primer targeting the constant region and a universal primer concatenated to the 5'end. In this method, RNA was first reverse transcribed using reverse transcriptase enzyme with terminal transferase activity, adding additional untemplated C nucleotides to the 3' end of the cDNA. This was followed by the anchoring of a template switch oligonucleotide containing a poly (G) to the untemplated poly (C) region, allowing the reverse transcriptase to switch templates and continue the cDNA extension until the end of the template switch oligonucleotide that contains a common adaptor sequence on the 5' end. In our experiments, the 5' template switch adaptor (SmartNNNa) added UMIs (unique molecular identifiers) to the 5' end of each cDNA molecule. Two PCR reactions followed this, with semi-nested and nested primers amplifying the VDJ region. The process is illustrated in **Figure 2.** UMIs are random nucleotides labeling individual cDNA molecules, allowing us to assign each sequencing read to a particular template cDNA molecule and, therefore, help minimize amplification and sequencing errors.

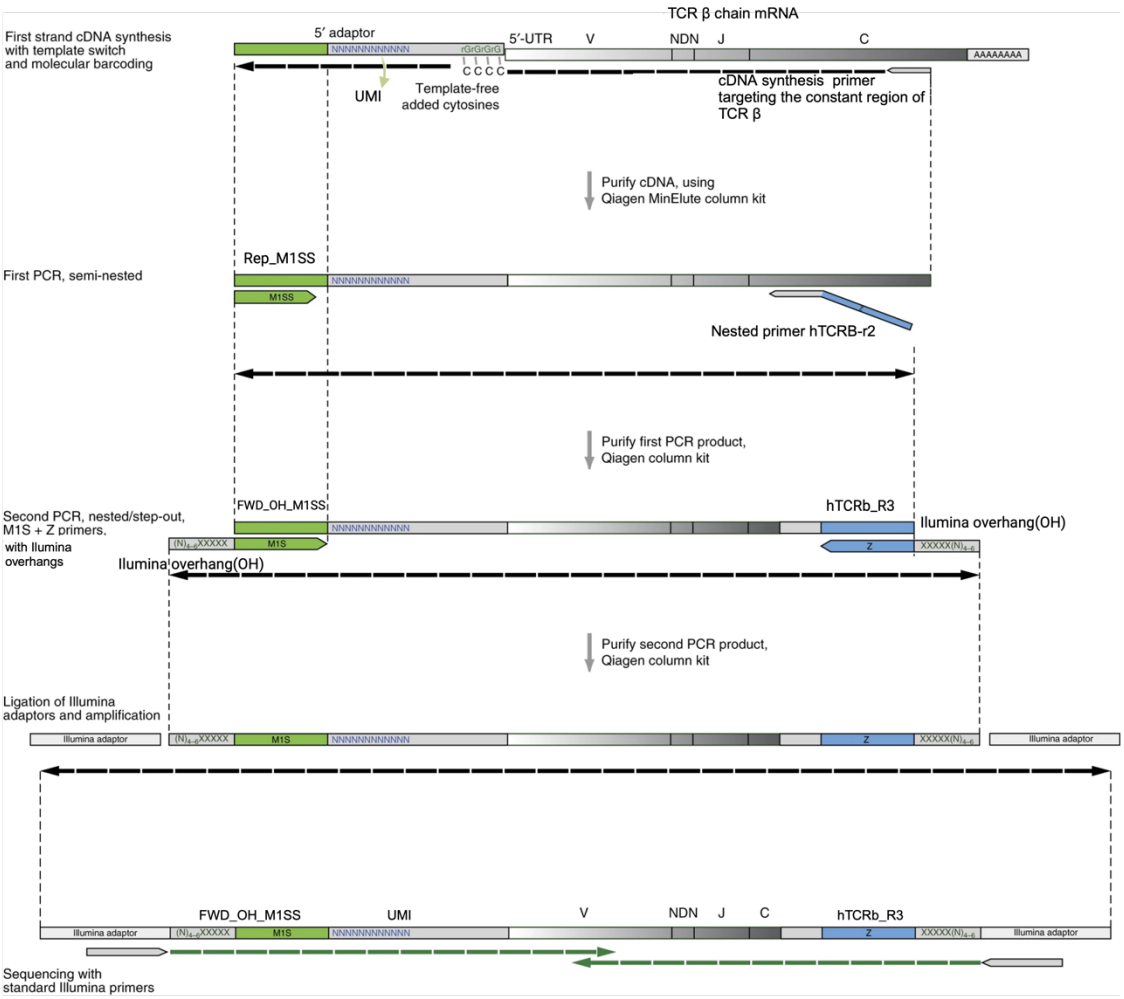

Figure 2. Schematic of the 5'RACE TCR library preparation protocol. The Figure shows the protocol steps and the region to be sequenced (Modified Turchaninova et al., 2016).

3.1.4.1 cDNA synthesis

For cDNA synthesis, RNA extracted from samples was taken from a -80 °C freezer and thawed on ice. Mix 1 was prepared in a sterile 0.2 ml reaction tube with a total volume of 8 µl **(Table 3)**. Mix 1 was then incubated at t 72°C for 3 minutes in a thermal cycler; post-incubation, the tubes were immediately chilled on ice. This step was followed by the addition of 12.5 µl of mix 2 **(Table 4)** to mix 1. The final reaction mix was gently resuspended and put into the thermal cycler at 42 °C for 60 minutes. Following the incubation, 1 µl of Uracyl DNA glycosylase (5U/µl, New England Biolabs) was added to the samples, and the samples

were once again put into the thermal cycler to incubate for 40 minutes at 37ºC. Uracyl DNA glycosylase treatment removes the residual template switch adapter, critical for accurately labeling starting cDNA molecules. Lastly, cDNA was purified with the Zymo DNA clean & concentrator kit (Zymo Research) according to the manufacturer's protocol. CDNA was eluted in 12 µl of DNA elution buffer. cDNA synthesis was done two times for each sample, and they were pooled on a single purification column (Zymo Research) to achieve desirable amounts of cDNA.

Table 3. cDNA synthesis reaction mix 1.

Component	**Amount (µl)**	**Final amount/concentration**
RNA	5	<500 ng
cDNA synthesis primer: hTCRB-r1 (10 µM)	2	1 µM
Nuclease-free water (Ambion, Thermo Scientific)	1	–

Table 4. cDNA synthesis reaction mix 2.

Component	**Amount (µl)**	**Final amount/concentration**
First-strand buffer (5x, Takara)	4	1x
DTT (20mM, Takara)	2	2 mM
5'-*template switch* adapter (10 µM) (SMARTNNNa)	2	1 µM
dNTP solution (10 mM)	2	1 mM
SMARTScribe Reverse Transcriptase (10×, Takara)	2	10 U/µl
Ribolock (40 U/µl, Thermo Scientific)	0.5	1.6 U/µl

3.1.4.2 First PCR amplification

The first semi-nested PCR reaction was carried out right after cDNA synthesis to minimize product loss. The following reagents were used for the first round of PCR amplification **(Table 5)**. The reaction was carried out in a total volume of 50 µl. PCR was performed using the parameters given in **Table 6**. PCR products were then purified using the Zymo DNA Clean & Concentrator kit (Zymo Research). The purified products were stored at 4 °C.

Table 5. First PCR amplification components and Final concentrations.

Component	Amount (µl)	Final amount/concentration
First-strand cDNA	12	–
Q5 Hot Start High Fidelity Polymerase Reaction Buffer (5x, New England Bi-olabs)	10	1x
dNTP solution (10 mM)	1	0.2 mM
Forward primer: Rep_M1SS	1	0.2 µM
Reverse primer: hTCRB-r2 (10 µM)	1	0.2 µM
Phusion Hot Start II DNA polymerase (Thermo Scientific) (2 U/µL)	0.5	0.02 U/µl
Nuclease-free water (Ambion, Thermo Scientific)	24.5	–

Table 6. First PCR program and its parameters.

Cycle	Denaturation	Annealing	Extension
1	98 °C 30 s	—	—
21	98 °C 10 s	55 °C 20 s	72 °C 50 s
1	—	—	72 °C 2 min

3.1.4.3 Second PCR amplification

The second PCR was also carried out in a volume of 50 µl, contained the components given in **Table 7**, and was carried out on the parameters in **Table 8**. The PCR product was purified within an hour after amplification, using the Zymo DNA Clean & Concentrator kit (Zymo Research), and eluted in 10 µl elution buffer.

Table 7. Second PCR amplification components and Final concentrations.

Component	Amount (µl)	Final amount/concentration
Purified first PCR product	2	–
Q5 Hot Start High Fidelity Polymerase Reaction Buffer (5x, New England Biolabs)	10	1x
dNTP solution (10 mM)	1	0.2 mM
Forward primer: Fwd_OH_M1S	1	0.2 µM
Reverse primer: hTCRb_R3+NextRev	1	0.2 µM
Phusion Hot Start II DNA polymerase (Thermo Scientific) (2 U/µL)	0.5	0.02 U/µl
Nuclease-free water (Ambion, Thermo Scientific)	34.5	–

Table 8. Second PCR program and its parameters.

Cycle	Denaturation	Annealing	Extension
1	98 °C 30 s	—	—
15	98 °C 10 s	58 °C 20 s	72 °C 50 s
1	—	—	72 °C 2 min

3.1.4.3 Sequencing library preparation

The concentration of the second PCR product was measured using the Qubit 2.0 fluorometer dsDNA with an HS Assay kit (Thermo Scientific) according to the manufacturer's protocol. For Library preparation, all second PCR products were diluted to a unified concentration of 10 ng/µl. This step was followed by indexing PCR to add Illumina adaptor indexes (Nextera (XT v2 Index Kit D kit (catalog number FC-131-2004, manufacturer Illumina)) to both ends of the samples. The reaction was carried out in a total volume of 15 µl **(Table 9)**, and the PCR reaction was performed using parameters provided in **Table 10**.

The products of the indexing PCR were further purified using AMPure XP purification beads (Beckman Coulter). For the bead purification, 9 µl of AMPure XP beads were added to 15 µl of each indexed PCR sample. The resulting solution was resuspended thoroughly using a pipette, and samples were left to incubate for 5 minutes at room temperature for maximum recovery; then, samples were placed on a magnet for two minutes to separate the beads from the solution. The clarified suspension was removed from the mixture on the magnet, leaving about 5 µl of supernatant. Furthermore, 200 µl of freshly made 70% ethanol was added to the samples, which were left to incubate for 30 seconds. Post incubation, ethanol was carefully removed. The ethanol wash was repeated a total of two times. The samples were then removed from the magnet, and 40 µl of RNase-free water (Qiagen) was added for elution, mixed 10 times with the pipette, and incubated at room temperature for 2 minutes until the solution was clarified. The samples were placed on a magnet for 1 minute to separate the beads from the solution. 35 µl of the elute was transferred to new sample tubes.

Table 9. Indexing PCR.

Component	Amount (µl)	Final amount/concentration
Purified second PCR product (10 ng/ µl)	2.5	–
2x KAPA HiFi HotStart PCR Mix (Kapa Biosystems)	7.5	1x
Nextera XT v2 Index 1 primer (i7) (Illumina)	2.5	–
Nextera XT v2 Index 2 primer (i5) (Illumina)	2.5	–

Table 10. Index PCR program and its parameters.

Cycle	Denaturation	Annealing	Extention
1	95°C 3 min	—	—
7	95 °C 3 sec	55 °C 30 s	72 °C 30 s
1	—	—	72 °C 5 min

1.4.7 Next-generation sequencing

Next-generation sequencing was carried out in the sequencing core facility laboratory of the Institute of Genomics at the University of Tartu using MiSeq (M01338) instrument using symmetric 301 bp paired-end sequencing with dual-index configuration. The sequencing kit used was MiSeq v3 600 cycles.

1.4.8 Bioinformatics analysis

The rocket cluster (HPC center, 2024) of the Centre for Scientific Computing at the University of Tartu was used for preliminary Bioinformatic analysis. FastQC (version 0.11.9, Andrews, 2014) was employed to control the quality of the sequencing data. Additionally, MultiQC (version v1.19, Ewels *et al*., 2016) was used for enhanced visualization of quality control results. MiXCR (version 4.3.2, Ewels *et al*., 2016) was used for the upstream analysis of raw data. The pipeline first aligned the raw sequencing reads against the reference database of V-, D-, J-, and C-gene segments. It then matched the tag pattern sequence and extracted UMIs, correcting sequencing and PCR errors within the barcode sequence to reduce false diversity caused by these errors. Additionally, the pipeline assembled clonotypes based on the CDR3 region, applying multiple layers of error correction, and ultimately generated a table of clonotypes for each sample.

For downstream analysis, the R programming language (version 4.3.3) was employed via the RStudio software (version 2023.12.1+402), with Immunarch (version 0.9.0, ImmunoMind Team, 2019) serving as the primary R package utilized for data analysis.

1.4.9 Enzyme-linked immunosorbent assay (ELISA)

Sample supernatants from 2 days post-stimulation of PBMCs were taken out of -20°C and thawed with the end goal of IFN-γ quantification. A dilution factor of 2 was selected for the supernatants used in the assay. The experiment was done using high-binding half-area 96 Microwell plates (Greiner bio-one), and the assay was carried out using the ELISA MAX™ Deluxe Set Human IFN-γ kit (Biolegend) and based on the manufacturer's protocol. The results were analyzed by GraphPad Prism 10.2.2.

1.5 RESULTS

1.5.1 Optimization of T-cell stimulation conditions

Flow cytometry allowed the comparison of different conditions for the proliferation of antigen-specific T-cells, including the presence and absence of human serum in the growth media. More importantly, it enabled us to assess the proliferation response to two different SARS-CoV-2 antigens: recombinant SARS-CoV-2 S Protein S1+S2 (R683A, R685A) and an S peptide pool containing immunodominant regions of the wild-type virus (124 peptides, 15-mers with 11 amino acid overlap). Proliferation was also compared between two different time points, 5 days post-stimulation **(Figure S3)** and 7 days post-stimulation **(Figure 3, 4)**.

We checked for CD4+ and CD8+ proliferating T-cells. The gating strategy can be found in the supplementary materials **(Figure S2)**.

T-cell proliferation was determined using cell trace violet staining. After each cell division, the daughter cells carry 50% of the parent cell fluorescence, allowing us to track and quantify the proliferation using flow cytometry.

Throughout the repetitions of the experiment, our results stayed consistent, and better proliferation could be observed in samples stimulated for 7 days with the protein antigen consisting of both S1 and S2 subunits of the SARS-CoV-2 spike protein.

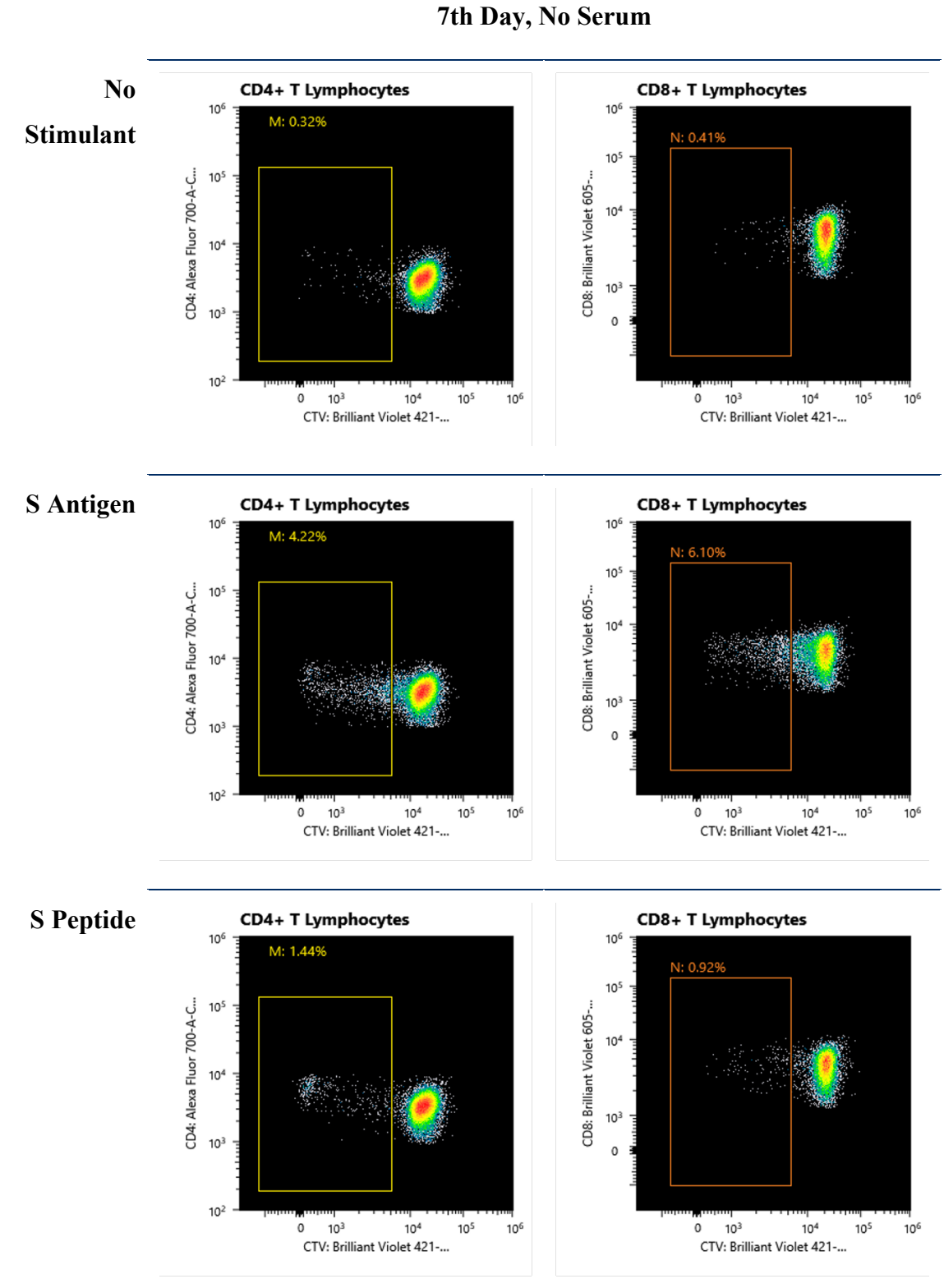

Figure 3. Flow cytometry results from the 7th-day post antigen stimulations with no human serum. The panels on the right represent the proliferation of CD4+ T-cells, while those on the left represent the proliferation of CD8+ T-cells.

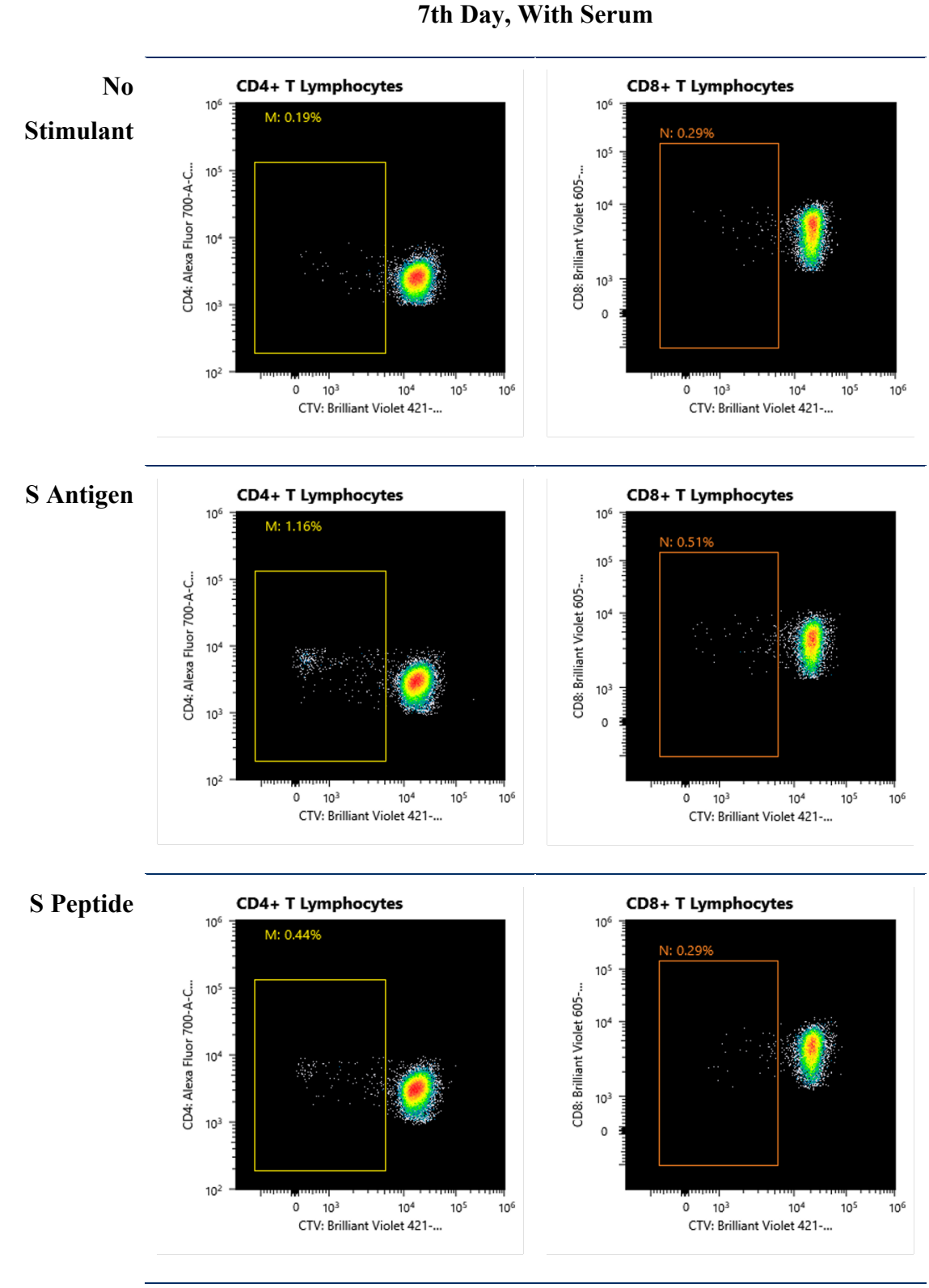

Figure 4. Flow cytometry results from the 7th-day post antigen stimulations with human serum. The panels on the right represent CD4+ T-cells, while those on the left represent CD8+ T-cells. The panels on the right represent the proliferation of CD4+ T-cells, while those on the left represent the proliferation of CD8+ T-cells.

1.5.2 Repertoire clonality

T-cell receptor repertoire clonality is defined as the number of different TCR sequences within one repertoire. One TCR clone has a unique sequence on a protein level resulting from a random VDJ recombination, and clonotype refers to all the TCRs found within a repertoire carrying a similar TCR sequence (similar clones). To have a general overview of the sizes of our repertoires, the numbers of clones and clonotypes from each repertoire were examined.

1.5.2.1 Number of clones and clonotypes

The total number of Clones in our library was 2,206,714 in all samples, and the average number of clones was 30,649. The maximum number of clones was represented in sample 31-S-Ag-1, belonging to the antibody-deficient patient group with 120,757 clones, and the minimum number of clones belonged to sample 1-S-Ag, belonging to the antibody-deficient patient group with 2355 Clones **(Figure 5)**.

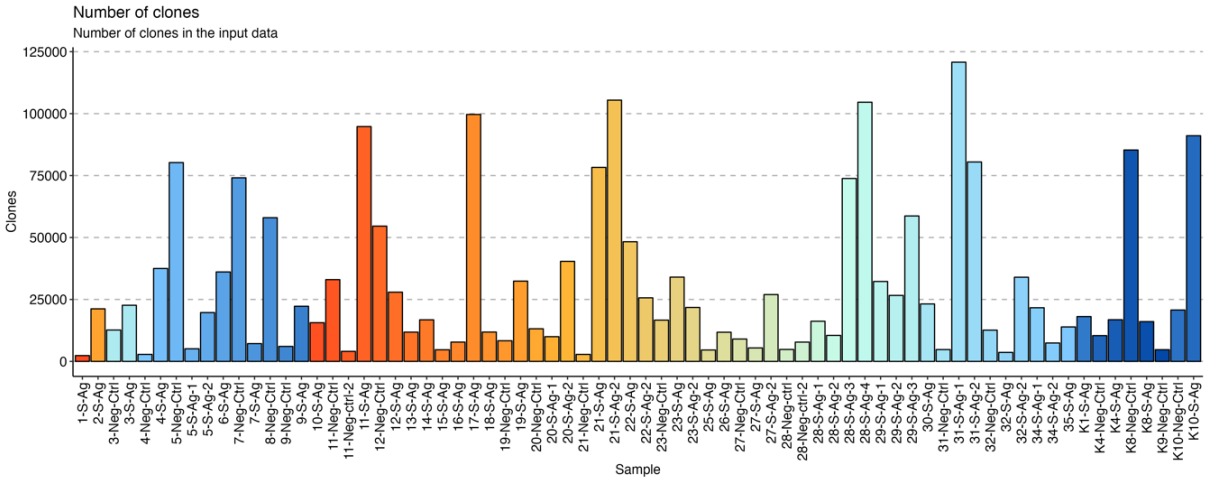

Figure 5. Number of Clones found within each repertoire. The X-axis represents the samples in our library; each sample is considered a singular repertoire. The Y-axis represents the number of clones.

The number of clonotypes represents the count of distinct T-cell receptor sequences carrying a unique CDR3 region. Each clonotype represents a unique combination of T-cell receptors

with the same CDR3 region. On average, there were 7,931 clonotypes among the samples. The maximum number of clonotypes belonged to sample 28-S-Ag-4, with 32,452 clonotypes belonging to the CVID group. The minimum number of clonotypes belonged to sample 1-S-Ag with 919 clonotypes. In total, our library represented 571,039 clonotypes **(Figure 6)**.

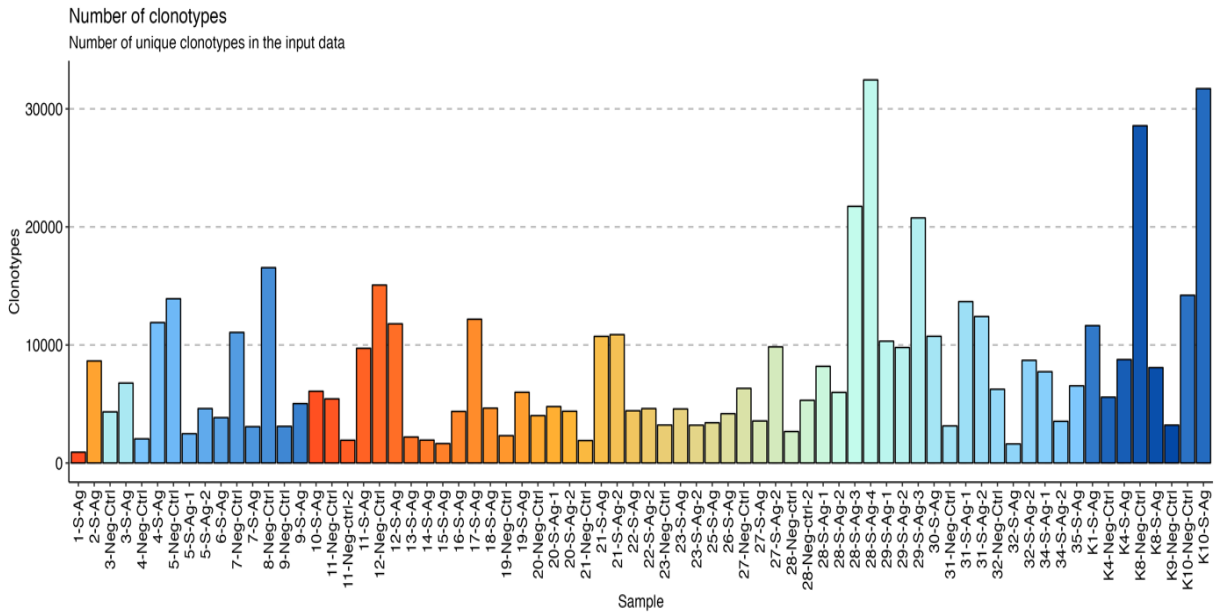

Figure 6. **Number of Clonotypes found within each repertoire.** The X-axis represents the samples in our library; each sample is considered a singular repertoire. The Y-axis represents the number of clonotypes.

1.5.2.2 Number of clonotypes within grouped data

The distribution of clonotypes within each condition was analyzed and compared to gain deeper insights into how the number of clonotypes varies across different conditions. First, the number of clonotypes among stimulated samples with S antigen and unstimulated samples was investigated **(Figure 7)**. Given the observed p-value, it was concluded that there is no statically significant difference in the number of clonotypes presented in stimulated versus unstimulated samples.

Moreover, the distribution of clonotypes among patients with different diagnoses (healthy controls, CVID, antibody deficiency, XLA) was also analyzed. Similarly, the distribution was not significantly different between the studied groups, given the p-values represented in the figure **(Figure 8)**.

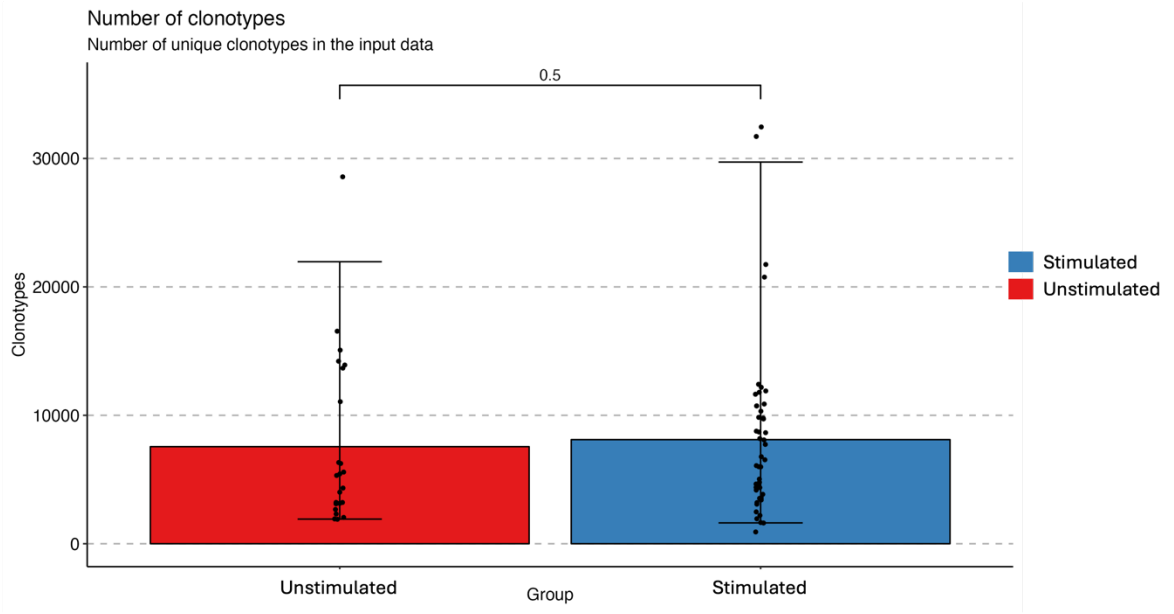

Figure 7. Distribution of clonotypes among stimulated and unstimulated samples. The X-axis represents grouped samples based on stimulation status, and the Y-axis represents the number of clonotypes in the input repertoires. P-value was calculated by the Wilcoxon rank sum test (a difference in mean rank values between two groups).

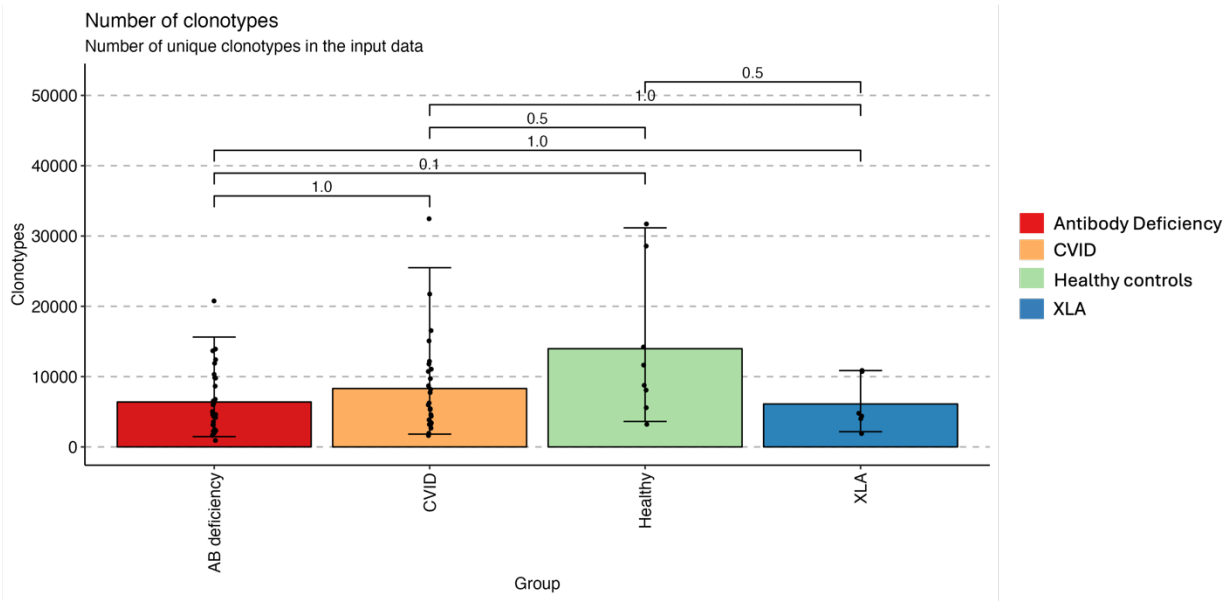

Figure 8. Distribution of clonotypes among samples with different Diagnosis. The X-axis represents grouped samples based on Diagnosis, and the Y-axis represents the number of clonotypes in the input repertoires. P-values were calculated by the Wilcoxon rank sum test (a difference in mean rank values between two groups).

1.5.2.3 Clonal proportions

Clonal proportions were also investigated to assess the diversity of the repertoires by considering the distribution of rare and abundant clonotypes within the TCR repertoires, looking into the top clonal proportions and rare clonal proportions among grouped repertoires (stimulated versus unstimulated samples and different diagnoses). This analysis is based on the number of clones within clonotypes and the frequency of those clonotypes in the repertoires. The top clonal proportion estimates the relative abundance of the most prevalent clonotypes (**Figure 9 B, D**), whereas the rare clonal proportion estimates the relative abundance for the groups of rare clonotypes with low counts (**Figure 9 A, C**).

Initially, both rare and top clonal proportions of stimulated and unstimulated samples were compared and investigated. Looking into the rare clonal proportion (**Figure 9 A**), considering that the X-axis represents the number of times a clonotype appears in each group, and the Y-axis represents the percentage that the clonotype takes up in the repertoire, it can be observed that almost 60% (~30% 2-3 and ~30% 4-10) of the repertoires fall into the abundance interval of 2-10, with no significant difference between stimulated and unstimulated samples. However, the repertoires of stimulated samples contain more clonotypes with abundances of 11-30 (p-value of 0.015). Clonotypes with counts of 31 and higher take up approximately 20% of the repertoire, with no significant difference between the stimulated and unstimulated samples. Furthermore, looking at the top clonal proportions (**Figure 9 B**), the X-axis indicates the indices of the clonotypes based on their abundance in the repertoire. The clonotype index is ordered by decreasing clonotype size. A low clonotype index indicates an expanded clonotype, whereas a high one indicates a rare clonotype group. In a way that index [1:10] shows the 10 most prevalent clonotypes in the respective repertoire, [11:100] represents the next, and so forth. The Y-axis represents the percentage that the clonotype takes up in the repertoire.

There is no statistically significant difference between stimulated and unstimulated samples. However, it can be observed that the most abundant clonotypes represent only ~10% of the respective repertoires, pointing to the diversity of the repertoire. The most frequently observed clonotypes belong to indices [101:1000] and [1001:3000], which comprise around 30% of the repertoire each.

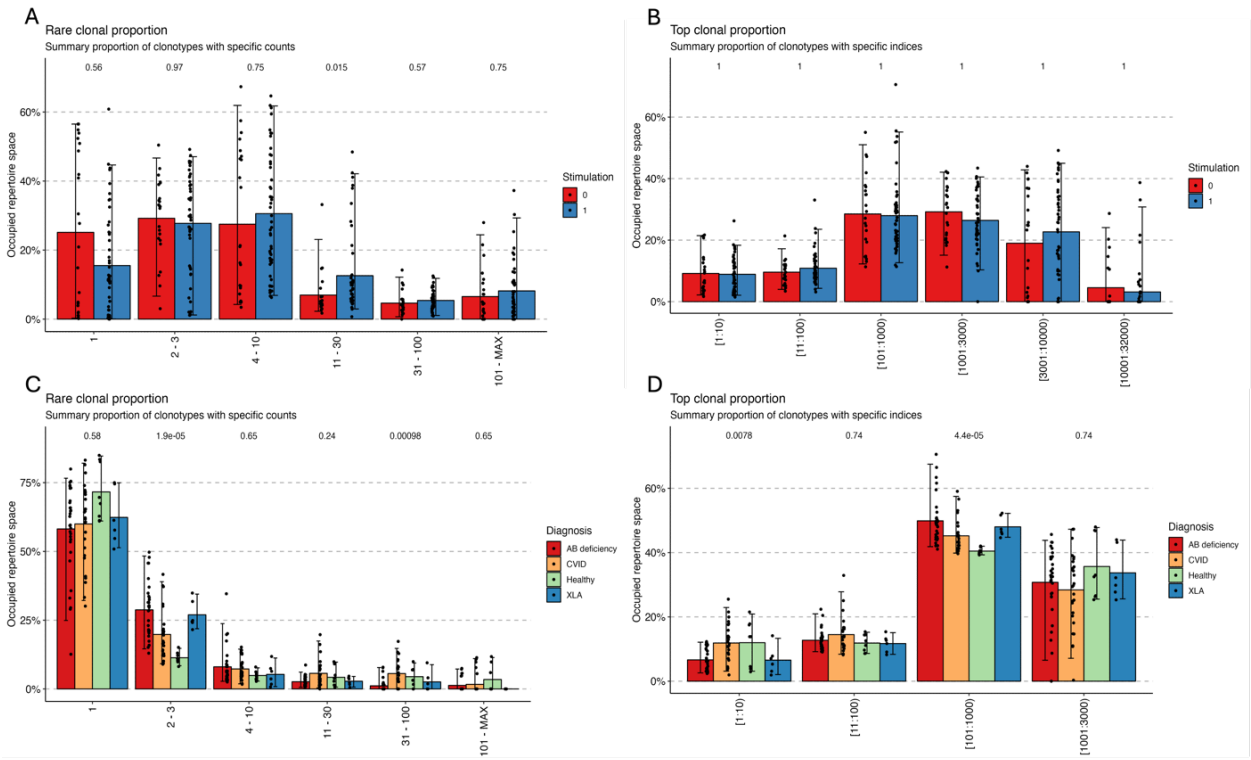

Figure 9. Representation of Top and Rare clonotypes among grouped repertoires. A: Rare clonal proportions among stimulated and unstimulated samples (0: unstimulated, 1: stimulated). The X-axis shows counts of clonotypes, and the Y-axis shows the percentage that the clonotype takes up in the repertoire. B: Top Clonal proportion among stimulated and unstimulated samples (0: unstimulated, 1: stimulated). The X-axis represents the indices of clonotypes, where the index indicates the clonotype's ranking from the most abundant (index 1) to the least abundant (index 32,000). P-values were calculated by the Wilcoxon rank sum test (a difference in mean rank values between two groups). C and D: Top and rare clonotypes among repertoires grouped by diagnosis. P-values were calculated by the Kruskal-Wallis test, which indicates that at least one sample stochastically dominates over another sample.

Next, the top and Rare clonal proportions of repertoires belonging to patients with different diagnoses were examined. For a more accurate analysis, data was downsampled to the size of the repertoire with the smallest number of clones (2355 Clones). Most repertoires across different diagnoses **(Figure 9 C)** consist of rare clonotypes (~60-70%) that have occurred only once with no statistically significant difference among the different groups. However, a statistically significant difference is observed within the rare clonotypes that have occurred

2-3 times, with repertoires of healthy individuals containing fewer of these clonotypes (p-value 1.9×10^{-5}). Statistical significance could also be observed within the repertoires of clonotypes occurring 31-100 times, with CVID patients exhibiting a greater abundance of such clonotypes and antibody-deficient patients displaying the least (p-value 0.00098).

Regarding the top clonal proportion among different diagnoses, the top 10 most prevalent clonotypes occupy less than 20% of the repertoire. CVID and healthy individuals contain more of the respective clonotypes (p-value 0.0078) (**Figure 9 D**). Clonotypes with indices [101:1000] occupy ~40-50% of respective repertoires and show another statistical significance with a p-value of 4.4×10^{-5} between antibody deficient and CVID patients versus healthy controls and XLA patients.

1.5.3 CDR3 sequence length

The length of detected CDR3 amino acids of each of the patient groups was analyzed and compared. CDR3 sequences across different patient groups and healthy controls were distributed according to their respective lengths using a histogram **(Figure 10)**. All sequences shorter than 10 amino acids and longer than 23 amino acids (outside the 95th percentile) were removed from the graph to better visualize the distribution. After the removal of the very short and very long sequences, the average amino acid length of CDR3 was 15.98, and a similar mean value was also observed within different patient groups and healthy controls (AB deficiency - 15.99, CVID - 16.00, Healthy - 16.00, XLA - 15.79).

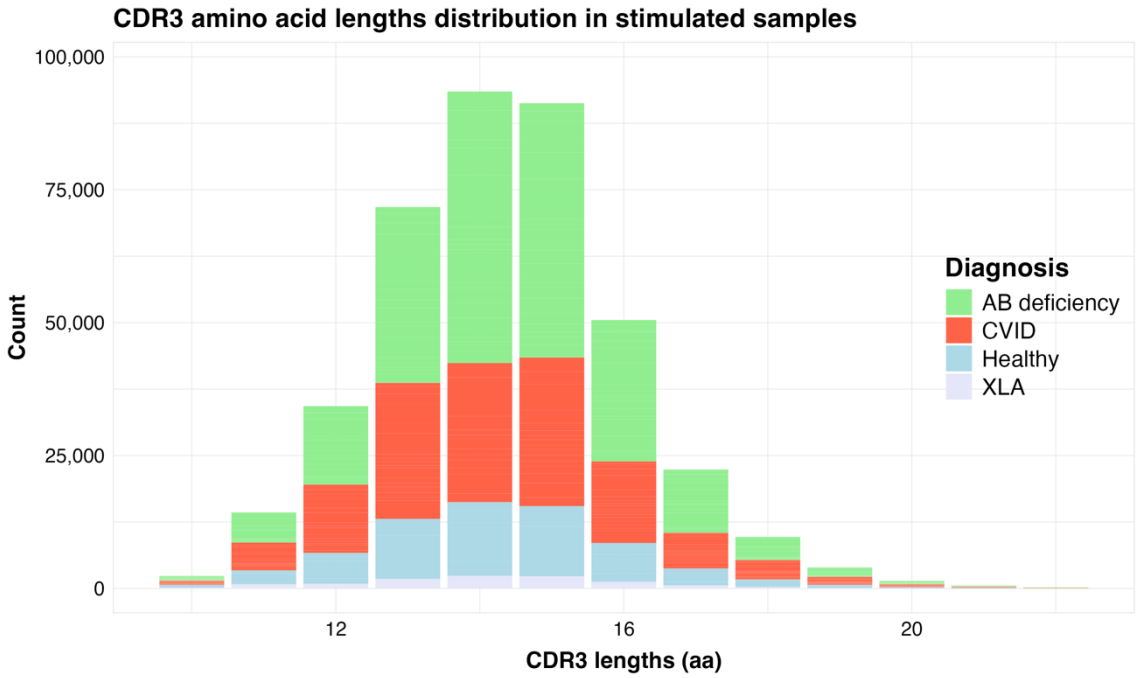

Figure 10. Distribution of CDR3 amino acid sequence length across different diagnoses in stimulated samples. The X-axis represents the CDR3 length in amino acids, and the Y-axis represents the number of sequences with the corresponding length.

1.5.4 Repertoire diversity

Repertoire Diversity was analyzed using two different indices: the D50 index and the Chao1 index.

1.5.4.1 D50 Index

The D50 index was used to indicate the percentage of unique CDR3 sequences or, in other words, clonotypes represented in 50% of the total sequencing reads, meaning that this diversity is dependent on the dominant and most prevalent clonotypes (Chaudhary & Wesemann, 2018; Lee et al., 2016). The higher the D50 index, the higher the diversity and the smaller the clonotypic expansion. Firstly, the D50 index was checked among stimulated and unstimulated samples; no statistically significant difference was observed between these two groups **(Figure 11)**. Next, the D50 diversity was investigated among repertoires belonging to different diagnoses **(Figure 12)** within the stimulated repertoires. Although the healthy controls showed a higher index, there was no statistically significant difference in D50 diversity among the different groups.

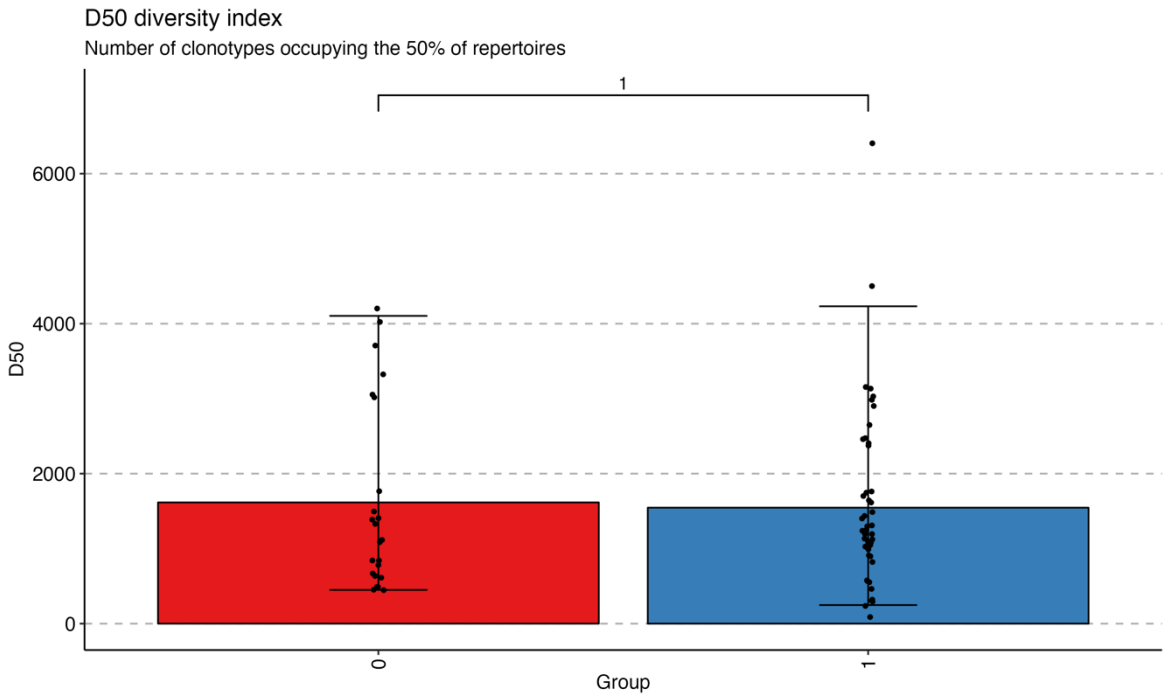

Figure 11. D50 diversity Index among stimulated and unstimulated samples. The X-axis represents the different groups compared (0: Unstimulated, 1: Stimulated). The Y-axis represents the corresponding D50 index. P-value was calculated by the Wilcoxon rank sum test (a difference in mean rank values between two groups)

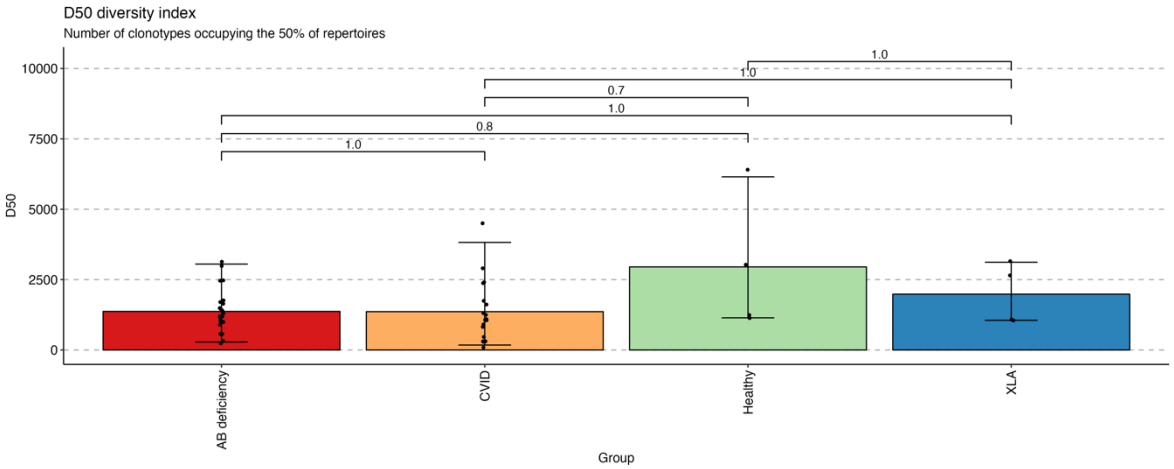

Figure 12. D50 diversity Index among different Diagnoses within stimulated repertoires. The X-axis represents the different groups compared. The Y-axis represents the corresponding D50 index. P-values were calculated by the Wilcoxon rank sum test (a difference in mean rank values between two groups).

1.5.4.2 Chao1 Index

Chao 1 index was the second index used for investigating the diversity among repertoires. Chao1 is an estimator of species richness, meaning that it provides information on the abundance of unique clones that exist within a repertoire, and it is dependent on the rare clonotypes that have occurred once or twice (Chaudhary & Wesemann, 2018; Kotagiri et al., 2022). First, the chao1 diversity was calculated and represented for stimulated and unstimulated samples, comparing the groups. No statistical significance was noted between the two **(Figure 13)**.

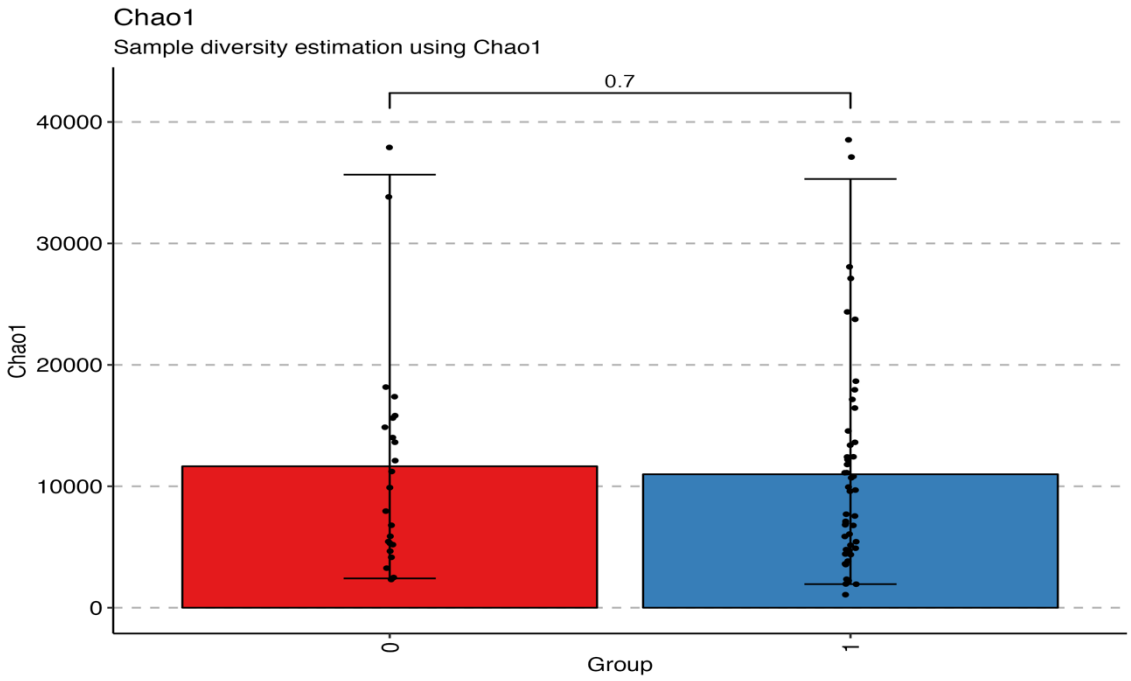

Figure 13. Chao 1 diversity Index among stimulated and unstimulated samples. The X-axis represents the different groups compared (0: Unstimulated, 1: Stimulated). The Y-axis represents the corresponding Chao1 index. P-value was calculated by the Wilcoxon rank sum test (a difference in mean rank values between two groups)

Chao 1 was then calculated for stimulated samples only across different diagnoses to compare diversity **(Figure 14)**. Significant differences were observed within patient subgroups of Healthy versus Antibody-deficient patients (p-value 0.005) in the stimulated repertoires.

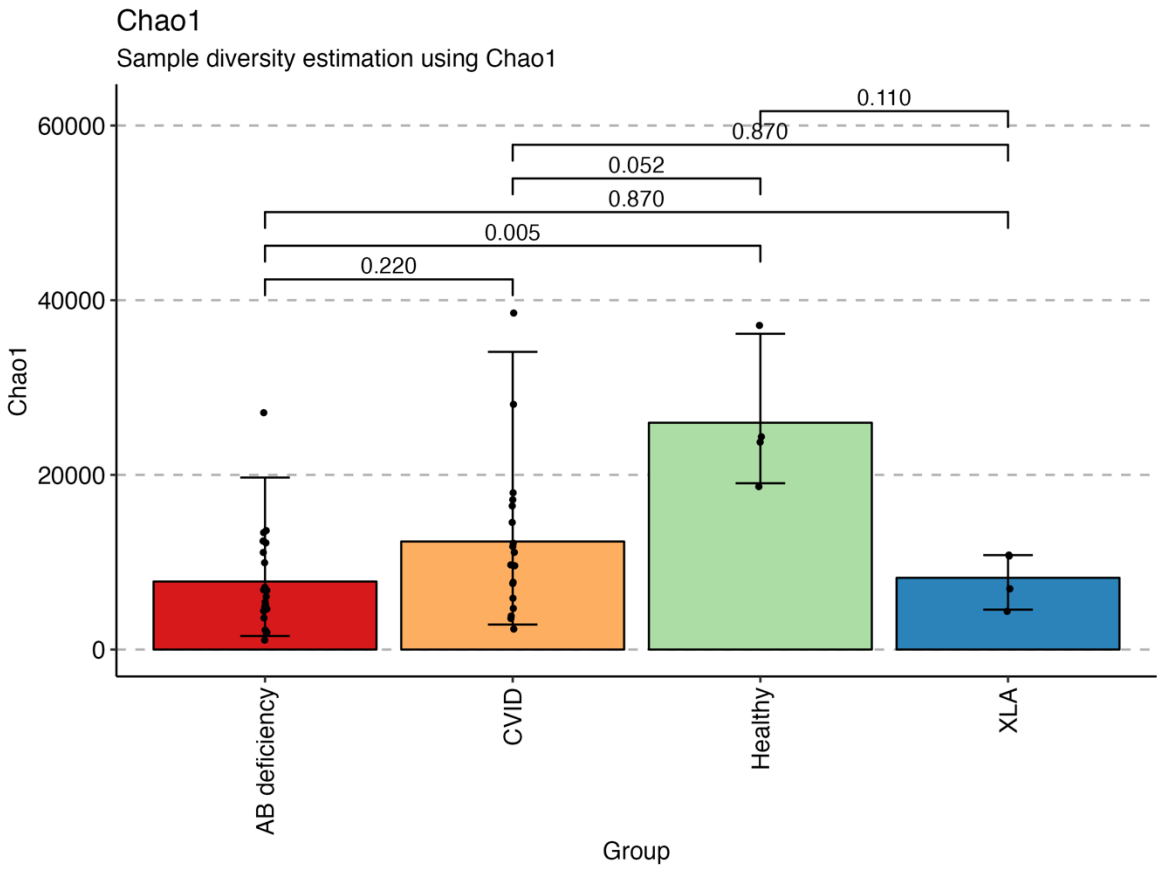

Figure 14. Chao 1 diversity Index among different stimulated samples within different Diagnoses. The X-axis represents the different groups compared. The Y-axis represents the corresponding Chao1 index. Here, only the stimulated samples are represented. P-values were calculated by the Wilcoxon rank sum test (a difference in mean rank values between two groups).

1.5.5 Gene segment usage

TCR V beta gene segment usage was investigated among patient subgroups and healthy controls to uncover if there were any disease-related patterns in how TCRs are generated concerning the v gene segments. TRBV-20-1 and TRBV-5-1 showed the most frequent usage in all subgroups.

However, seeing a statistically significant difference between TRBV-15 (p-value 0.037) **(Figure 15)** usage between the studied groups and similar patterns within each population, parallel analysis of each diagnosis versus healthy controls was also examined.

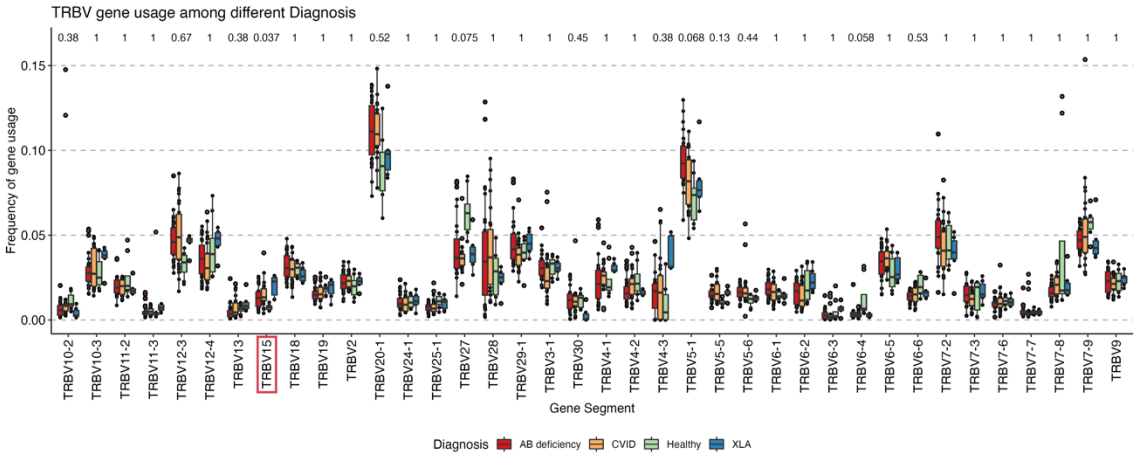

Figure 15. TRBV gene usage among patient subgroups and healthy controls. P-values were calculated by the Kruskal-Wallis test, which indicates that at least one sample stochastically dominates one other sample. The X-axis represents different TRBV gene segments, and the Y-axis represents the respective frequency of usage. P-values were calculated by the Kruskal-Wallis test, which indicates that at least one sample stochastically dominates one other sample.

Comparing healthy controls to CVID patients, significant differences were observed in the frequency of usage of TRBV15 with more frequent usage within the CVID subgroup (P-value 0.017). Conversely, TRBV27 (P-value 0.0028) and TRBV6-4 (P-value 0.02) were more frequently used in healthy controls compared to CVID **(Figure 16)**.

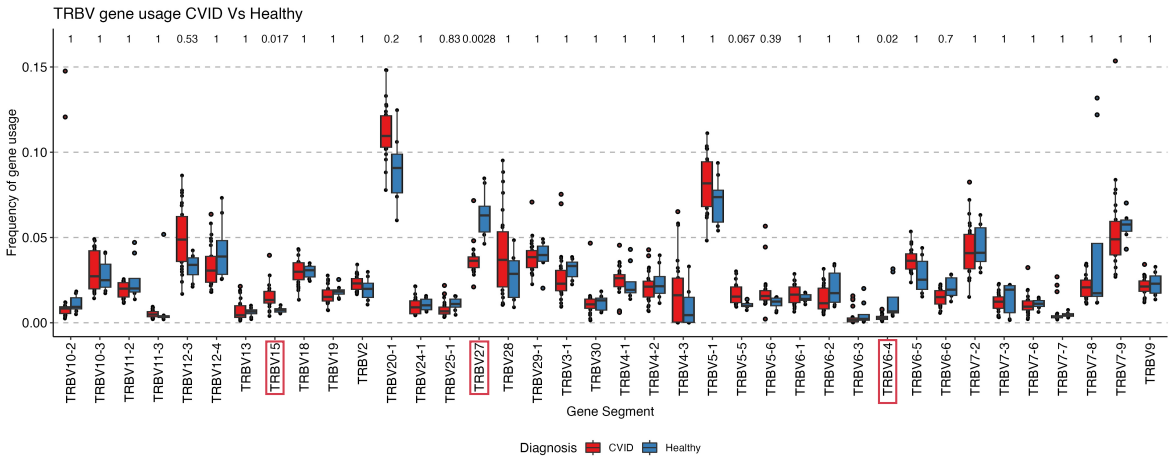

Figure 16. TRBV gene usage among CVID patients and healthy controls. P-values were calculated by the Wilcoxon rank sum test (a difference in mean rank values between two groups). The X-axis represents different TRBV gene segments, and the Y-axis represents the respective frequency of usage. P-values were calculated by the Wilcoxon rank sum test (a difference in mean rank values between two groups)

Next, the frequency of gene usage was investigated among antibody-deficient patients and healthy controls. Similarly to the previous comparison, TRBV6-4 exhibited higher usage levels in healthy controls than in the patient group (p-value 0.01). However, TRBV5-1 and TRBV5-5 were more commonly utilized in the repertoires of antibody-deficient patients (p-values 0.045 and 0.017, respectively) **(Figure 17)**.

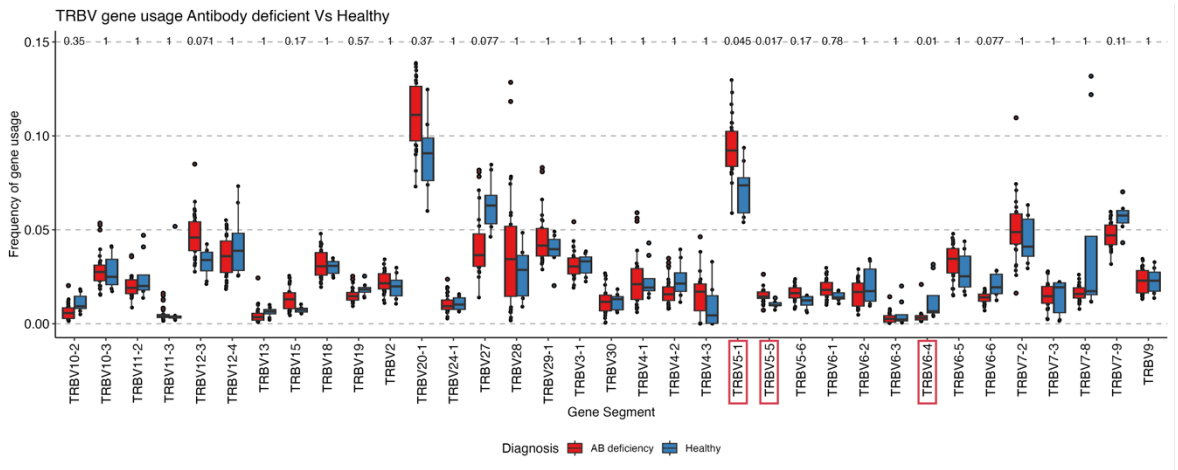

Figure 17. TRBV gene usage among antibody-deficient patients and healthy controls. P-values were calculated by the Wilcoxon rank sum test (a difference in mean rank values between two groups). The X-axis represents different TRBV gene segments, and the Y-axis represents the respective frequency of usage. P-values were calculated by the Wilcoxon rank sum test (a difference in mean rank values between two groups)

Lastly, a comparison was carried out between XLA patients and healthy controls. In contrast to the two prior findings, no statistically significant differences were noted within the respective repertoires regarding TRBV gene usage **(Figure 18)**.

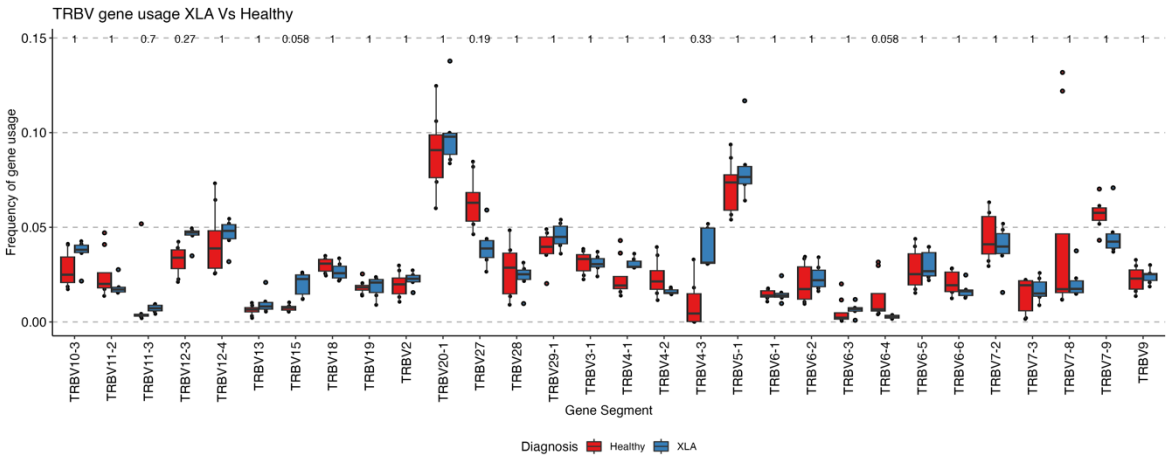

Figure 18. TRBV gene usage among XLA patients and healthy controls. P-values were calculated by the Wilcoxon rank sum test (a difference in mean rank values between two groups). The X-axis represents different TRBV gene segments, and the Y-axis represents the respective frequency of usage. P-values were calculated by the Wilcoxon rank sum test (a difference in mean rank values between two groups)

1.5.6 Clonotype tracking

Clonal expansion within the repertoires was investigated between stimulated and unstimulated samples of each patient and healthy controls to observe whether antigen stimulation led to any detectable expansions among the top ten prevalent clonotypes. Clonotype tracking was conducted for all samples, although only selected ones are presented here, with the remainder available in supplementary figures.

1.5.6.1 Clonotype tracking in healthy controls

Considerable expansion was observed within the 10 most prevalent clonotypes in repertoires of control K10 and K8 stimulated samples **(Figure 19 A, B)**. In donor K10, within the 10 most prevalent clonotypes, 7 clonotypes showed noticeable expansion, and donor K8 showed a similar trend, with 8 clonotypes demonstrating notable expansion. These expanded clonotypes, such as CASSFQPNTGELFF in K10 **(Figure 19 A)**, are hypothesized to belong to SARS-CoV-2 specific T-cells.

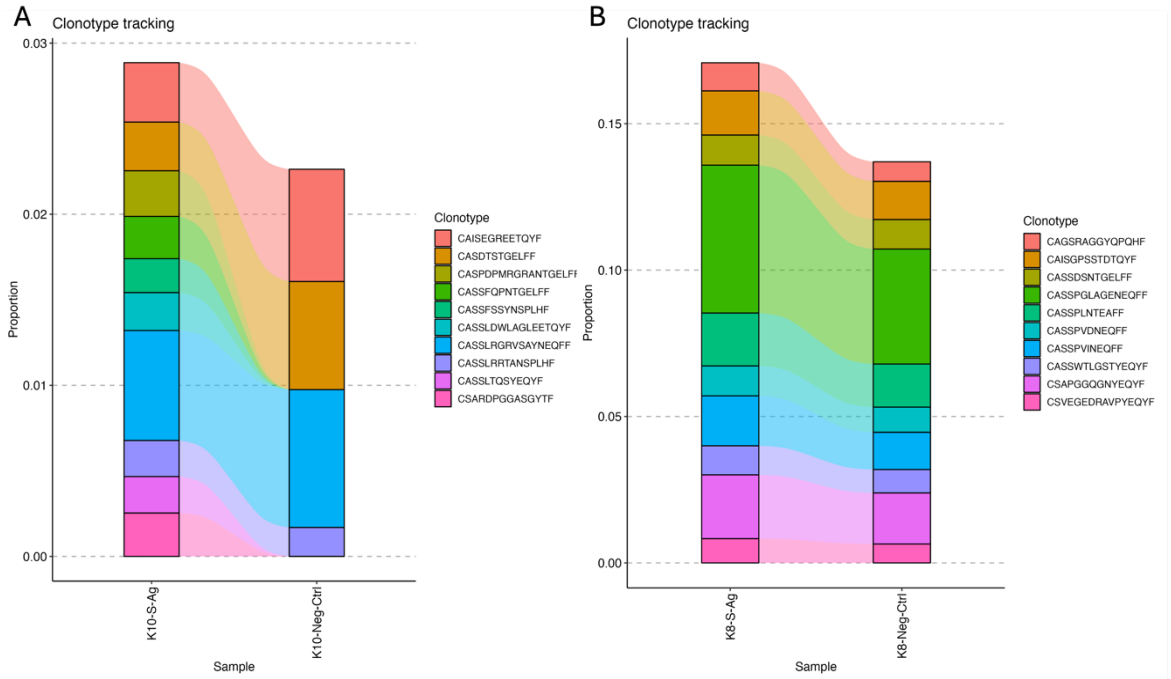

Figure 19. Clonotype tracking in k10 (A) and k8 (B) healthy controls within the top 10 most prevalent clonotypes. The X-axis represents the stimulated (S-Ag) and unstimulated sample (Neg-Ctrl) belonging to each individual. The Y-axis shows the proportion of each clonotype within the repertoire. Clonotype aa sequences are color-coded in the legends of the figures. A: Healthy control K10, B: Healthy control K8.

1.5.6.2 Clonotype tracking in XLA

Each XLA patient (PID 20 and 21) had a parallel stimulated sample. Initially, clonotype tracking was done on each sample with the respective unstimulated sample within each repertoire's 10 most prevalent clonotypes. Next, the common clonotypes between the two were compared and represented in **Figure 20.** In the case of sample number 20 **(Figure 20 A)**, expansion could be observed in CASSPPGMNTGELFF and CASSSWNNEQFF clonotypes within the 5 shared clonotypes between all three samples. Regarding sample number 21, all 6 common sequences within the 10 most prevalent clonotypes showed expansion in both stimulated samples compared to the unstimulated sample. These clonotypes are hypothesized to be of SARS-CoV-2 specific T-cells.

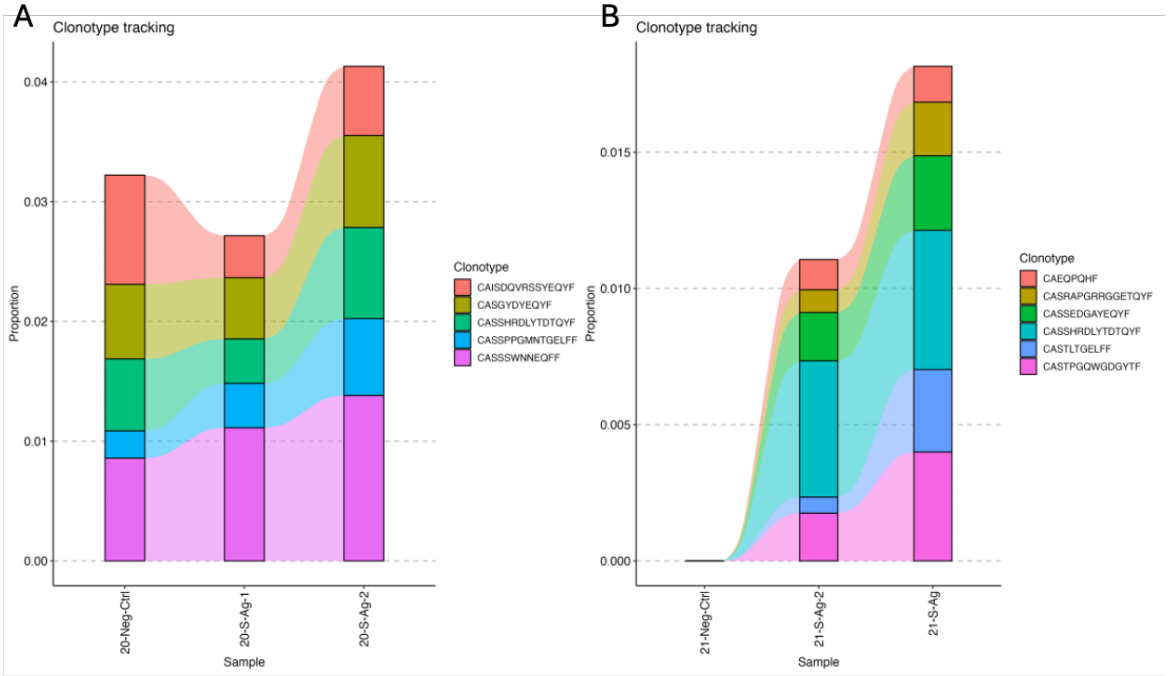

Figure 20. Clonotype tracking in XLA patient 21 and XLA patient 20. The X-axis represents the stimulated (S-Ag) and unstimulated samples (Neg-Ctrl) belonging to each individual. The Y-axis shows the proportion of each clonotype within the repertoire. Clonotype aa sequences are color-coded in the legends of the figures. A: Patient 20, B: Patient 21.

1.5.6.3 Clonotype tracking in CVID

Clonotype tracking for CVID patients was done in a similar pattern by first examining the top 10 clonotypes in parallel samples, identifying the common CDR3 amino acid sequences, and tracking those common clonotypes between the two stimulated parallels and the respective unstimulated sample as represented in **Figure 21**. In the case of sample 23 **(Figure 21 A)**, all 7 common clonotypes were expanded in both stimulated parallels compared to the unstimulated sample. This expansion is mainly recognized in CASSPIGAGPHNSPLHF, CASSPLLGVFPYEQYF, and CSAPDRGGQPQHF CDR3 amino acid sequences. With regards to sample 32, out of the 7 common clonotypes between the parallels, 4 expanded clonotypes could be pinpointed: CASSFKGLAGSSSSYNEQFF, CASSLGIDTQYF, CASSSFWDGRGSAGELFF, and CASSTTGQMGAEQYF **(Figure 21 B)**.

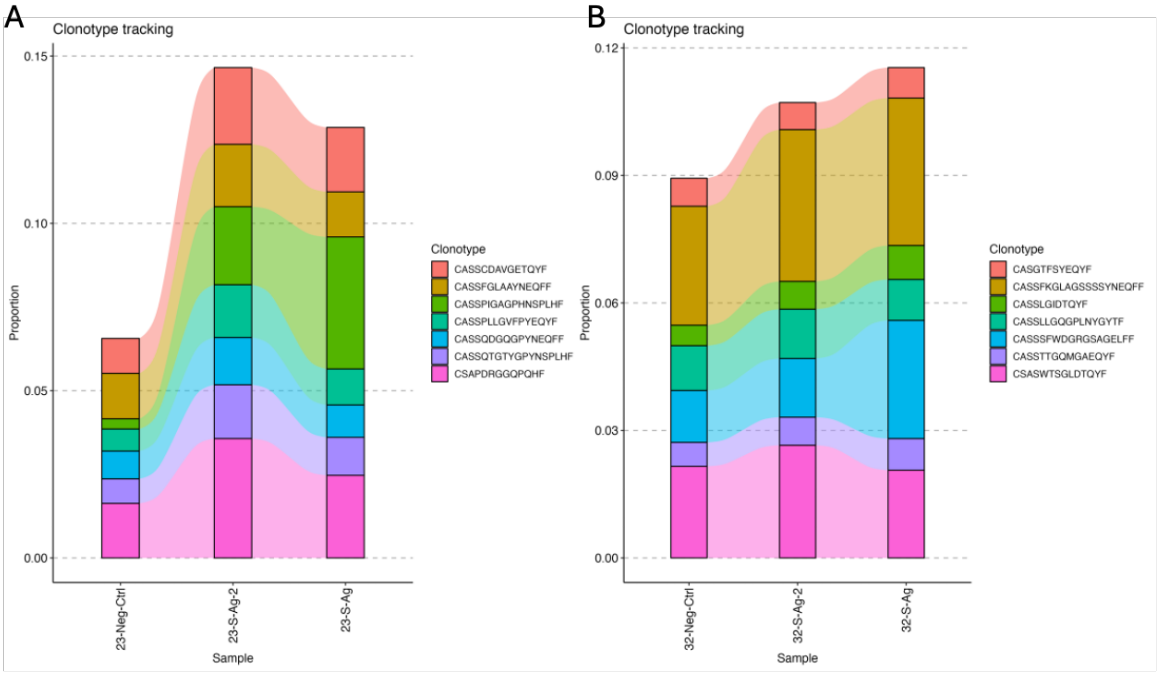

Figure 21. Clonotype tracking in CVID patients 23 and 32. The X-axis represents the stimulated (S-Ag) and unstimulated samples (Neg-Ctrl) belonging to each individual. The Y-axis shows the proportion of each clonotype within the repertoire. Clonotype aa sequences are color-coded in the legends of the figures. A: Patient 23, B: Patient 32.

A similar pattern of expansion was recognized within other repertoires belonging to CVID patients; nevertheless, the pattern was disrupted in the case of patient 28. Despite the prior examples, although common sequences could be identified within 4 stimulated and unstimulated samples, no solid expansion was observed within the common sequences **(Figure 22)**.

The inconsistency could be explained by the patient's autoimmune condition of Crohn's disease and their use of immunosuppressive medication.

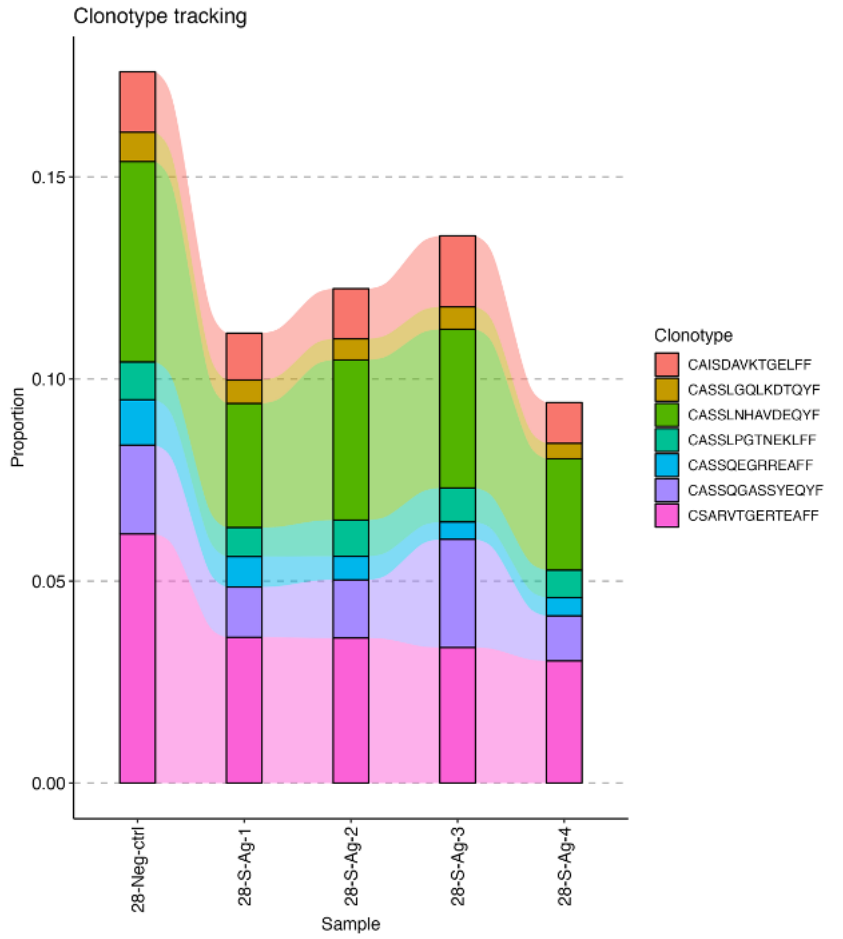

Figure 22. Clonotype tracking in CVID patients 28. The X-axis represents the stimulated (S-Ag) and unstimulated samples (Neg-Ctrl) belonging to the individual. The Y-axis shows the proportion of each clonotype within the repertoires. Clonotype aa sequences are color-coded in the legends of the figures.

1.5.6.4 Clonotype tracking in antibody deficiency

Clonotype tracking was also investigated for the antibody-deficient subgroup. Patient 5 shared 9 common clonotypes among the top 10 most prevalent clonotypes between the stimulated parallels and the unstimulated control, out of which expansion could be observed within 6 of these clonotypes in the stimulated parallels, specifically the CASSYRPTSGSGEQFF clonotype **(Figure 23 A)**. Within the repertoire of patient 27, out of the 10 most detected clonotypes, 4 clonotypes were captured within both stimulated samples and the unstimulated belonging to this patient. Out of the 4 common clonotypes, clonotype

CASLSPGVLTLHF and CASSYVPGNEQFF showed clear expansion in stimulated samples compared to the unstimulated control. The expanded clonotypes are hypothesized to be SARS-CoV-2 specific.

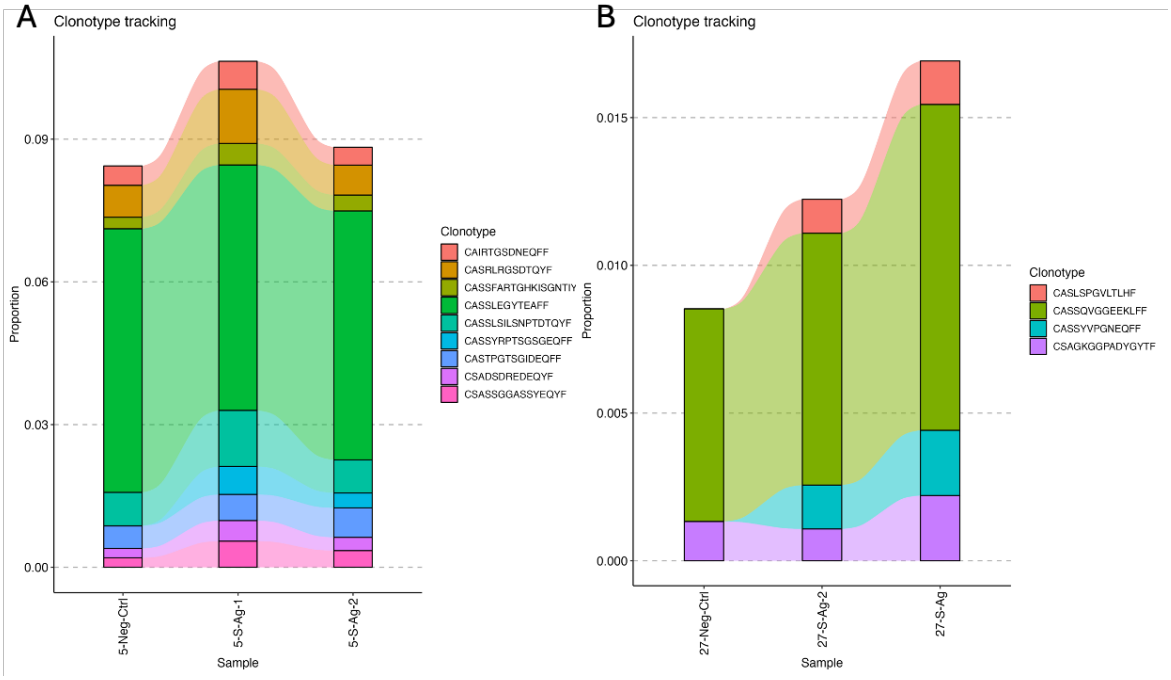

Figure 23. Clonotype tracking in antibody deficient patients 27 and 5. The X-axis represents the stimulated (S-Ag) and unstimulated samples (Neg-Ctrl) belonging to each individual. The Y-axis shows the proportion of each clonotype within the repertoire. Clonotype aa sequences are color-coded in the legends of the figures. A: Patient 5, B: Patient 27

1.6 DISCUSSION

Common variable immunodeficiency (CVID) patients are characterized by low levels of serum immunoglobulins of at least two types with possible abnormalities of both B lymphocytes and T lymphocytes, with a number of studies pointing to T-cell abnormalities (Conley et al., 1999; Giovannetti et al., 2007). Thus, it is essential to study vaccine responses in this population, as data regarding how these patients respond to vaccination is highly variable due to the complexity and variability of the disease. Studying the T-cell receptor repertoire post-vaccination would help understand the cellular response dynamics in these patients. However, their TCR repertoire is highly under-studied.

In this master's thesis, the TCR repertoire of patients with primary immunodeficiencies (CVID, XLA, selective IgG deficiencies) 6 months post the second dose of vaccination with Pfizer-BioNTech Comirnaty-BNT162b2 vaccine against COVID-19 was studied, with more focus on CVID patients.

The experiment included samples from 33 diseased individuals, 13 of which belonged to the CVID cohort, 2 to XLA, 18 to patients exhibiting selective antibody deficiencies, and 5 healthy individuals as controls. To study their TCR repertoire dynamics post-vaccination, the spike antigen-stimulated and unstimulated samples were obtained.

Furthermore, the TCR-β chain libraries were prepared using Rapid Amplification of cDNA Ends (5'RACE) with unique molecular identifiers (UMI) based on the modified method discussed by Turchaninova *et al*., 2016.

Despite the under-representation of some of the libraries due to suboptimal sequencing quality (mean phred score falling below 25 before 200bp) and under-sequencing (regarding the theoretical number of T-cells that were processed, the number of reads was relatively low), we obtained 9,627,320 total sequencing reads, out of which 7,207,398 (74.86%) were successfully aligned reads with 3,275,792 reads covering the CDR3 region (45.45% of the successfully aligned reads). These reads resulted in a total of 2,206,714 clones and 571,039 clonotypes. Despite this limitation, significant results were obtained reflecting on the repertoire characteristics of these individuals.

5'RACE with an introduction of UMIs was chosen in this work to minimize PCR amplification biases and errors associated with other methods, such as multiplex PCR. Moreover,

the choice of RNA rather than genomic DNA as the starting material allows for more sensitive detection of TCR sequences owing to higher copy numbers of RNA templates (Nguyen et al., 2011; Shugay et al., 2014; Woodsworth et al., 2013). Reportedly, DNA-based methods have shown a lowered signal-to-noise ratio due to DNA from irrelevant V and J segments that are not part of the rearranged sequences and lower amplification efficacy (Genolet et al., 2023). Furthermore, the DNA contains both TCR-β alleles, yet most T-cells express only one allele due to allelic exclusion (Genolet et al., 2023).

Few studies have been done on the T-cell receptor repertoire of CVID patients. However, there have been findings pointing at lowered diversity in the CD8+ T-cell receptor repertoire of subgroups of this disease, which is explained by the oligoclonal expansion of the late differentiated CD8+ T-cells. This has often been seen in rare subgroups of CVID with a low CD4:CD8 ratio due to CD4 lymphopenia with higher counts of CD8+ T-cells (Viallard et al., 2013; Wong et al., 2016). In this study, only a tendency for a higher chao1 diversity index was seen in healthy controls compared to CVID, pointing to a higher frequency of clonotypes with rare counts in healthy controls and possibly a more diverse repertoire. However, this observation was not statistically significant **(Figure 14)**. This could be explained by several influencing factors, including the heterogeneity of this disease, normal CD4 and CD8 T-cell counts of CVID patients within our cohort with rather ambiguous immunophenotypes, and lastly our repertoire consisting of both CD4+ and CD8+ TCR-β chain. The earlier-mentioned sequencing limitation could also influence this. Another potential limitation that may have influenced our observations regarding diversity is the absence of age integration within the analysis due to our cohort's uneven age distribution. Aging is associated with lower diversity of the repertoire.

Previous work on the TCR repertoire of ATM-deficient patients characterized by immunological abnormalities, including antibody deficiencies and lymphopenia, had shown shorter CDR3 length than healthy controls (M. Fang et al., 2022). In this study, no difference was observed in the CDR3 amino acid length distribution between the patient groups and healthy controls **(Figure 10)**. However, exploring potential changes in CDR3 length post-vaccination could provide valuable insights into the impact of vaccination on this aspect by analyzing samples prior to vaccination.

Furthermore, V gene segment usage was also examined and compared between different groups. It has been previously suggested that TCR V beta gene usage is dominated by the

germ-line locus factor of recombination machinery, and bias towards specific V gene segments might alter clonotypic expansion in response to antigens (Zvyagin et al., 2014). Other results have also suggested a particular bias toward certain rearrangements, possibly explained by thymic selection or common antigen exposures (Robins et al., 2010). This is aligned with our observations of higher frequency of TRBV-15 usage and lower TRBV-27 and TRBV6-4 in CVID patients compared to healthy controls **(Figure 16)**. Similarly, in the case of antibody-deficient patients, when compared to healthy controls, we observed more frequent use of TRBV5-1 and TRBV5-5 in the patients and less frequent use of TRBV6-4 **(Figure 17)**. However, the reason behind this phenomenon is still unknown, and further clarifications are required to explain this occurrence and bias.

Previous studies have suggested that patients with primary low B-cell counts from CVID or pharmacologic B-cell deficiencies have heightened effector and memory T-cell responses to SARS-CoV-2 after mRNA vaccination, especially with memory CD8+ T-Cells (Zonozi et al., 2023). Thus, clonotypic expansions among the 10 most prevalent clonotypes were examined between S antigen-stimulated and unstimulated samples to study the TCR dynamics post-vaccination. We failed to establish a connection between B-cell counts or anti-SARS-CoV-2 IgG found in the serum of CVID patients and T-cell expansions. However, this finding is aligned with the expansions observed in XLA patients in this work who have absent mature circulating B-cells in their blood with severe antibody deficiencies but an intact T-cell compartment (Suri *et al*., 2016).

Clonal expansions were observed in all stimulated samples of CVID patients regardless of high or low B-cell counts or IgG levels, except for patient 28 **(Figure 22)**; the inconsistency could be explained by the patient's autoimmune condition of Crohn's disease and their use of immunosuppressive medication. However, this confirms our method's applicability to study expansion, although further verifications are needed to verify the COVID-19 specificity of the expanded clones as we could not find identical aa sequences in public databases. This could be explained by the vast diversity of TCR repertoire (Robins et al., 2009), with currently available methods capturing only a limited fraction of this diversity (Genolet et al., 2023). Nevertheless, we saw a few motif similarities between our identified sequences and S-specific CDR3 aa sequences available in the VDJdb public database (Goncharov et al., 2022) **(Figure S8)**.

In conclusion, the results obtained in this work contribute to filling the massive gap in what's known about the TCR repertoire of primary immunodeficient patients, especially patients with CVID. Despite the limitations encountered, this study shed light on the repertoire characteristics of the PID patients post-vaccination included in the cohort of this study. This work provides a reasonable basis for future investigations that could lead to the development of personalized medicine in the form of SARS-CoV-2 T-cell-based vaccines for this vulnerable group of patients with B-cell impairments.

SUMMARY

In this study, we employed high-throughput sequencing to profile and characterize the dynamics of the TCR repertoire of a group of PID patients with more focus on those with CVID 6 months post-second dose of the Pfizer-BioNTech Comirnaty-BNT162b2 vaccination against COVID-19. On average, we obtained 30,649 clones and 7,931 clonotypes per sample in our repertoires, with an approximately equal distribution between the different groups in our cohort. Our repertoires mostly consisted of rare clonotypes, and the top clonotypes were scarce. This confirmed high levels of diversity within the repertoires. A relative tendency for a higher chao1 diversity was observed in the healthy controls. Looking at the CDR3 amino acid length, we report no difference between patients and healthy controls within our cohort.

A comparison of TCR V beta gene segment usage between CVID patients and healthy controls revealed a higher frequency of TRBV-15 usage and lower frequencies of TRBV-27 and TRBV6-4 in CVID patients relative to healthy controls. A similar comparison between healthy and antibody-deficient patients showed more frequent use of TRBV5-1 and TRBV5-5 in the patients and less frequent use of TRBV6-4. This finding could be associated with possible differences in the thymic selection process or common antigenic exposure.

T-cell response post-vaccination can be induced by the vaccine antigen, and the TCR repertoire dynamics can be studied. Tracking the clonal expansions among the top 10 most prevalent clonotypes between S antigen-stimulated and unstimulated samples identified possible SARS-CoV-2 specific TCR CDR3 amino acid sequences. Expansions were observed in all individuals within our cohort except for one CVID patient undergoing immunosuppressive treatment. This further approved our method for identifying specific SARS-Cov-2 TCRs; however, further verifications would be necessary. The identical expanded clonotypes were not found in public databases. However, CDR3 amino acid similarities were found between our sequences and those found in the VDJdb public database. This is significant given the considerable variability and diversity of TCR repertoires.

This work provides novel and important clues regarding the dynamics of the TCR repertoire of PID patients post-second dose of Pfizer-BioNTech Comirnaty-BNT162b2 vaccination. This lays the groundwork for a better understanding of the immune response of this vulnerable group to vaccination and the development of personalized medicine in the form of SARS-CoV-2 T-cell-based vaccines.

REFERENCES

Abraham, R. S., Marshall, J. M., Kuehn, H. S., Rueda, C. M., Gibbs, A., Guider, W., Stewart, C., Rosenzweig, S. D., Wang, H., Jean, S., Peeples, M., King, T., Hunt, W. G., Honegger, J. R., Ramilo, O., Mustillo, P. J., Mejias, A., Ardura, M. I., & Shimamura, M. (2021). Severe SARS-CoV-2 disease in the context of a NF-κB2 loss-of-function pathogenic variant. *Journal of Allergy and Clinical Immunology*, *147*(2). https://doi.org/10.1016/j.jaci.2020.09.020

Amaya-Uribe, L., Rojas, M., Azizi, G., Anaya, J. M., & Gershwin, M. E. (2019). Primary immunodeficiency and autoimmunity: A comprehensive review. In *Journal of Autoimmunity* (Vol. 99). https://doi.org/10.1016/j.jaut.2019.01.011

Ameratunga, R., Longhurst, H., Steele, R., Lehnert, K., Leung, E., Brooks, A. E. S., & Woon, S. T. (2021). Common Variable Immunodeficiency Disorders, T-Cell Responses to SARS-CoV-2 Vaccines, and the Risk of Chronic COVID-19. *The Journal of Allergy and Clinical Immunology: In Practice*, *9*(10), 3575–3583. https://doi.org/10.1016/J.JAIP.2021.06.019

Arroyo-Sánchez, D., Cabrera-Marante, O., Laguna-Goya, R., Almendro-Vázquez, P., Carretero, O., Gil-Etayo, F. J., Suàrez-Fernández, P., Pérez-Romero, P., Rodríguez de Frías, E., Serrano, A., Allende, L. M., Pleguezuelo, D., & Paz-Artal, E. (2022). Immunogenicity of Anti-SARS-CoV-2 Vaccines in Common Variable Immunodeficiency. *Journal of Clinical Immunology*, *42*(2). https://doi.org/10.1007/s10875-021-01174-5

Bitzenhofer, M., Suter-Riniker, F., Moor, M. B., Sidler, D., Horn, M. P., Gschwend, A., Staehelin, C., Rauch, A., Helbling, A., & Jörg, L. (2022). Humoral response to mRNA vaccines against SARS-CoV-2 in patients with humoral immunodeficiency disease. *PLoS ONE*, *17*(6 June). https://doi.org/10.1371/journal.pone.0268780

Blanco-Melo, D., Nilsson-Payant, B. E., Liu, W. C., Uhl, S., Hoagland, D., Møller, R., Jordan, T. X., Oishi, K., Panis, M., Sachs, D., Wang, T. T., Schwartz, R. E., Lim, J. K., Albrecht, R. A., & tenOever, B. R. (2020). Imbalanced Host Response to SARS-CoV-2 Drives Development of COVID-19. *Cell*, *181*(5). https://doi.org/10.1016/j.cell.2020.04.026

Bonilla, F. A., & Geha, R. S. (2009). Common Variable Immunodeficiency. *Pediatric Research 2009 65:7*, *65*(7), 13–19. https://doi.org/10.1203/pdr.0b013e31819dbf88

Bonilla, F. A., Khan, D. A., Ballas, Z. K., Chinen, J., Frank, M. M., Hsu, J. T., Keller, M., Kobrynski, L. J., Komarow, H. D., Mazer, B., Nelson, R. P., Orange, J. S., Routes, J. M., Shearer, W. T., Sorensen, R. U., Verbsky, J. W., Bernstein, D. I., Blessing-Moore, J., Lang, D., … Wallace, D. (2014). Practice parameter for the diagnosis and management of primary immunodeficiency. *Journal of Allergy and Clinical Immunology*, *136*(5). https://doi.org/10.1016/j.jaci.2015.04.049

Bousfiha, A., Jeddane, L., Al-Herz, W., Ailal, F., Casanova, J. L., Chatila, T., Conley, M. E., Cunningham-Rundles, C., Etzioni, A., Franco, J. L., Gaspar, H. B., Holland, S. M., Klein, C., Nonoyama, S., Ochs, H. D., Oksenhendler, E., Picard, C., Puck, J. M., Sullivan, K. E., & Tang, M. L. K. (2015). The 2015 IUIS Phenotypic Classification for Primary Immunodeficiencies. *Journal of Clinical Immunology*, *35*(8). https://doi.org/10.1007/s10875-015-0198-5

Bradley, P., & Thomas, P. G. (2019). Using T Cell Receptor Repertoires to Understand the Principles of Adaptive Immune Recognition. In *Annual Review of Immunology* (Vol. 37). https://doi.org/10.1146/annurev-immunol-042718-041757

Brandtzaeg, P. (2015). Immunobiology of the Tonsils and Adenoids. *Mucosal Immunology: Fourth Edition*, *2–2*, 1985–2016. https://doi.org/10.1016/B978-0-12-415847-4.00103-8

Braun, J., Loyal, L., Frentsch, M., Wendisch, D., Georg, P., Kurth, F., Hippenstiel, S., Dingeldey, M., Kruse, B., Fauchere, F., Baysal, E., Mangold, M., Henze, L., Lauster, R., Mall, M. A., Beyer, K., Röhmel, J., Voigt, S., Schmitz, J., … Thiel, A. (2020). SARS-CoV-2-reactive T cells in healthy donors and patients with COVID-19. *Nature*, *587*(7833). https://doi.org/10.1038/s41586-020-2598-9

Buchholz, V. R., & Busch, D. H. (2019). Back to the Future: Effector Fate during T Cell Exhaustion. In *Immunity* (Vol. 51, Issue 6). https://doi.org/10.1016/j.immuni.2019.11.007

Cagigi, A., & Loré, K. (2021). Immune Responses Induced by mRNA Vaccination in Mice, Monkeys and Humans. *Vaccines*, *9*(1), 1–14. https://doi.org/10.3390/VACCINES9010061

Cascella, M., Rajnik, M., Cuomo, A., Dulebohn, S. C., & Di Napoli, R. (2023a). Features, Evaluation, and Treatment of Coronavirus (COVID-19). *StatPearls*. https://www.ncbi.nlm.nih.gov/books/NBK554776/

Cascella, M., Rajnik, M., Cuomo, A., Dulebohn, S. C., & Di Napoli, R. (2023b). Features, Evaluation, and Treatment of Coronavirus (COVID-19). *StatPearls*. https://www.ncbi.nlm.nih.gov/books/NBK554776/

Chaudhary, N., & Wesemann, D. R. (2018). Analyzing immunoglobulin repertoires. In *Frontiers in Immunology* (Vol. 9, Issue MAR). https://doi.org/10.3389/fimmu.2018.00462

Conley, M. E., Notarangelo, L. D., & Etzioni, A. (1999). Diagnostic criteria for primary immunodeficiencies. Representing PAGID (Pan-American Group for Immunodeficiency) and ESID (European Society for Immunodeficiencies). *Clinical Immunology (Orlando, Fla.)*, *93*(3).

Corey, L., Mascola, J. R., Fauci, A. S., & Collins, F. S. (2020). A strategic approach to COVID-19 vaccine R&D. *Science (New York, N.Y.)*, *368*(6494), 948–950. https://doi.org/10.1126/SCIENCE.ABC5312

Covid-19 vaktsiinid | Ravimiamet. (n.d.). Retrieved March 20, 2024, from https://ravimiamet.ee/ravimid-ja-ohutus/covid-19/covid-19-vaktsiinid

Crotty, S. (2019). T Follicular Helper Cell Biology: A Decade of Discovery and Diseases. *Immunity*, *50*(5), 1132–1148. https://doi.org/10.1016/J.IMMUNI.2019.04.011

Cunningham-Rundles, C., & Ponda, P. P. (2005). Molecular defects in T- and B-cell primary immunodeficiency diseases. In *Nature Reviews Immunology* (Vol. 5, Issue 11). https://doi.org/10.1038/nri1713

da Rosa Mesquita, R., Francelino Silva Junior, L. C., Santos Santana, F. M., Farias de Oliveira, T., Campos Alcântara, R., Monteiro Arnozo, G., Rodrigues da Silva Filho, E., Galdino dos Santos, A. G., Oliveira da Cunha, E. J., Salgueiro de Aquino, S. H., & Freire de Souza, C. D. (2021). Clinical manifestations of COVID-19 in the general population: systematic review. *Wiener Klinische Wochenschrift*, *133*(7–8), 377–382. https://doi.org/10.1007/S00508-020-01760-4/TABLES/2

Davis, M. M., & Bjorkman, P. J. (1988). Erratum: T-cell antigen receptor genes and T-cell recognition (Nature (1988) 334 (395-402)). In *Nature* (Vol. 335, Issue 6192). https://doi.org/10.1038/335744b0

Dudakov, J. A., Hanash, A. M., & Van Den Brink, M. R. M. (2015). Interleukin-22: Immunobiology and pathology. In *Annual Review of Immunology* (Vol. 33). https://doi.org/10.1146/annurev-immunol-032414-112123

Elsner, R. A., & Shlomchik, M. J. (2020). Germinal Center and Extrafollicular B Cell Responses in Vaccination, Immunity, and Autoimmunity. In *Immunity* (Vol. 53, Issue 6). https://doi.org/10.1016/j.immuni.2020.11.006

Esakandari, H., Nabi-Afjadi, M., Fakkari-Afjadi, J., Farahmandian, N., Miresmaeili, S.-M., & Bahreini, E. (n.d.). *A comprehensive review of COVID-19 characteristics*. https://doi.org/10.1186/s12575-020-00128-2

Fang, E., Liu, X., Li, M., Zhang, Z., Song, L., Zhu, B., Wu, X., Liu, J., Zhao, D., & Li, Y. (2022). Advances in COVID-19 mRNA vaccine development. *Signal Transduction and Targeted Therapy*, *7*(1). https://doi.org/10.1038/S41392-022-00950-Y

Fang, M., Su, Z., Abolhassani, H., Zhang, W., Jiang, C., Cheng, B., Luo, L., Wu, J., Wang, S., Lin, L., Wang, X., Wang, L., Aghamohammadi, A., Li, T., Zhang, X., Hammarström, L., & Liu, X. (2022). T Cell Repertoire Abnormality in Immunodeficiency Patients with DNA Repair and Methylation Defects. *Journal of Clinical Immunology*, *42*(2). https://doi.org/10.1007/s10875-021-01178-1

Fink, K. (2019). Can we improve vaccine efficacy by targeting T and B cell repertoire convergence? In *Frontiers in Immunology* (Vol. 10, Issue FEB). https://doi.org/10.3389/fimmu.2019.00110

Fischer, A., Provot, J., Jais, J. P., Alcais, A., Mahlaoui, N., Adoue, D., Aladjidi, N., Amoura, Z., Arlet, P., Armari-Alla, C., Bader-Meunier, B., Barlogis, V., Bayart, S., Beaurain, B., Bertrand, Y., Bienvenu, B., Blanche, S., Bodet, D., Bonnotte, B., … Viallard, J. F. (2017). Autoimmune and inflammatory manifestations occur frequently in patients with primary immunodeficiencies. *Journal of Allergy and Clinical Immunology*, *140*(5), 1388-1393.e8. https://doi.org/10.1016/J.JACI.2016.12.978

Fudenberg, H., Good, R. A., Goodman, H. C., Hitzig, W., Kunkel, H. G., Roitt, I. M., Rosen, F. S., Rowe, D. S., Seligmann, M., & Soothill, J. R. (1971). PRIMARY

IMMUNODEFICIENCIES Report of a World Health Organization Committee. *Pediatrics*, *47*(5), 927–946. https://doi.org/10.1542/PEDS.47.5.927

Genolet, R., Bobisse, S., Chiffelle, J., Arnaud, M., Petremand, R., Queiroz, L., Michel, A., Reichenbach, P., Cesbron, J., Auger, A., Baumgaertner, P., Guillaume, P., Schmidt, J., Irving, M., Kandalaft, L. E., Speiser, D. E., Coukos, G., & Harari, A. (2023). TCR sequencing and cloning methods for repertoire analysis and isolation of tumor-reactive TCRs. *Cell Reports Methods*, *3*(4). https://doi.org/10.1016/j.crmeth.2023.100459

Giovannetti, A., Pierdominici, M., Mazzetta, F., Marziali, M., Renzi, C., Mileo, A. M., De Felice, M., Mora, B., Esposito, A., Carello, R., Pizzuti, A., Paggi, M. G., Paganelli, R., Malorni, W., & Aiuti, F. (2007). Unraveling the Complexity of T Cell Abnormalities in Common Variable Immunodeficiency. *The Journal of Immunology*, *178*(6). https://doi.org/10.4049/jimmunol.178.6.3932

Goncharov, M., Bagaev, D., Shcherbinin, D., Zvyagin, I., Bolotin, D., Thomas, P. G., Minervina, A. A., Pogorelyy, M. V., Ladell, K., McLaren, J. E., Price, D. A., Nguyen, T. H. O., Rowntree, L. C., Clemens, E. B., Kedzierska, K., Dolton, G., Rius, C. R., Sewell, A., Samir, J., … Shugay, M. (2022). VDJdb in the pandemic era: a compendium of T cell receptors specific for SARS-CoV-2. In *Nature Methods*. https://doi.org/10.1038/s41592-022-01578-0

Grifoni, A., Weiskopf, D., Ramirez, S. I., Mateus, J., Dan, J. M., Moderbacher, C. R., Rawlings, S. A., Sutherland, A., Premkumar, L., Jadi, R. S., Marrama, D., de Silva, A. M., Frazier, A., Carlin, A. F., Greenbaum, J. A., Peters, B., Krammer, F., Smith, D. M., Crotty, S., & Sette, A. (2020). Targets of T Cell Responses to SARS-CoV-2 Coronavirus in Humans with COVID-19 Disease and Unexposed Individuals. *Cell*, *181*(7). https://doi.org/10.1016/j.cell.2020.05.015

Guchelaar, N. A. D., van Laar, J. A. M., Hermans, M. A. W., van der Houwen, T. B., Atmaca, S., van Maaren, M. S., Brkic, Z., van Daele, P. L. A., Dalm, V. A. S. H., van Hagen, P. M., & Rombach, S. M. (2021). Characteristics of COVID-19 infection and antibody formation in patients known at a tertiary immunology department. *Journal of Translational Autoimmunity*, *4*. https://doi.org/10.1016/j.jtauto.2021.100084

Hagin, D., Freund, T., Navon, M., Halperin, T., Adir, D., Marom, R., Levi, I., Benor, S., Alcalay, Y., & Freund, N. T. (2021). Immunogenicity of Pfizer-BioNTech COVID-19

vaccine in patients with inborn errors of immunity. *Journal of Allergy and Clinical Immunology*, *148*(3). https://doi.org/10.1016/j.jaci.2021.05.029

Hartenian, E., Nandakumar, D., Lari, A., Ly, M., Tucker, J. M., & Glaunsinger, B. A. (2020). The molecular virology of coronaviruses. *The Journal of Biological Chemistry*, *295*(37), 12910. https://doi.org/10.1074/JBC.REV120.013930

Hartmann, E., Graefe, H., Hopert, A., Pries, R., Rothenfusser, S., Poeck, H., Mack, B., Endres, S., Hartmann, G., & Wollenberg, B. (2006). Analysis of plasmacytoid and myeloid dendritic cells in nasal epithelium. *Clinical and Vaccine Immunology*, *13*(11), 1278–1286. https://doi.org/10.1128/CVI.00172-06

Hu, B., Guo, H., Zhou, P., & Shi, Z. L. (2020). Characteristics of SARS-CoV-2 and COVID-19. *Nature Reviews Microbiology 2020 19:3*, *19*(3), 141–154. https://doi.org/10.1038/s41579-020-00459-7

Hurme, A., Jalkanen, P., Marttila-Vaara, M., Heroum, J., Jokinen, H., Vara, S., Liedes, O., Lempainen, J., Melin, M., Julkunen, I., & Kainulainen, L. (2023). T cell immunity following COVID-19 vaccination in adult patients with primary antibody deficiency – a 22-month follow-up. *Frontiers in Immunology*, *14*. https://doi.org/10.3389/fimmu.2023.1146500

Juno, J. A., Tan, H. X., Lee, W. S., Reynaldi, A., Kelly, H. G., Wragg, K., Esterbauer, R., Kent, H. E., Batten, C. J., Mordant, F. L., Gherardin, N. A., Pymm, P., Dietrich, M. H., Scott, N. E., Tham, W. H., Godfrey, D. I., Subbarao, K., Davenport, M. P., Kent, S. J., & Wheatley, A. K. (2020). Humoral and circulating follicular helper T cell responses in recovered patients with COVID-19. *Nature Medicine*, *26*(9). https://doi.org/10.1038/s41591-020-0995-0

Kinoshita, H., Durkee-Shock, J., Jensen-Wachspress, M., Kankate, V. V., Lang, H., Lazarski, C. A., Keswani, A., Webber, K. C., Montgomery-Recht, K., Walkiewicz, M., Notarangelo, L. D., Burbelo, P. D., Fuss, I., Cohen, J. I., Bollard, C. M., & Keller, M. D. (2021). Robust Antibody and T Cell Responses to SARS-CoV-2 in Patients with Antibody Deficiency. *Journal of Clinical Immunology*, *41*(6). https://doi.org/10.1007/s10875-021-01046-y

Kotagiri, P., Mescia, F., Rae, W. M., Bergamaschi, L., Tuong, Z. K., Turner, L., Hunter, K., Gerber, P. P., Hosmillo, M., Hess, C., Clatworthy, M. R., Goodfellow, I. G., Matheson,

N. J., McKinney, E. F., Wills, M. R., Gupta, R. K., Bradley, J. R., Bashford-Rogers, R. J. M., Lyons, P. A., & Smith, K. G. C. (2022). B cell receptor repertoire kinetics after SARS-CoV-2 infection and vaccination. *Cell Reports*, *38*(7). https://doi.org/10.1016/j.celrep.2022.110393

Lam, J. H., Smith, F. L., & Baumgarth, N. (2020). B cell activation and response regulation during viral Infections. *Viral Immunol.*, *33*(4), 294–306. https://doi.org/10.1089/vim.2019.0207

Lee, Y. N., Frugoni, F., Dobbs, K., Tirosh, I., Du, L., Ververs, F. A., Ru, H., De Bruin, L. O., Adeli, M., Bleesing, J. H., Buchbinder, D., Butte, M. J., Cancrini, C., Chen, K., Choo, S., Elfeky, R. A., Finocchi, A., Fuleihan, R. L., Gennery, A. R., … Notarangelo, L. D. (2016). Characterization of T and B cell repertoire diversity in patients with RAG deficiency. *Science Immunology*, *1*(6). https://doi.org/10.1126/sciimmunol.aah6109

Liu, H., Pan, W., Tang, C., Tang, Y., Wu, H., Yoshimura, A., Deng, Y., He, N., & Li, S. (2021). The methods and advances of adaptive immune receptors repertoire sequencing. *Theranostics*, *11*(18). https://doi.org/10.7150/thno.61390

Liu, X., & Wu, J. (2018). History, applications, and challenges of immune repertoire research. In *Cell Biology and Toxicology* (Vol. 34, Issue 6). https://doi.org/10.1007/s10565-018-9426-0

Løken, R. Ø., & Fevang, B. (2023). Cellular immunity in COVID-19 and other infections in Common variable immunodeficiency. In *Frontiers in Immunology* (Vol. 14). https://doi.org/10.3389/fimmu.2023.1124279

Manso, T., Folch, G., Giudicelli, V., Jabado-Michaloud, J., Kushwaha, A., Nguefack Ngoune, V., Georga, M., Papadaki, A., Debbagh, C., Pégorier, P., Bertignac, M., Hadi-Saljoqi, S., Chentli, I., Cherouali, K., Aouinti, S., El Hamwi, A., Albani, A., Elhassani, M. E., Viart, B., … Kossida, S. (2022). IMGT® databases, related tools and web resources through three main axes of research and development. *Nucleic Acids Research*, *50*(D1). https://doi.org/10.1093/nar/gkab1136

Martínez-Flores, D., Zepeda-Cervantes, J., Cruz-Reséndiz, A., Aguirre-Sampieri, S., Sampieri, A., & Vaca, L. (2021). SARS-CoV-2 Vaccines Based on the Spike Glycoprotein and Implications of New Viral Variants. *Frontiers in Immunology*, *12*, 701501. https://doi.org/10.3389/FIMMU.2021.701501

McCusker, C., Upton, J., & Warrington, R. (2018). Primary immunodeficiency. *Allergy, Asthma, and Clinical Immunology : Official Journal of the Canadian Society of Allergy and Clinical Immunology*, *14*(Suppl 2), 61. https://doi.org/10.1186/S13223-018-0290-5

McGonagle, D., Sharif, K., O'Regan, A., & Bridgewood, C. (2020). The Role of Cytokines including Interleukin-6 in COVID-19 induced Pneumonia and Macrophage Activation Syndrome-Like Disease. In *Autoimmunity Reviews* (Vol. 19, Issue 6). https://doi.org/10.1016/j.autrev.2020.102537

Meckiff, B. J., Ramírez-Suástegui, C., Fajardo, V., Chee, S. J., Kusnadi, A., Simon, H., Eschweiler, S., Grifoni, A., Pelosi, E., Weiskopf, D., Sette, A., Ay, F., Seumois, G., Ottensmeier, C. H., & Vijayanand, P. (2020). Imbalance of Regulatory and Cytotoxic SARS-CoV-2-Reactive CD4+ T Cells in COVID-19. *Cell*, *183*(5). https://doi.org/10.1016/j.cell.2020.10.001

Mistry, P., Barmania, F., Mellet, J., Peta, K., Strydom, A., Viljoen, I. M., James, W., Gordon, S., & Pepper, M. S. (2022). SARS-CoV-2 Variants, Vaccines, and Host Immunity. *Frontiers in Immunology*, *12*, 809244. https://doi.org/10.3389/FIMMU.2021.809244/BIBTEX

Miyasaka, A., Yoshida, Y., Wang, T., & Takikawa, Y. (2019). Next-generation sequencing analysis of the human T-cell and B-cell receptor repertoire diversity before and after hepatitis B vaccination. *Human Vaccines and Immunotherapeutics*, *15*(11). https://doi.org/10.1080/21645515.2019.1600987

Nahum, A., Sharfe, N., Broides, A., Dadi, H., Naghdi, Z., Mandola, A. B., Vong, L., Arbiv, A., Dalal, I., Brami, I., Wormser, O., Levy, J., & Roifman, C. M. (2020). Defining the biological responses of IL-6 by the study of a novel IL-6 receptor chain immunodeficiency. *Journal of Allergy and Clinical Immunology*, *145*(3). https://doi.org/10.1016/j.jaci.2019.11.015

Nguyen, P., Ma, J., Pei, D., Obert, C., Cheng, C., & Geiger, T. L. (2011). Identification of errors introduced during high throughput sequencing of the T cell receptor repertoire. *BMC Genomics*, *12*. https://doi.org/10.1186/1471-2164-12-106

Nikolich-Žugich, J., Slifka, M. K., & Messaoudi, I. (2004). The many important facets of T-cell repertoire diversity. In *Nature Reviews Immunology* (Vol. 4, Issue 2). https://doi.org/10.1038/nri1292

Peng, Y., Mentzer, A. J., Liu, G., Yao, X., Yin, Z., Dong, D., Dejnirattisai, W., Rostron, T., Supasa, P., Liu, C., López-Camacho, C., Slon-Campos, J., Zhao, Y., Stuart, D. I., Paesen, G. C., Grimes, J. M., Antson, A. A., Bayfield, O. W., Hawkins, D. E. D. P., … Knight, J. C. (2020). Broad and strong memory CD4+ and CD8+ T cells induced by SARS-CoV-2 in UK convalescent individuals following COVID-19. *Nature Immunology 2020 21:11*, *21*(11), 1336–1345. https://doi.org/10.1038/s41590-020-0782-6

Petes, C., Odoardi, N., & Gee, K. (2017). The Toll for trafficking: Toll-like receptor 7 delivery to the endosome. In *Frontiers in Immunology* (Vol. 8, Issue SEP). https://doi.org/10.3389/fimmu.2017.01075

Pogorelyy, M. V., Minervina, A. A., Touzel, M. P., Sycheva, A. L., Komech, E. A., Kovalenko, E. I., Karganova, G. G., Egorov, E. S., Komkov, A. Y., Chudakov, D. M., Mamedov, I. Z., Mora, T., Walczak, A. M., & Lebedev, Y. B. (2018). Precise tracking of vaccine-responding T cell clones reveals convergent and personalized response in identical twins. *Proceedings of the National Academy of Sciences of the United States of America*, *115*(50). https://doi.org/10.1073/pnas.1809642115

Pormohammad, A., Zarei, M., Ghorbani, S., Mohammadi, M., Razizadeh, M. H., Turner, D. L., & Turner, R. J. (2021). Efficacy and Safety of COVID-19 Vaccines: A Systematic Review and Meta-Analysis of Randomized Clinical Trials. *Vaccines*, *9*(5). https://doi.org/10.3390/VACCINES9050467

Primorac, D., Vrdoljak, K., Brlek, P., Pavelić, E., Molnar, V., Matišić, V., Erceg Ivkošić, I., & Parčina, M. (2022). Adaptive Immune Responses and Immunity to SARS-CoV-2. *Frontiers in Immunology*, *13*, 1. https://doi.org/10.3389/FIMMU.2022.848582

Qi, H., Liu, B., Wang, X., & Zhang, L. (2022). The humoral response and antibodies against SARS-CoV-2 infection. *Nature Immunology 2022 23:7*, *23*(7), 1008–1020. https://doi.org/10.1038/s41590-022-01248-5

Quinti, I., Lougaris, V., Milito, C., Cinetto, F., Pecoraro, A., Mezzaroma, I., Mastroianni, C. M., Turriziani, O., Bondioni, M. P., Filippini, M., Soresina, A., Spadaro, G., Agostini,

C., Carsetti, R., & Plebani, A. (2020). A possible role for B cells in COVID-19? Lesson from patients with agammaglobulinemia. *Journal of Allergy and Clinical Immunology*, *146*(1). https://doi.org/10.1016/j.jaci.2020.04.013

Raje, N., & Dinakar, C. (2015). Overview of Immunodeficiency Disorders. In *Immunology and Allergy Clinics of North America* (Vol. 35, Issue 4). https://doi.org/10.1016/j.iac.2015.07.001

Robbiani, D. F., Gaebler, C., Muecksch, F., Lorenzi, J. C. C., Wang, Z., Cho, A., Agudelo, M., Barnes, C. O., Gazumyan, A., Finkin, S., Hägglöf, T., Oliveira, T. Y., Viant, C., Hurley, A., Hoffmann, H. H., Millard, K. G., Kost, R. G., Cipolla, M., Gordon, K., … Nussenzweig, M. C. (2020). Convergent antibody responses to SARS-CoV-2 in convalescent individuals. *Nature*, *584*(7821), 437–442. https://doi.org/10.1038/s41586-020-2456-9

Robins, H. S., Campregher, P. V, Srivastava, S. K., Wacher, A., Turtle, C. J., Kahsai, O., Riddell, S. R., Warren, E. H., & Carlson, C. S. (2009). Comprehensive assessment of T-cell receptor beta-chain diversity in alphabeta T cells. In *Blood* (Vol. 114, Issue 19).

Robins, H. S., Srivastava, S. K., Campregher, P. V., Turtle, C. J., Andriesen, J., Riddell, S. R., Carlson, C. S., & Warren, E. H. (2010). Overlap and effective size of the human CD8+ T cell receptor repertoire. *Science Translational Medicine*, *2*(47). https://doi.org/10.1126/scitranslmed.3001442

Rydyznski Moderbacher, C., Ramirez, S. I., Dan, J. M., Grifoni, A., Hastie, K. M., Weiskopf, D., Belanger, S., Abbott, R. K., Kim, C., Choi, J., Kato, Y., Crotty, E. G., Kim, C., Rawlings, S. A., Mateus, J., Tse, L. P. V., Frazier, A., Baric, R., Peters, B., … Crotty, S. (2020). Antigen-Specific Adaptive Immunity to SARS-CoV-2 in Acute COVID-19 and Associations with Age and Disease Severity. *Cell*, *183*(4). https://doi.org/10.1016/j.cell.2020.09.038

Salinas, A. F., Mortari, E. P., Terreri, S., Quintarelli, C., Pulvirenti, F., Di Cecca, S., Guercio, M., Milito, C., Bonanni, L., Auria, S., Romaggioli, L., Cusano, G., Albano, C., Zaffina, S., Perno, C. F., Spadaro, G., Locatelli, F., Carsetti, R., & Quinti, I. (2021). SARS-CoV-2 Vaccine Induced Atypical Immune Responses in Antibody Defects: Everybody Does their Best. *Journal of Clinical Immunology*, *41*(8). https://doi.org/10.1007/s10875-021-01133-0

Schulien, I., Kemming, J., Oberhardt, V., Wild, K., Seidel, L. M., Killmer, S., Sagar, Daul, F., Salvat Lago, M., Decker, A., Luxenburger, H., Binder, B., Bettinger, D., Sogukpinar, O., Rieg, S., Panning, M., Huzly, D., Schwemmle, M., Kochs, G., … Neumann-Haefelin, C. (2021). Characterization of pre-existing and induced SARS-CoV-2-specific CD8+ T cells. *Nature Medicine*, *27*(1). https://doi.org/10.1038/s41591-020-01143-2

Sekine, T., Perez-Potti, A., Rivera-Ballesteros, O., Strålin, K., Gorin, J. B., Olsson, A., Llewellyn-Lacey, S., Kamal, H., Bogdanovic, G., Muschiol, S., Wullimann, D. J., Kammann, T., Emgård, J., Parrot, T., Folkesson, E., Akber, M., Berglin, L., Bergsten, H., Brighenti, S., … Buggert, M. (2020). Robust T Cell Immunity in Convalescent Individuals with Asymptomatic or Mild COVID-19. *Cell*, *183*(1). https://doi.org/10.1016/j.cell.2020.08.017

Sette, A., & Crotty, S. (2021). Adaptive immunity to SARS-CoV-2 and COVID-19. *Cell*, *184*(4), 861–880. https://doi.org/10.1016/J.CELL.2021.01.007

Shugay, M., Britanova, O. V., Merzlyak, E. M., Turchaninova, M. A., Mamedov, I. Z., Tuganbaev, T. R., Bolotin, D. A., Staroverov, D. B., Putintseva, E. V., Plevova, K., Linnemann, C., Shagin, D., Pospisilova, S., Lukyanov, S., Schumacher, T. N., & Chudakov, D. M. (2014). Towards error-free profiling of immune repertoires. *Nature Methods*, *11*(6). https://doi.org/10.1038/nmeth.2960

Spencer, S., Bal, S. K., Egner, W., Allen, H. L., Raza, S. I., Ma, C. A., Gürel, M., Zhang, Y., Sun, G., Sabroe, R. A., Greene, D., Rae, W., Shahin, T., Kania, K., Ardy, R. C., Thian, M., Staples, E., Pecchia-Bekkum, A., Worrall, W. P. M., … Thaventhiran, J. E. D. (2019). Loss of the interleukin-6 receptor causes immunodeficiency, atopy, and abnormal inflammatory responses. *Journal of Experimental Medicine*, *216*(9). https://doi.org/10.1084/jem.20190344

Steiner, S., Schwarz, T., Corman, V. M., Gebert, L., Kleinschmidt, M. C., Wald, A., Gläser, S., Kruse, J. M., Zickler, D., Peric, A., Meisel, C., Meyer, T., Staudacher, O. L., Wittke, K., Kedor, C., Bauer, S., Besher, N. Al, Kalus, U., Pruß, A., … Hanitsch, L. G. (2022). SARS-CoV-2 T Cell Response in Severe and Fatal COVID-19 in Primary Antibody Deficiency Patients Without Specific Humoral Immunity. *Frontiers in Immunology*, *13*. https://doi.org/10.3389/fimmu.2022.840126

Steiner, S., Sotzny, F., Bauer, S., Na, I. K., Schmueck-Henneresse, M., Corman, V. M., Schwarz, T., Drosten, C., Wendering, D. J., Behrends, U., Volk, H. D., Scheibenbogen, C., & Hanitsch, L. G. (2020). HCoV- and SARS-CoV-2 Cross-Reactive T Cells in CVID Patients. *Frontiers in Immunology*, *11*. https://doi.org/10.3389/fimmu.2020.607918

Suthar, M. S., Zimmerman, M. G., Kauffman, R. C., Mantus, G., Linderman, S. L., Hudson, W. H., Vanderheiden, A., Nyhoff, L., Davis, C. W., Adekunle, O., Affer, M., Sherman, M., Reynolds, S., Verkerke, H. P., Alter, D. N., Guarner, J., Bryksin, J., Horwath, M. C., Arthur, C. M., … Wrammert, J. (2020). Rapid Generation of Neutralizing Antibody Responses in COVID-19 Patients. *Cell Reports Medicine*, *1*(3). https://doi.org/10.1016/j.xcrm.2020.100040

Tangye, S. G., Al-Herz, W., Bousfiha, A., Chatila, T., Cunningham-Rundles, C., Etzioni, A., Franco, J. L., Holland, S. M., Klein, C., Morio, T., Ochs, H. D., Oksenhendler, E., Picard, C., Puck, J., Torgerson, T. R., Casanova, J. L., & Sullivan, K. E. (2020). Human Inborn Errors of Immunity: 2019 Update on the Classification from the International Union of Immunological Societies Expert Committee. *Journal of Clinical Immunology*, *40*(1). https://doi.org/10.1007/s10875-019-00737-x

Tezuka, H., Abe, Y., Asano, J., Sato, T., Liu, J., Iwata, M., & Ohteki, T. (2011). Prominent Role for Plasmacytoid Dendritic Cells in Mucosal T Cell-Independent IgA Induction. *Immunity*, *34*(2), 247–257. https://doi.org/10.1016/J.IMMUNI.2011.02.002

Tong, J. Y., Wong, A., Zhu, D., Fastenberg, J. H., & Tham, T. (2020). The Prevalence of Olfactory and Gustatory Dysfunction in COVID-19 Patients: A Systematic Review and Meta-analysis. *Otolaryngology–Head and Neck Surgery*, *163*(1), 3–11. https://doi.org/10.1177/0194599820926473

Tortorici, M. A., & Veesler, D. (2019). Structural insights into coronavirus entry. *Advances in Virus Research*, *105*, 93–116. https://doi.org/10.1016/BS.AIVIR.2019.08.002

Turchaninova, M. A., Davydov, A., Britanova, O. V., Shugay, M., Bikos, V., Egorov, E. S., Kirgizova, V. I., Merzlyak, E. M., Staroverov, D. B., Bolotin, D. A., Mamedov, I. Z., Izraelson, M., Logacheva, M. D., Kladova, O., Plevova, K., Pospisilova, S., & Chudakov, D. M. (2016). High-quality full-length immunoglobulin profiling with

unique molecular barcoding. *Nature Protocols*, *11*(9). https://doi.org/10.1038/nprot.2016.093

Turner, S. J., Doherty, P. C., McCluskey, J., & Rossjohn, J. (2006). Structural determinants of T-cell receptor bias in immunity. In *Nature Reviews Immunology* (Vol. 6, Issue 12). https://doi.org/10.1038/nri1977

Viallard, J. F., Ruiz, C., Guillet, M., Pellegrin, J. L., & Moreau, J. F. (2013). Perturbations of the CD8+ T-cell repertoire in CVID patients with complications. *Results in Immunology*, *3*. https://doi.org/10.1016/j.rinim.2013.05.004

Walls, A. C., Park, Y. J., Tortorici, M. A., Wall, A., McGuire, A. T., & Veesler, D. (2020). Structure, Function, and Antigenicity of the SARS-CoV-2 Spike Glycoprotein. *Cell*, *181*(2), 281-292.e6. https://doi.org/10.1016/J.CELL.2020.02.058

Weiskopf, D., Bangs, D. J., Sidney, J., Kolla, R. V., De Silva, A. D., De Silva, A. M., Crotty, S., Peters, B., & Sette, A. (2015). Dengue virus infection elicits highly polarized CX3CR1+ cytotoxic CD4+ T cells associated with protective immunity. *Proceedings of the National Academy of Sciences of the United States of America*, *112*(31). https://doi.org/10.1073/pnas.1505956112

Weiskopf, D., Schmitz, K. S., Raadsen, M. P., Grifoni, A., Okba, N. M. A., Endeman, H., van den Akker, J. P. C., Molenkamp, R., Koopmans, M. P. G., van Gorp, E. C. M., Haagmans, B. L., de Swart, R. L., Sette, A., & de Vries, R. D. (2020). Phenotype and kinetics of SARS-CoV-2-specific T cells in COVID-19 patients with acute respiratory distress syndrome. *Science Immunology*, *5*(48). https://doi.org/10.1126/SCIIMMUNOL.ABD2071

Wheatley, A. K., Juno, J. A., Wang, J. J., Selva, K. J., Reynaldi, A., Tan, H. X., Lee, W. S., Wragg, K. M., Kelly, H. G., Esterbauer, R., Davis, S. K., Kent, H. E., Mordant, F. L., Schlub, T. E., Gordon, D. L., Khoury, D. S., Subbarao, K., Cromer, D., Gordon, T. P., … Kent, S. J. (2021). Evolution of immune responses to SARS-CoV-2 in mild-moderate COVID-19. *Nature Communications 2021 12:1*, *12*(1), 1–11. https://doi.org/10.1038/s41467-021-21444-5

Wiersinga, W. J., Rhodes, A., Cheng, A. C., Peacock, S. J., & Prescott, H. C. (2020). Pathophysiology, Transmission, Diagnosis, and Treatment of Coronavirus Disease

2019 (COVID-19): A Review. *JAMA*, *324*(8), 782–793. https://doi.org/10.1001/JAMA.2020.12839

Wong, G. K., Millar, D., Penny, S., Heather, J. M., Mistry, P., Buettner, N., Bryon, J., Huissoon, A. P., & Cobbold, M. (2016). Accelerated Loss of TCR Repertoire Diversity in Common Variable Immunodeficiency. *The Journal of Immunology*, *197*(5). https://doi.org/10.4049/jimmunol.1600526

Woodruff, M. C., Ramonell, R. P., Nguyen, D. C., Cashman, K. S., Saini, A. S., Haddad, N. S., Ley, A. M., Kyu, S., Howell, J. C., Ozturk, T., Lee, S., Suryadevara, N., Case, J. B., Bugrovsky, R., Chen, W., Estrada, J., Morrison-Porter, A., Derrico, A., Anam, F. A., … Sanz, I. (2020). Extrafollicular B cell responses correlate with neutralizing antibodies and morbidity in COVID-19. *Nat. Immunol.*, *21*(12), 1506–1516. https://doi.org/10.1038/s41590-020-00814-z

Woodsworth, D. J., Castellarin, M., & Holt, R. A. (2013). Sequence analysis of T-cell repertoires in health and disease. In *Genome Medicine* (Vol. 5, Issue 10). https://doi.org/10.1186/gm502

Zander, R., Schauder, D., Xin, G., Nguyen, C., Wu, X., Zajac, A., & Cui, W. (2019). CD4+ T Cell Help Is Required for the Formation of a Cytolytic CD8+ T Cell Subset that Protects against Chronic Infection and Cancer. *Immunity*, *51*(6). https://doi.org/10.1016/j.immuni.2019.10.009

Zhang, J., Ejikemeuwa, A., Gerzanich, V., Nasr, M., Tang, Q., Simard, J. M., & Zhao, R. Y. (2022). Understanding the Role of SARS-CoV-2 ORF3a in Viral Pathogenesis and COVID-19. In *Frontiers in Microbiology* (Vol. 13). Frontiers Media S.A. https://doi.org/10.3389/fmicb.2022.854567

Zhao, J., Zhao, J., Mangalam, A. K., Channappanavar, R., Fett, C., Meyerholz, D. K., Agnihothram, S., Baric, R. S., David, C. S., & Perlman, S. (2016). Airway Memory CD4+ T Cells Mediate Protective Immunity against Emerging Respiratory Coronaviruses. *Immunity*, *44*(6). https://doi.org/10.1016/j.immuni.2016.05.006

Zonozi, R., Walters, L. C., Shulkin, A., Naranbhai, V., Nithagon, P., Sauvage, G., Kaeske, C., Cosgrove, K., Nathan, A., Tano-Menka, R., Gayton, A. C., Getz, M. A., Senjobe, F., Worrall, D., John Iafrate, A., Fromson, C., Montesi, S. B., Rao, D. A., Sparks, J. A., … Gaiha, G. D. (2023). *T cell responses to SARS-CoV-2 infection and vaccination are*

elevated in B cell deficiency and reduce risk of severe COVID-19. https://www.science.org

Zvyagin, I. V., Pogorelyy, M. V., Ivanova, M. E., Komech, E. A., Shugay, M., Bolotin, D. A., Shelenkov, A. A., Kurnosov, A. A., Staroverov, D. B., Chudakov, D. M., Lebedev, Y. B., & Mamedov, I. Z. (2014). Distinctive properties of identical twins' TCR repertoires revealed by high-throughput sequencing. *Proceedings of the National Academy of Sciences of the United States of America*, *111*(16). https://doi.org/10.1073/pnas.1319389111

Appendix

I. Supplementary material

Table S1. List of primers used for 5'RACE to prepare the libraries.

Primer	Sequence
1st strand cDNA synthesis:	
SmartNNNa	AAGCAGUGGTAUCAACGCAGAGUNNNNUNNNNUNNN-NUCTT(rG)4
hTCRB-r1	GTATCTGGAGTCATTGA
1st PCR amplification:	
Rep_M1SS	AAGCAGTGGTATCAACGCA
hTCRB-r2	TGCTTCTGATGGCTCAAACAC
2nd PCR amplification:	
Fwd_OH_M1S	TCGTCGGCAGCGTCAGATGTGTATAAGAGACAGNNNNNCAGTGGTATCAACGCAGAG
hTCRb_R3+NextRev	GTCTCGTGGGCTCGGAGATGTGTATAAGAGACAGNNNNN+ACACSTTKTTCAGGTCCTC

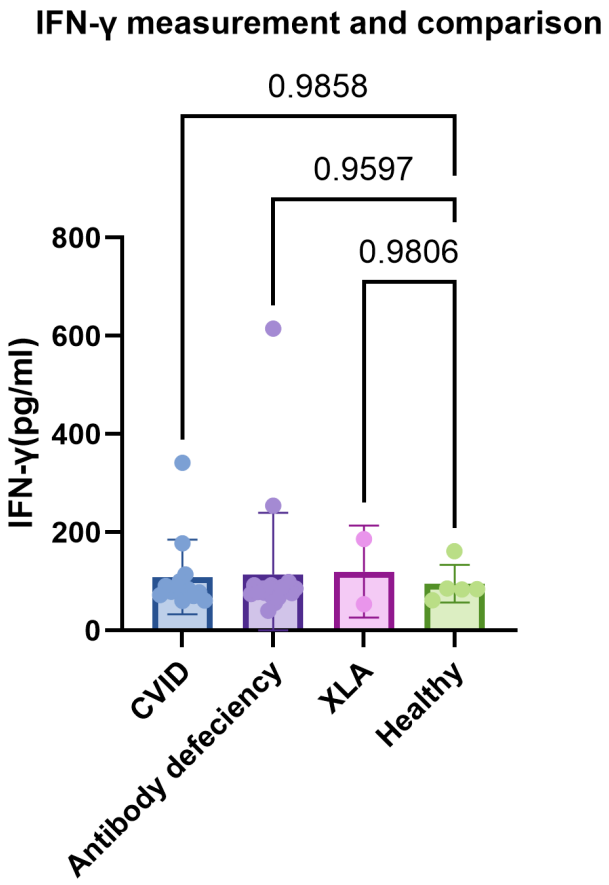

Figure S1. Interferon-gamma (IFN-γ) measurements and comparison of PID vs Healthy by ELISA. The X-axis represents the different groups, and the Y-axis is the concentration of the measured IFN-γ in stimulated samples. P-values were obtained by the ANOVA test comparing the mean of each diagnosis with Healthy.

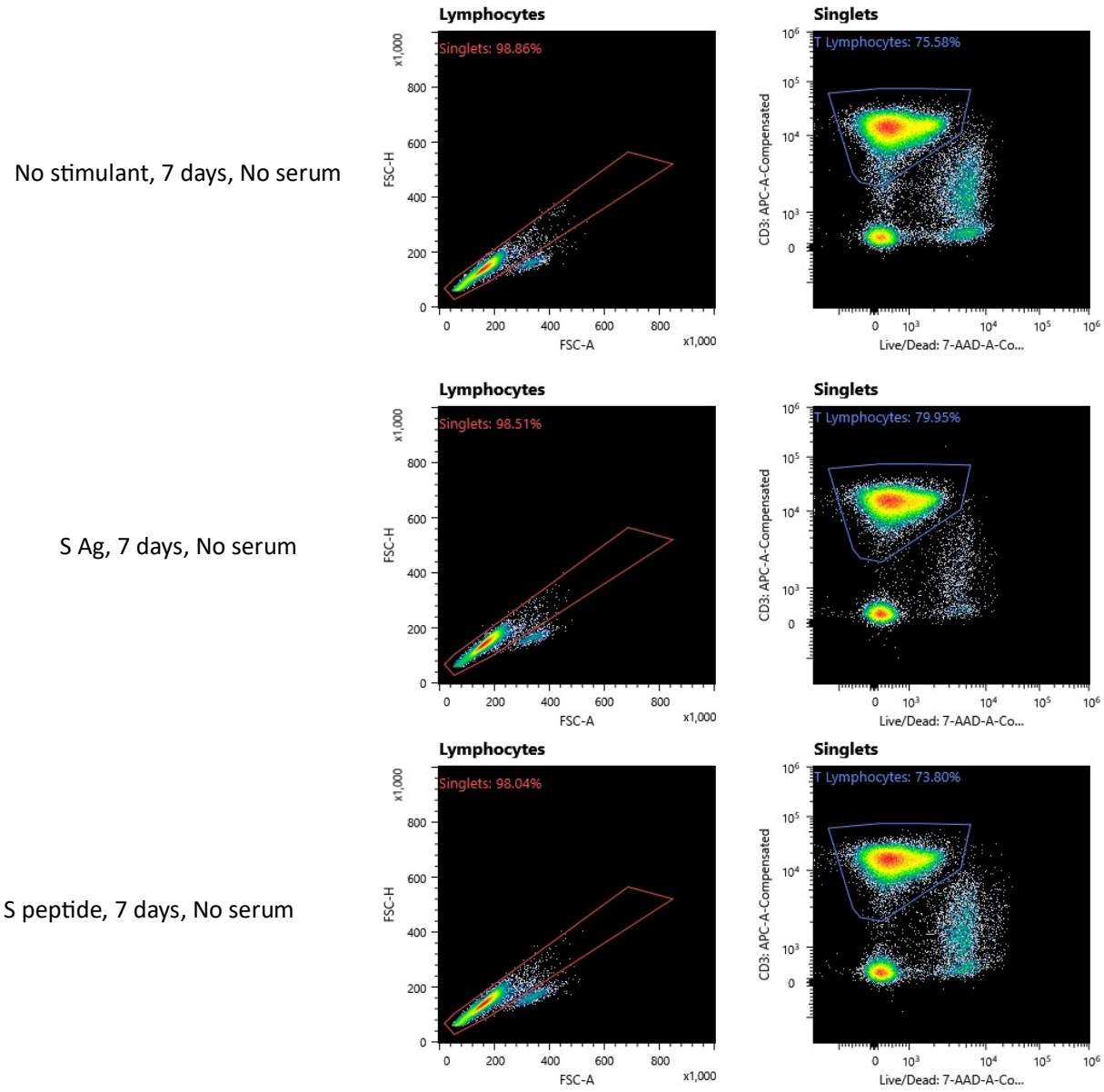

Figure S2. Gating strategy for selection of live T-lymphocytes. On the right, the singlet gates on lymphocytes are shown, with the X-axis representing forward scatter area (FSC-A) and the Y-axis representing forward scatter-height (FSC-H). On the left, live T lymphocytes are identified and gated by CD3+ and 7-AAD-.

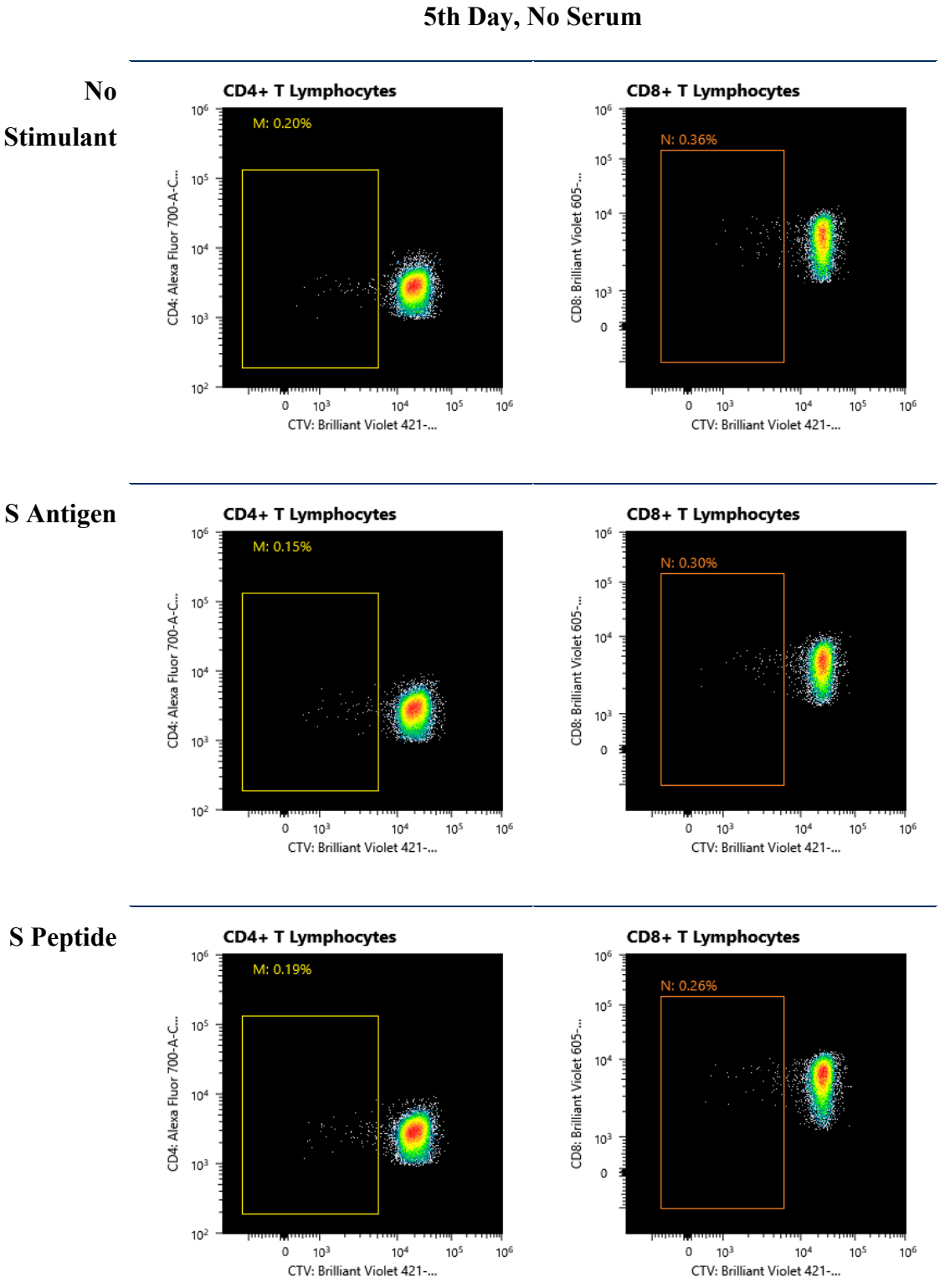

Figure S3. Flow cytometry results from the 5th-day post antigen stimulations with no human serum. The panels on the right represent CD4+ T-cells, while those on the left represent CD8+ T-cells.

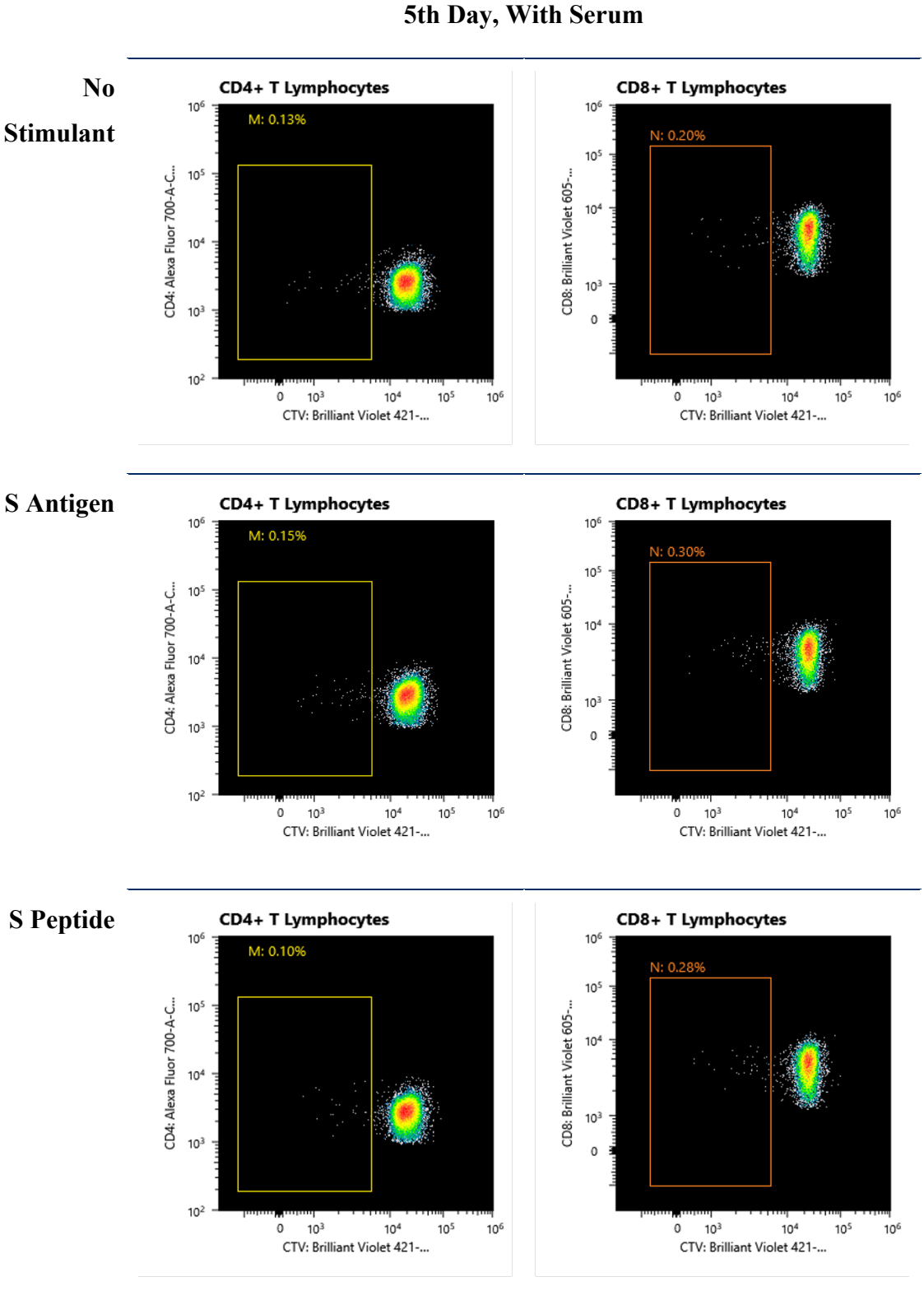

Figure S4. Flow cytometry results from the 5th-day post antigen stimulations with human serum. The panels on the right represent CD4+ T-cells, while those on the left represent CD8+ T-cells.

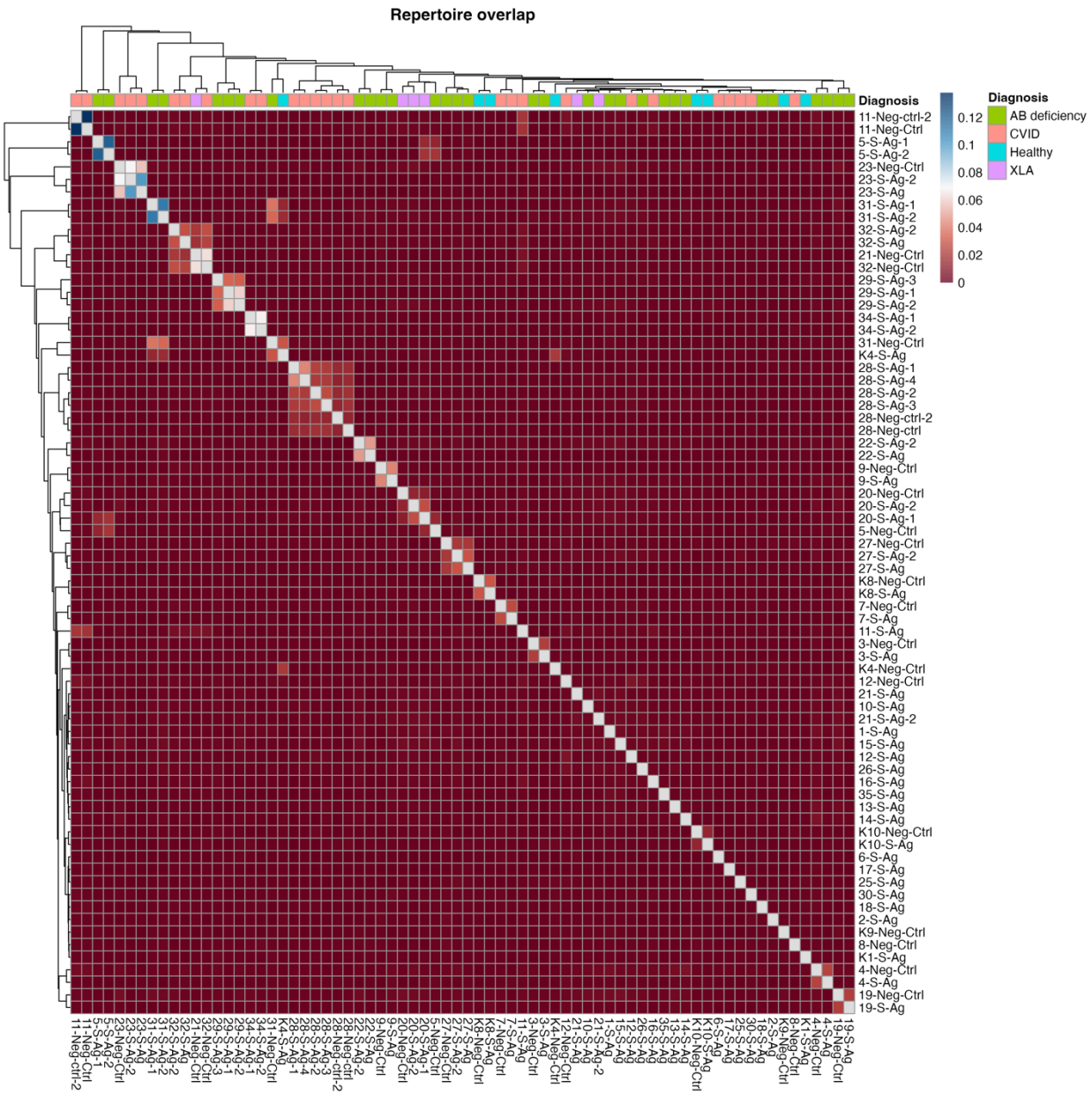

Figure S5. Repertoire overlap by Jaccard index. The heat map shows the overlap of samples by the Jaccard index, showing the cluster of samples by the color-coded diagnosis in the top row. Data was downsampled to the lowest number of clones. Each box shows the overlap between two samples.

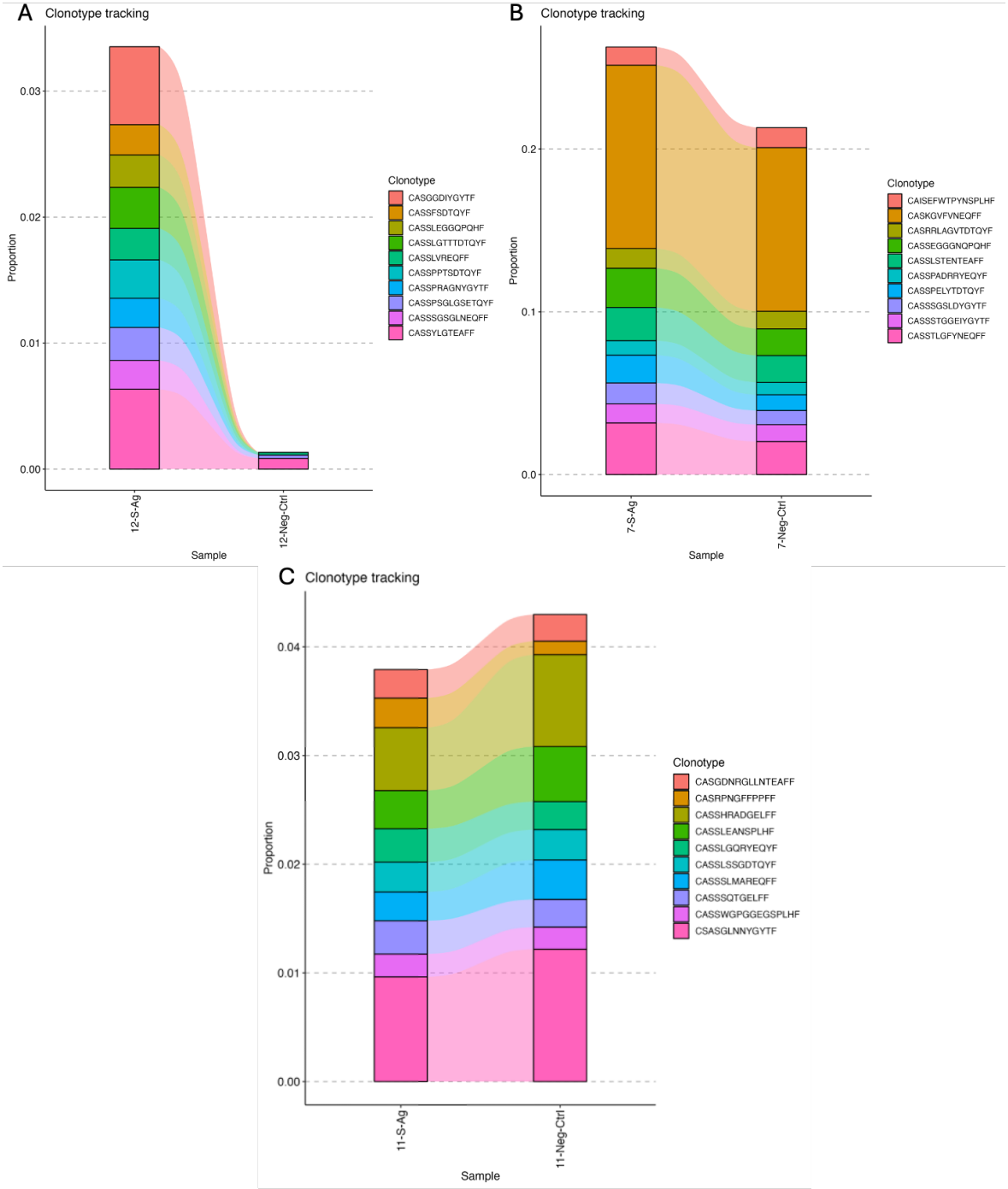

Figure S6. Clonotype tracking in CVID patients 12, 7, and 11. The X-axis represents the stimulated (S-Ag) and unstimulated samples (Neg-Ctrl) belonging to each individual. The Y-axis shows the proportion of each clonotype within the repertoire. Clonotype aa sequences are color-coded in the legends of the figures. A: Patient 12, B: Patient 7, C: Patient 11

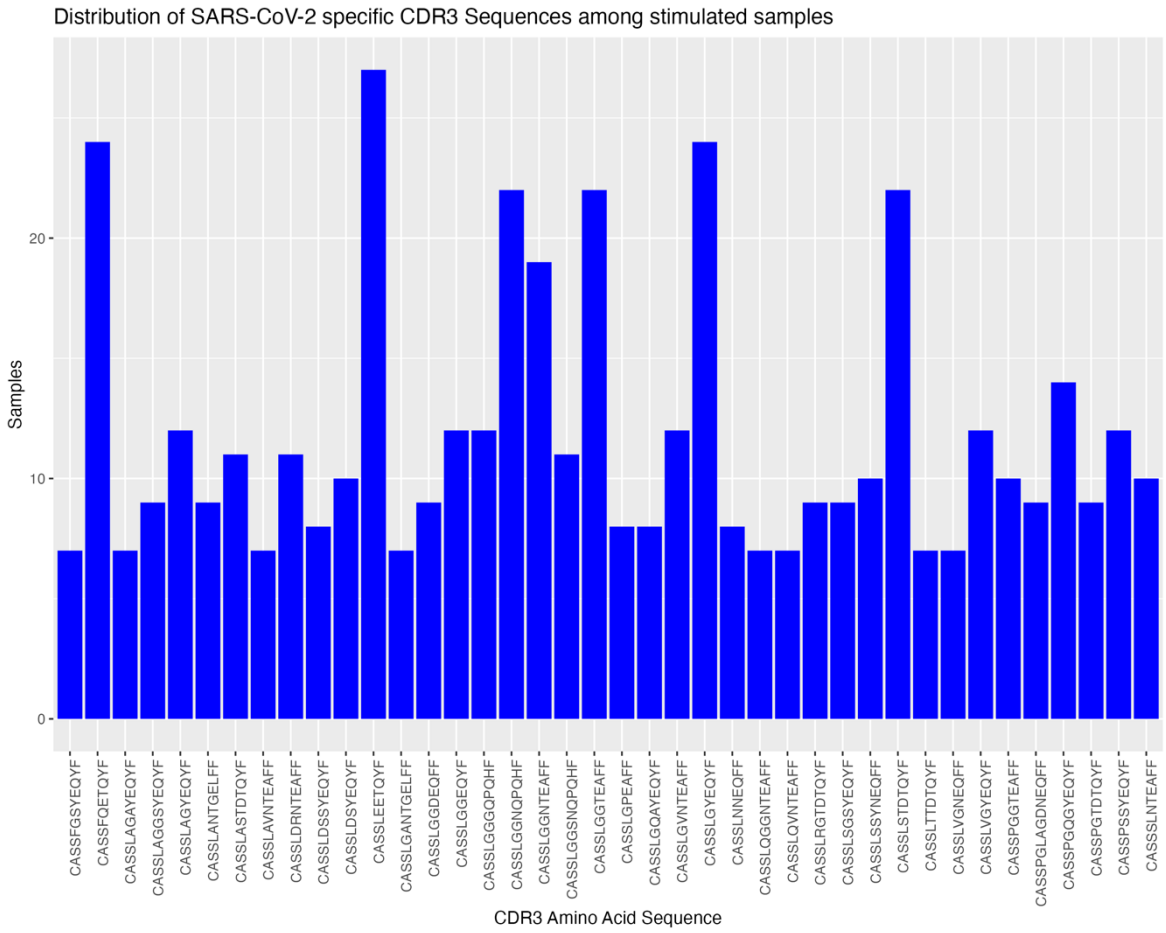

Figure S7. The annotated SARS-CoV-2 specific CDR3 amino acids among stimulated Samples. Annotations were done using the public VDJdb database (Goncharov et al., 2022). The X-axis represents the identified SARS-CoV-2 specific CDR3 aa among the stimulated samples and the Y-axis represents the number of samples that contained the TCR.

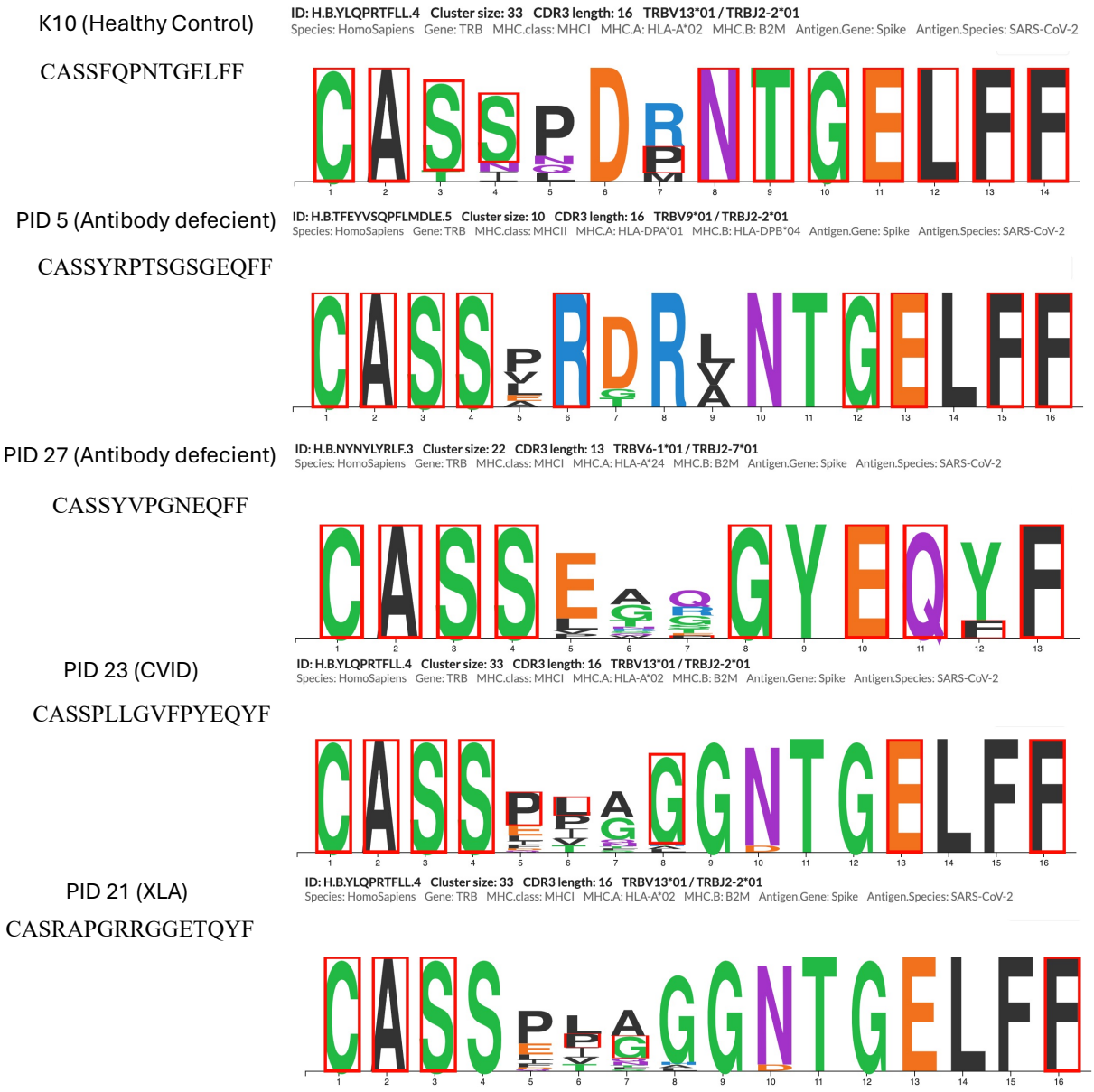

Figure S8. Comparison of Expanded Clonotypes with Known SARS-CoV-2 Spike Associated Clonotypes. Comparisons were done using the public VDJdb database (Goncharov et al., 2022). The patient ID, diagnosis, and expanded clonotype are presented on the left. The visualization of the amino acid motif similarity with clusters of known SARS-CoV-2 Spike-specific CDR3 sequences and the expanded clonotype is displayed on the right. The amino acid positions highlighted in red represent similarities between identified Spike-specific sequences and the input clonotype.

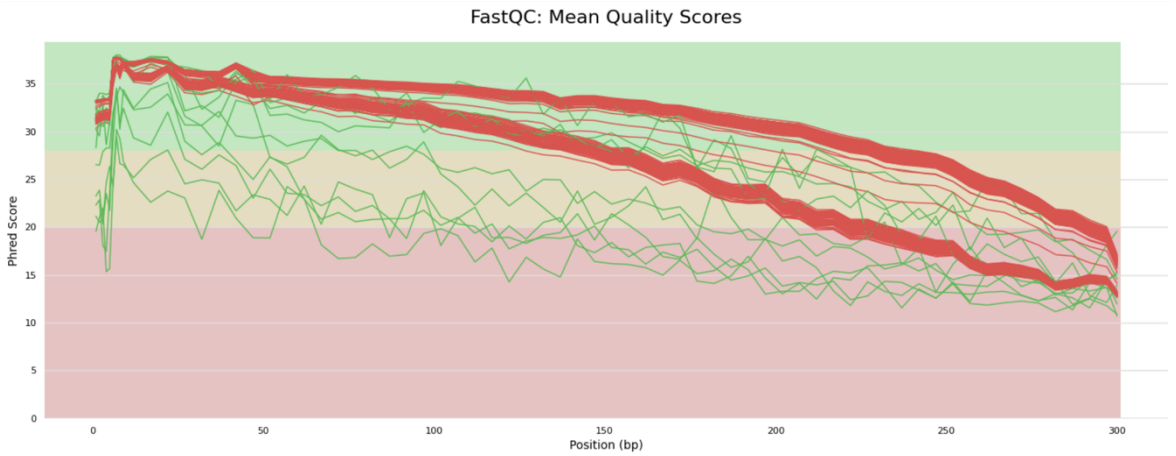

Figure S9. Mean quality scores of sequences from FastQC. The X-axis represents the length of the sequencing reads in base pairs, and the Y-axis shows the corresponding phred score.

NON-EXCLUSIVE LICENCE TO REPRODUCE THESIS AND MAKE THESIS PUBLIC

I, Avishan Aghayari

1. herewith grant the University of Tartu a free permit (non-exclusive licence) to

reproduce, for the purpose of preservation, including for adding to the DSpace digital archives until the expiry of the term of copyright,

"**T-cell receptor repertoire analysis in CVID pa-tients post Comirnaty vaccination**"

supervised by Alexandra Elaskova, and Prof. Kai Kisand

2. I grant the University of Tartu a permit to make the work specified in p. 1 available to the public via the web environment of the University of Tartu, including via the DSpace digital archives, under the Creative Commons licence CC BY NC ND 3.0, which allows, by giving appropriate credit to the author, to reproduce, distribute the work and communicate it to the public, and prohibits the creation of derivative works and any commercial use of the work until the expiry of the term of copyright.

3. I am aware of the fact that the author retains the rights specified in p. 1 and 2.

4. I certify that granting the non-exclusive licence does not infringe other persons' intellectual property rights or rights arising from the personal data protection legislation.

Avishan Aghayari

22/05/2024